

IDENTIFICATION OF POWDERY MILDEW DISEASE AND GENETIC  
IMPROVEMENTS IN HAZELNUT

by  
İPEK BİLGE

Submitted to the Graduate School of Engineering and Natural Sciences  
in partial fulfilment of the requirements for the degree of  
Doctor of Philosophy

Sabancı University

December 2020

IDENTIFICATION OF POWDERY MILDEW DISEASE AND GENETIC  
IMPROVEMENTS IN HAZELNUT

APPROVED BY:

[Redacted signature]

[Redacted signature]

[Redacted signature]

[Redacted signature]

[Redacted signature]

[Redacted signature]

DATE OF APPROVAL: 18/12/2020

© İpek Bilge 2020  
All Rights Reserved

# Identification of Powdery Mildew Disease and Genetic Improvements in Hazelnut

İpek BİLGE

BIO, Doctor of Philosophy, 2020

Thesis Supervisor: Prof. Dr. Selim ÇETİNER

Keywords: Powdery mildew, *Corylus avellana*, *Erysiphe corylacearum*, *Phylactinia guttata*, Loop mediated Isothermal Amplification (LAMP), Mildew Locus O (MLO) Gene family

## ABSTRACT

*Corylus avellana* L. (hazelnut) is an economically important nut crop worldwide due to its nutritional and nutraceutical properties. Powdery mildew is a fungal infection caused by obligate biotrophic fungal plant pathogens distributed nearly worldwide and infects a wide range of plants. Being a highly contagious pathogen that effects the crop quality, a fast and correct genetic diagnosis efforts are highly demanded. In the content on this thesis work initial effort is given to identify the types and characteristics of two pathogens of powdery mildews that mostly infects hazelnut leaves in Turkey. As a result of unique microscopy analysis and genetical ancestor tracing they have been identified as *Erysiphe corylacearum* and *Phylactinia guttata* where first is more abundant and destructive and latter is less frequently observed. In order to be able to diagnose the type of pathogen on-field, a novel fast and cost-effective methodology based on the use of newly designed *E. corylacearum* and *P. guttata* specific primers is developed. Results suggest that the proposed approach reduces the pathogen diagnosis time 10 to 1 when compared with diagnosis with the use of conventional ITS primers. Focusing specifically on *E. corylacearum* specific primers limit of detection is identified quantitatively with calculation of pathogen copy number. Loop Mediated Isothermal Amplification (LAMP) method is employed with *E. corylacearum* specific 28S-LAMP primers that enables the on-field identification of pathogen. Lastly, the genome sequencing of *Corylus avellana* cv. Tombul have been correctly sequenced that enabled the identification of resistant gene family *Mildew Locus O* (MLO) that paves way to powdery mildew resistant hazelnut crops.

# Fındıkta Külleme hastalığının tanımlanması ve Genetik olarak iyileştirilmesi

İpek BİLGE

BIO, Doktora Tezi, 2020

Tez Danışmanı: Prof. Dr. Selim ÇETİNER

Anahtar kelimeler: Külleme hastalığı, *Corylus avellana*, *Erysiphe corylacearum*, *Phylactinia guttata*, Loop mediated Isothermal Amplification (LAMP), *Mildew Locus O* (MLO) Gen ailesi

## ÖZET

*Corylus avellana* L. (fındık), besleyici ve nutrasötik özellikleri nedeniyle dünya çapında ekonomik açıdan önemli bir kuruyemiş türüdür. Külleme hastalığı, tüm dünyaya yayılan zorunlu biyotrofik mantar bitki patojenlerinin neden olduğu bir mantar enfeksiyonudur ve çeşitli bitkileri enfekte eder. Ürün kalitesini etkileyen oldukça bulaşıcı bir patojen olduğu için hızlı ve doğru bir genetik tanımlama yönteminin geliştirilmesi gerekmektedir. Bu tez çalışmasının içeriğinde, Türkiye'deki fındık yapraklarını etkileyen iki külleme patojeninin türlerini ve özelliklerini belirlemek için çalışılmıştır. Mikroskopi analizi ve genetik tanımlama sonucunda, bu patojenler *Erysiphe corylacearum* ve *Phylactinia guttata* olarak tanımlanmışlardır; patojenlerden ilki daha çok rastlanılan ve hasata zara verirken ikincisi daha az sıklıkla görülür. Sahada patojen tipini teşhis edebilmek için, yeni tasarlanmış *E. corylacearum* ve *P. guttata*'ya özgü primerlerin kullanımına dayanan yeni, hızlı ve uygun maliyetli bir metodoloji geliştirilmiştir. Sonuçlar, önerilen yaklaşımın, geleneksel ITS primerlerinin kullanımı ile tanıya kıyasla patojen tanı süresini 10 günden 1 güne düşürmüştür. Özellikle *E. corylacearum*'a özgü primerler saptama sınırına odaklanıldığında, patojen kopya sayısının hesaplanmasıyla kantitatif olarak tanımlanır. Döngü Aracılı İzotermal Amplifikasyon (LAMP) yöntemi, adapte edilebilecek mekanizma ile patojenin sahada tanımlanmasını sağlayan *E. corylacearum*'a özgü 28S-LAMP primerleri ile kullanılabilir. Son olarak, *Corylus avellana* cv. Tombul genomu kullanılarak, küllemeye dirençli fındık ekinlerinin yolunu açan gen familyası *Mildew Locus O* (MLO) biyoinformatik olarak tesbit edilip, Genomda kopyalarının bulunduğu deneysel olarak kanıtlanılmıştır.

## ACKNOWLEDGEMENTS

Well after many sleepless nights, multiple tears, tons of brainstorming, studied articles that reached to my height, lots of discussions and group meetings. But these times were not melancholic at all, I meet the best advisor, my caramel macchiato husband, adopted four crazy cats and lifelong friends.

I gratefully thank to my advisor Stuart J. Lucas for his guidance throughout my whole PhD journey. His patient towards my endless questions, dedication for teaching scientific studies, countless encouragements and great family values.

I gratefully thank to my advisor Prof. Dr. Selim Çetiner for accepting me and helping me to complete this journey.

I would like to thank members of my thesis jury, Dr. Bahar Soğutmaz Özdemir, Dr. Meltem Elitaş, Dr. Fatma Aydınoglu and Prof. Dr. Levent Öztürk for accepting being in my jury and spending their valuable time for me.

I would like to express my eternal love to my family, My dad, mum and grandma for their endless support, encouragement and love. Unfortunately, I lost my grandma at the beginning of my PhD journey, but she will always be remembered. My enthusiastic husband and future susam... hopefully life await us with many joys.

Lastly, I am grateful to my friends from astroleg, yılan, the last gossip, bacıcode and güzellikler diyarı always encouraging me to never give up and put a smile on my face.

## TABLE OF CONTENT

List of Tables	viii
List of Figures	ix
1 INTRODUCTION.....	1
1.1 Overview.....	1
1.2 Hazelnut .....	2
1.2.1 Hazelnut Diversity.....	2
1.2.2 Hazelnut cultivars from Turkey:.....	6
1.2.3 Hazelnut genome.....	8
1.3 Powdery mildew disease.....	10
1.3.1 Corylus Fungal pathogens.....	10
1.3.2 Powdery Mildew Disease.....	15
1.3.3 Powdery mildew Disease on <i>Corylus avellana</i> .....	18
1.3.4 Powdery Mildew morphological identification.....	19
1.3.5 Powdery mildew Genetic identification.....	21
1.3.5.1 DNA Barcoding.....	21
1.3.5.2 Loop Mediated Isothermal Amplification (LAMP).....	24
1.3.3 Powdery mildew disease Intervention.....	26
1.3.3.1 Fungicide.....	26
1.3.3.2 Fungal Hyperparasites.....	28
1.4 Issue to Address .....	30
1.5 Proposed Approach .....	30
2 MATERIALS AND METHODS.....	32
2.1 Orchards selection and weather station locations.....	32
2.2 Pathogen Diagnosis Algorithm .....	33
2.3 Leaf sample collection.....	34
2.4 Initial Inspection by Microscopy.....	35
2.5 DNA extraction .....	35
2.6 Polymerase Chain Reaction (PCR) Analysis .....	36
2.7 Sanger Sequencing .....	37
2.8 Specific PCR primer design.....	37
2.9 Quantitative-PCR (qPCR) Analysis.....	38
2.10 Loop Mediated Isothermal Amplification (LAMP) assay.....	38
2.11 RNA extraction.....	39

3 RESULTS AND DISCUSSION.....	41
3.1. Hazelnut orchards and Environmental factors: .....	41
3.2 Visual Analysis of Collected Leaf Samples.....	49
3.3. Morphology of Powdery mildew pathogen observed on leaf samples.....	53
3.4 Fungal pathogen identification by PCR analysis with Universal ITS primers.....	57
3.5 PCR analysis using Universal ITS primers for <i>E. corylacearum</i> infected leaf sample.....	60
3.6 Designing <i>Erysiphe corylacearum</i> specific primers.....	65
3.7 Analyzing collected leaf samples with newly designed <i>E.corylacearum</i> specific primers.....	67
3.8 Powdery mildew infection copy number calculation.....	70
3.9 Limit of detection for <i>E. corylaearum</i> infection.....	73
3.10 Loop Mediated Isothermal Amplification Assay (LAMP): .....	76
3.11 <i>Phylactinia guttata</i> identification by Universal primers .....	78
3.12 <i>Phylactinia guttata</i> specific primer design.....	81
3.14 Identification of MLO gene family .....	82
3.15 Mildew Locus O (MLO) gene family experimentally validation for <i>Corylus avellana</i> .....	84
4. CONCLUSION.....	86
APPENDIX.....	99
A. Location data for sample collected orchards in Turkey .....	99
B. List of collected leaf samples.....	101

## LIST OF TABLES

<b>Table 1:</b> Subsection distribution of <i>Corylus</i> species, known common names and the harvest yield location are given .....	5
<b>Table 2:</b> List of Ascomycota species that can be find on <i>Corylus sp.</i> leaves. ....	12
<b>Table 3:</b> List of universal ITS primer for fungi .....	23
<b>Table 4:</b> Annealing temperature of primers used in thesis .....	37
<b>Table 5:</b> Designed primer for <i>Erysiphe corylacearum</i> specific fungal identification. ....	65
<b>Table 6:</b> Status of <i>E. corylacearum</i> infection by limit of detection. ....	75
<b>Table 7:</b> Designed LAMP primers. ....	76
<b>Table 8:</b> <i>Phylactinia guttata</i> specific primers. ....	81
<b>Table 9:</b> Hazelnut orchard location and selected weather stations.....	99

## LIST OF FIGURES

<b>Figure 1:</b> Involucre of <i>Corylus avellana</i> cv. Tombul.....	3
<b>Figure 2:</b> Dendrogram of 18 hazelnut cultivars .....	7
<b>Figure 3:</b> Hazelnut cultivars Allahverdi, Tombul and Çakıldak breed in Turkey. ....	8
<b>Figure 4:</b> Powdery mildew infection.....	16
<b>Figure 5:</b> Schematic view of powdery mildew life cycle.. ....	18
<b>Figure 6:</b> <i>P. guttata</i> and <i>E. corylacearum</i> morphology under light microscope .....	21
<b>Figure 7:</b> Algorithm of the pathogen diagnosis. ....	33
<b>Figure 8:</b> Sample collection cutter. ....	38
<b>Figure 9:</b> Weather graphs of 2018 data from Pasalar station.....	42
<b>Figure 10:</b> Weather graphs of 2019 data from Pasalar station.....	43
<b>Figure 11:</b> Weather graphs of 2018 data from Ballıkaya station. ....	43
<b>Figure 12:</b> Weathergraphs of 2019 data from Ballıkaya station. ....	44
<b>Figure 13:</b> Weather graphs of 2019 data from Kovancı station.....	45
<b>Figure 14:</b> Weather graphs of 2019 data from Eynesil station.. ....	46
<b>Figure 15:</b> <i>C. avellana</i> leaf collected from Sabancı University. 50	
<b>Figure 16:</b> Sakarya infected leaf samples.....	51
<b>Figure 17:</b> Düzce leaf samples.....	51
<b>Figure 18:</b> Ordu leaf samples .....	52
<b>Figure 19:</b> Giresun leaf samples .....	52
<b>Figure 20:</b> Powdery mildew agent <i>E.corylacearum</i> collected from hazelnut orchards .....	54
<b>Figure 21:</b> Powdery mildew infected leaf sample collected from Düzce field trip.....	55
<b>Figure 22:</b> SEM image of chasmothecium of powdery mildew pathogens. ....	56
<b>Figure 23:</b> 28S rRNA gene isolated from the collected samples.. ....	58
<b>Figure 24:</b> Phylogenetic tree analysis with sequenced samples .....	59
<b>Figure 25:</b> <i>C. avellana</i> cv. Tombul leaf samples. ....	61
<b>Figure 26:</b> <i>C.avellana</i> cv. Çakıldak leaf samples. ....	63
<b>Figure 27:</b> <i>C.avellana</i> cv. Tombul and Çakıldak gel electrophoresis. ....	63
<b>Figure 28:</b> Phylogenetic tree of sequenced samples .....	64
<b>Figure 29:</b> Sequence differences of the <i>Erysiphe corylacearum</i> and other leaf infecting fungal pathogens.....	65
<b>Figure 30:</b> Gel results of newly designed primers for <i>Erysiphe corylacearum</i> .....	66
<b>Figure 31:</b> 2018 samples sent from Sakarya and Düzce orchards gel image .....	68
<b>Figure 32:</b> Ordu orchard samples gel image result .....	69
<b>Figure 33:</b> Different hazelnut cultivar gel image result .....	69
<b>Figure 34:</b> Düzce orchard samples gel image result.....	69
<b>Figure 35:</b> Gel result of the 2019 season leaf samples tested with Ec_F1-R3 primers. ....	71
<b>Figure 36:</b> Amplication curves of plant, <i>E.corylacearum</i> amplicon and diluted samples .....	72
<b>Figure 37:</b> Gel electrophoresis result of PCR with Ec_F1-R3 primers and qPCR analysis. ....	74
<b>Figure 38:</b> Time dependent amplification of LAMP primers .....	77
<b>Figure 39:</b> <i>E. corylacearum</i> specific LAMP primers. ....	78
<b>Figure 40:</b> Fungal pathogen identification with universal primers NL1-TW14 for Düzce trip samples.....	79
<b>Figure 41:</b> Fungal pathogen identification with universal primers ITS4-ITS5 for Düzce trip samples.....	79
<b>Figure 42:</b> <i>P. guttata</i> infected leaf sample sequence analysis .....	80
<b>Figure 43:</b> Gel electrophoresis result of <i>P. guttata</i> specific primer Pg1.. ....	81

**Figure 44:** Gel electrophoresis result of *P. guttata* specific primer Pg2.....82  
**Figure 45:** A. Phylogenetic clustering of *C. avellana* MLO gene models .....83

## **LIST OF SYMBOLS AND ABBREVIATIONS**

ITS: Internal transcribed spacer

LAMP: Loop mediated isothermal amplification

MLO: Mildew Locus O

PCR: Polymerase chain reaction

SEM: Scanning electron microscope

## 1. Introduction

### 1.1. Overview

*Corylus avellana* L. (hazelnut) is an economically important nut crop worldwide due to its nutritional and nutraceutical properties. Turkey have the leading position in production and export of hazelnuts as well as 66% of the world's cultivation area. Hazelnut production extends along the Black Sea region, from the Georgian border in the east, to Istanbul in the west. In Turkey 33 provinces have hazelnut growing areas, and 16 of them are licensed for commercial hazelnut production.

Powdery mildew is a fungal infection caused by obligate biotrophic fungal plant pathogens distributed nearly worldwide and infect a wide range of plants. Powdery mildew can be observed by naked eye with formation of white powdery like patches. *Erysiphe corylacearum* and *Phylactinia guttata* are two pathogens of powdery mildew that infect *Corylus avellana* L. In 2005 *Phylactinia guttata* have been reported on hazelnuts in Washington, USA. The observations conclude that powdery mildew cause no significant damage to hazelnut scrub and unlikely to threaten the long-term survival of infected scrubs.

Between 2014 and 2015 *C. avellana* L. cultivation areas throughout the eastern Black Sea region started to develop significant damages on hazelnut scrubs due to the Powdery Mildew. By 2016 all 16 provinces that are licensed for hazelnut cultivation orchards were showing traces of destructive powdery mildew. The destructive powdery mildew agent is identified as *Erysiphe corylacearum*. Destructive powdery mildew agent *Erysiphe corylacearum* was also identified by 2017 in Iran, by 2018 in Azerbaijan, and by 2019 in Ukraine, Switzerland and central Europe. Destructive powdery mildew propagates rapidly throughout Asia and Europe.

Several methods are being used for powdery mildew intervention. These methods can be group into three as; fungicide, hyperparasite, and resistant genes. Fungicides are widely used to control fungal disease and safeguard crop yield and quality of harvest. Unfortunately, the cost, difficulty of discovering and registration requirements for new fungicide development combined with the public attitude and environmental concerns

towards the use of pesticides, as well as the development of powdery mildew resistant strains to different fungicides have reduced the appeal of fungicide application.

Hyper-parasites are natural biological control mechanisms for powdery mildew, that are achieved by using well-known natural antagonists of powdery mildews pathogens. However, to maintain control with hyperparasite a certain level of powdery mildew infection should be tolerated, since hyperparasite can only attack to already developed infection. Also, growth, sporulation and expansion of hyperparasite should be faster than host pathogen to reduce its severity and damaging effects on the infected plants. Hyperparasite usage for destructive powdery mildew infection is impractical because powdery mildew epidemics usually reach damaging levels before hyperparasite arrest growth and sporulation of pathogens.

Most promising results for destructive powdery mildew intervention are obtain by loss-of-function mutation in the gene *Mildew resistance Locus O* (MLO). Naturally occurring MLO mutation was found to confer durable resistance to barley powdery mildew pathogen, *Blumeria graminis f.sp. hordei*. Although powdery mildew in barley is caused by different fungal species, resistance to powdery mildew by MLO mutants are identified on many plants. By gene editing introduction of MLO mutation seems to be functionally working for various plant species and could present a promising target for developing powdery mildew resistance.

Classification of *Corylus* species, and Turkey specific cultivars will be discussed. Importance of hazelnut for industry and for Turkish producers is explained.

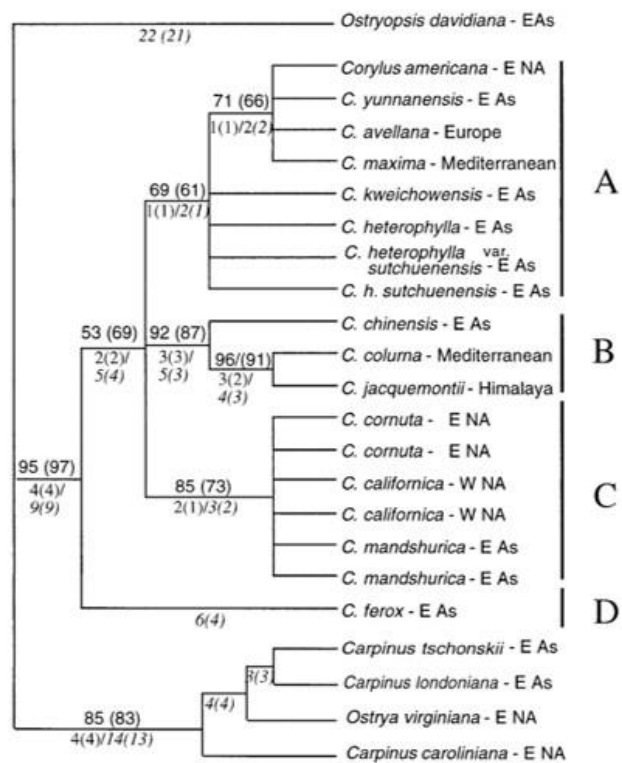
## **1.2 Hazelnut**

### **1.2.1 Hazelnut Diversity**

The *Corylus* L. genus belongs to the *Betulaceae* family of the order *Fagales* and contain wide variety of deciduous shrub and tree species that are important for many forests and produce edible nuts. The number of species within the genus *Corylus* varies between 9 and 25, depending on the taxonomic authority, with current revisions based on morphological, molecular and hybridization studies suggesting 13 major species assigned

to 4 subsections (Molnar 2011) (Helmstetter et al., 2019). *Corylus* species are divided into four subsections depending on the shape and distribution of involucre (Figure1);

- A. Subsection “*Corylus*”; species with leafy, overlapping, bell-shaped involucre covering the nuts,
- B. Subsection “*Colurnaea*”; species with deeply dissected involucre,
- C. Subsection “*Siphonochlamys*”; species with tubular, bristle-covered involucre,
- D. Subsection “*Acanthochlamys*”; contain *C. ferox* Wall, which has a spiny chestnut-like involucre.



- A Section *Corylus* subsection *Corylus*; bell-shaped involucre
- B Section *Corylus* subsection *Colurnae*; tree habit
- C Section *Corylus* subsection *Siphonochlamys*; tubular involucre
- D Section *Acanthochlamys*; spiny involucre

**Figure 1:** Involucre of *Corylus avellana* cv. Tombul is highlighted as yellow square. Phylogenetic tree of *Corylus* species. A. *Corylus* subsection, B. *Colurnae* subsection, C. *Siphonochlamys* subsection and D. *Acanthochlamys* subsection and the *Corylus* species under these subsections.

The genus *Corylus* range in size from small, multi-stemmed bushes (1 m) to large trees (up to 40 m). All members of the species are deciduous, with simple, alternate leaves. Hazelnuts are monoecious plants that male and female flowers are located on different part of plant. *Corylus* plays an important role in soil and water conservation owing to its strong root system and contributes to the sustainability of forests (Ma et al., 2013). The average lifespan of *Corylus sp.* is around 80-90 years. *C. avellana* has a long generation time (up to 8 years to reach full productivity) and displays sporophytic self-incompatibility, with genetically similar individuals unable to pollinate each other. Self-incompatibility induce high heterozygosity level by causing the pistil to reject the pollen of genetically close individuals (Marinoni et al. 2009).

There are about 13 species of *Corylus* around the world, widely distributed in temperate regions of Asia, Europe, and America. Some *Corylus* species are given a common name for public references (Table1). *Corylus avellana* L. also known as European hazelnut is most widely known and well-studied species and is an economically important nut crop worldwide due to its nutritional and nutraceutical properties (Lamichnane, Fabi, Ridolfi, & Varvaro, 2013).

Breeding programs are initiated in the 1960s for improving the climatic adaptations and hazelnut quality that benefits to food industry, health and pharmaceutical applications. In addition, for the long-term control of hazelnut diseases the environmental concerns and high cost of pruning and fungicide applications, host genetic resistance remains the most desirable and economical approach. Breeding program are initiated for creating resistance lines for diseases and parasites such as Eastern filbert blight (EFB) and bud mites (*Phytopus avellanae*) and aiming to improve nut quality by producing medium to large-size round nuts with high quality kernels that nuts drop free of the husks easy. Breeding programs select the parents depending the on the targeted characteristics. Selection of *C. americana* for wide variety of EFB-resistance and adaptation to wider range of climates, *C. avellana* for nut production quality and finally *C. heterophylla* and *C. colurna* for enhancing genetic diversity (Molnar, 2012). Hazelnut genomic and transcriptomic sequence resources allow breeders the opportunity to exploit the wealth of genetic diversity when choosing parents from among the hundreds of accessions worldwide (Rowley et al., 2012).

Hazelnut is a kind of favorite dried fruit which can be eaten raw and dried, not only delicious, but also has high calorific value. In the food industry, hazelnut can be processed in cakes, confectionery, chocolates, snacks and some senior nutrition such as ground hazelnut and hazelnut milk. Hazelnut can be processed in oil. It is a kind of high-quality edible oil rich in unsaturated fatty acid which has yellow color and flavor. Besides the edible function, hazelnut oil also has an economic value since it can also be processed in paint, soap, cosmetics, candles, etc (Ramadan 2019).

**Table 1:** Subsection distribution of *Corylus* species, known common names and the harvest yield location are given

Subsection	Species	Common name	Location
<i>A.Corylus</i>	<i>C. avellana</i>	European hazel	Europe, Caucasus, Western Asia
	<i>C. americana</i>	American hazel	Eastern North America
	<i>C. heterophylla</i>	Siberian hazel	Northeast China, Japan, Korea, Russia
	<i>C.kweichowensis</i>	Guizhou hazel	Middle-southern China
	<i>C. yunnanensis</i>	Yunnan hazel	China
<i>B.Columnaea</i>	<i>C. colurna</i>	Turkish tree hazel	Balkans, Turkey and Georgia
	<i>C. jacquemontii</i>	Indian tree hazel	Northern India and Pakistan
	<i>C. chinensis</i>	Chinese tree hazel	Middle - southern China
	<i>C. fargesii</i>	Paperbark tree hazel	Middle southern China
<i>C.Siphonochlamys</i>	<i>C. cornuta</i>	Beaked hazel	Appalachian Mountains (USA) to Gaspè peninsula (Quebec) to central British Columbia (Canada)

	<i>C. californica</i>	California hazel	Southern British Columbia (Canada) to central California (USA)
	<i>C. sieboldiana</i>	–	Japan, Korea, northeast China, Russian far east
<i>D.Acanthochlamys</i>	<i>C. ferox</i>	Tibetan hazel	Southcentral China to Tibet, Bhutan and Nepal

*C. avellana* is the most widely distributed variety in the world and according to the statistics of The Food and Agriculture Organization of the United Nations (FAO), Turkey has the leading position in production and export of hazelnuts as well as 66% of the world's cultivation area followed by Italy (16%), United States of America (4,64%) and Azerbaijan (4,57%). Annual production of hazelnut had reached to 850,000 tons worldwide by 2018 (FAOSTAT, 2018). There is a rapid increase in the number of hazelnuts growing countries and fortification of hazelnut cultivated areas within the major producing countries.

### 1.2.2 Hazelnut cultivars from Turkey

Hazelnut commercial production expands in regions with climates moderated by large amount of rain, cool summers and mild winters. *C. avellana* are preferred to grow in warm and humid climate, with plenty of light, and have ability to adapt variety of soils. Hazelnut production extends along the Black Sea region, from the Georgian border in the east, to Istanbul in the west. Hazelnut (*Corylus avellana*) is Turkey's most valuable agricultural export, and essential source of income for many families in Black Sea Region. Although 33 provinces have hazelnut growing areas, only 16 of them are licensed for commercial hazelnut production. Most of the production (90%) is carried out in six provinces: Ordu, Giresun, Trabzon, Samsun, Sakarya and Düzce (TUIK, 2018).

More than 400 cultivars of hazelnut are described around the world. Turkey have several *Corylus avellana* cultivars, In the past these cultivars were classified based on morphological characters such as the shape of the nut and quality of the kernel, but with the usage of the molecular markers including randomly amplified polymorphicDNA (RAPD), amplified fragment length polymorphism (AFLP) and simple sequence repeat

(SSR) molecular markers are developed for the classification. 18 hazelnut cultivars are identified with RAPD, ISSR, and AFLP markers (Figure 2). Acı, Allahverdi, Cavcava, Çakıldak, Foşa, Kalinkara, Kan, Karafındık, Kargalak, Kuş, İncelkara, Mincane, Palaz, Sivri, Tömbül, Uzunmasa, Yassıbadem, Yuvarlak badem (Kafkas et al., 2009).

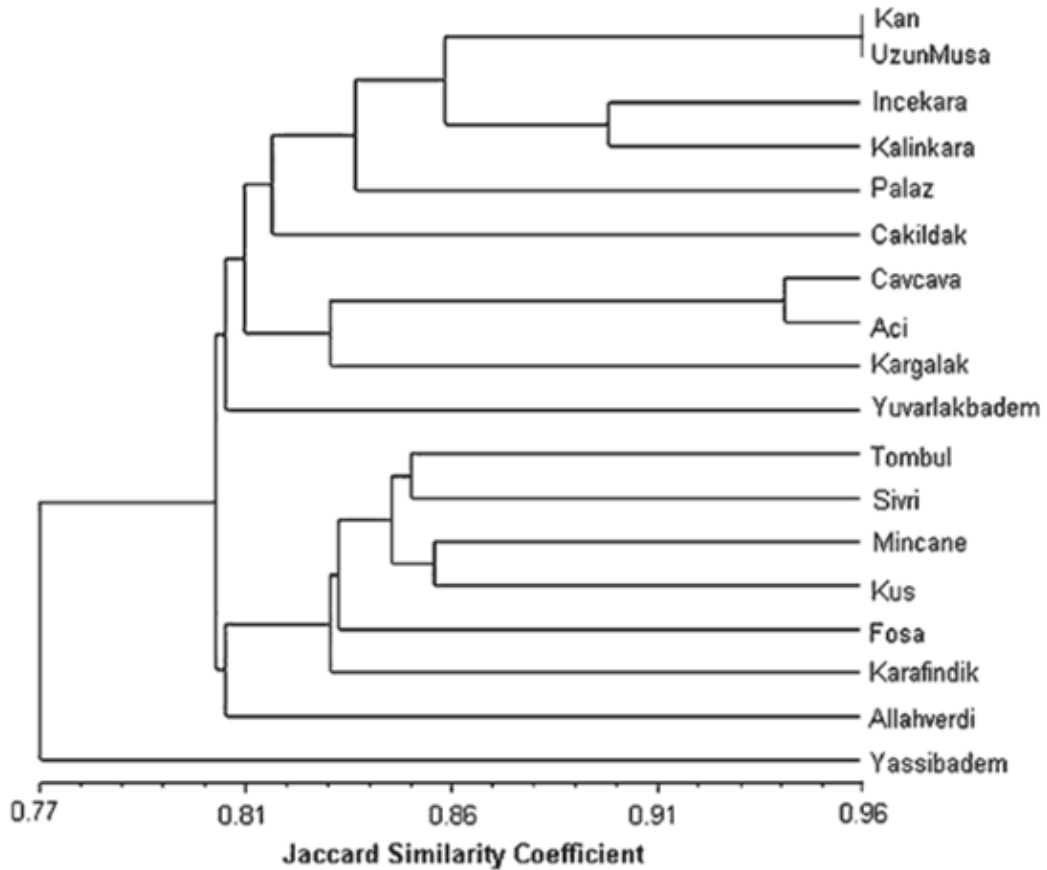


**Figure 2:** Dendrogram of 18 hazelnut cultivars (Kafkas et al., 2009).

Tömbül cultivars are most important hazelnut cultivar for Turkish economy since these cultivars have high value in international market (Figure 3). Allahverdi is created by HRI researchers through selective breeding. When Allahverdi cultivar is compared with Tömbül cultivar it has higher number of male flowers and the pollen spreading time is one week longer, empty fruit formation is quite low, the yield per area is twice more, less sensitive to arid, frost, disease and pests. Çakıldak cultivar flowers awakens much later than other hazelnut varieties, so it suffers little damage from late frosts of spring, and the yield of this variety, which can easily adapt to any climate and soil conditions, is

very high. The taste and quality of fruits that are quite large and relatively long are not good.



**Figure 3:** Hazelnut cultivars Allahverdi, Tombul and Çakıldak that breed in Turkey.

Demands to hazelnut, cause Hazelnut producers to expand their hazelnut orchards. Middle and higher elevations around Ordu renewed the orchards with Çakıldak, Tombul is used in Giresun and west of Trabzon, Foşa and Giresun Yabanisi in other parts of Trabzon. Yomra which is a synonym of Foşa is also being planted in renewals in the plains of Samsun. Orchards in the Western Black Sea region (Bartın, Zonguldak, Düzce, Sakarya, Kocaeli, Bolu) consist of mixed such as Karafındık, Mincane, Çakıldak and Foşa but mostly Tombul has been planted in renewals (Al-Khayri, J. M., Jain, S. M., & Johnson, 2019).

### 1.2.3 Hazelnut genome

*Corylus avellana* L. is a diploid with 11 chromosomes ( $2n = 2x = 22$ ), monoecious, dichogamous, wind-pollinated tree.

*Corylus sp.* genome analysis studies have been carried out to develop disease resistance or climate related adaptation. Eastern filbert blight is a fungal disease cause by *Anisogramma anomala* pathogen that generate small lesions on *Corylus americana* but causes severe cankers and branch die back on *Corylus avellana*. The growth of the cankers that slowly spread to branches, limbs, and tree trunks leading to failures in leaf growth and eventually the death of the tree, the EFB is mostly seen in United States (Johnson et al., 1996). To fight with Eastern filbert blight (EFB) disease *A. anomala*

infective behavior and reproductive system have been analyzed leading the development of fungicides and creating genetic resistant cultivars. Gasaway has a high-level resistance to EFB and it was discovered in nature free of disease symptoms. EFB resistance is controlled by a dominant allele at a single locus. EFB-resistant *C.avellana* cultivar that is created the heterozygous state with dominant allele for EFB resistance from Gasaway and enhance in commercial quality nut is named as Jefferson. A bacterial artificial chromosome (BAC) genomic library of Jefferson with an estimated 12× genome coverage was constructed to support contig assembly and map-based cloning of the EFB resistance locus is reported (Sathuvalli & Mehlenbacher, 2011) (V. Sathuvalli et al., 2017). Further 6,8Gb of hazelnut transcriptome data was assembled (Rowley et al., 2012).

A genetic linkage map of *C. avellana* L. was constructed by random amplified polymorphic DNA (RAPD) and simple sequence repeat (SSR) markers (Mehlenbacher et al., 2006). Additional polymorphic markers and microsatellite enriched libraries improve the available genome and transcriptome data (Gürcan et al., 2010)(Gürcan & Mehlenbacher, 2010)(Colburn et al., 2017). European hazelnut is defined as a diploid with 11 chromosomes ( $2n=2x=22$ ) and a genome of 378 Mbp. A draft genome is assembled by 93x coverage and have completed a denovo genome assembly, capturing 91 percent of the genome (345 Mbp). By homology-based functional annotation 34,910 protein coding loci was predicted. Polymorphism are identified between seven *C.avellana* L. cultivars and Jefferson (Rowley et al., 2018). *C. avellana* cv. Tombul genome was partially sequenced yielding 29.2% of hazelnut genome. These partially sequenced genome lead the design of novel SSR markers that are used to characterize genetic diversity between Turkish and European hazelnut varieties (Öztürk et al., 2018).

Two wild hazelnut species, *C. heterophylla* Fisch. and *C. mandshurica* (synonym to *C. sieboldiana*) transcriptome sequences are also available. *C. mandshurica* and *C. avellana* have highly differentiated genes that correlates with local adaptation of the two species. (Chen et al., 2014; Ma et al., 2013).

Finally, a reference genome of *C. avellana* cv. Tombul was developed in our group. Sequenced genome assembly consisting of 11 pseudomolecules with a total length of 370 Mb covering 97.8% of the estimated genome size *C. avellana* cv. Tombul is used for generating a de novo chromosome-scale genome assembly by applying a hybrid next-

generation sequencing strategy combining short-read, long-read and physical proximity sequencing. The study shows that the genome carries 27,316 high-confidence protein-coding genes, and over 20,000 were functionally annotated to known plant proteins. Study also focus on hazelnut allergens and Mlo (*Mildew resistance locus o*) proteins to understand the differentiate between members of these families and identify novel homologs that may be important in mildew disease and hazelnut allergy. Further this de novo chromosome-scale genome assembly will be helpful for identifying structural relationships between genes and facilitating rapid mapping of candidate genes from molecular markers for traits of interest (Lucas et al., 2019).

### **1.3 Powdery mildew disease**

*C. avellana* prefer to grow at humid climates and mild winters in nature. These climates are perfect for growth of many opportunistic fungus too. First opportunistic fungal pathogens that grow on hazelnut leaf will be discuss. Powdery mildew disease will be described, life cycle and plant infecting mechanism will be explained. Powdery mildew in hazelnut, the pathogens and identification methods will be defined.

#### **1.3.1 Corylus Fungal pathogens**

Major group of Ascomycota species use *Corylus sp.* as a host and some species use the invading fungi (hyperparasites) as a host, table 2 summarizes the fungal pathogen that infect or isolated from hazelnut leaves

*Alternaria sp.* are an opportunistic plant pathogen that cause brown-blackish necrosis on many organs of various plant species including walnut, cherry, barley and pistachio. *A. alternate*, *A. arborescens* and *A. tenuissima* are shown to infect hazelnut and causes early fruit drop at infected plant (Hong et al., 2006)(Figuli et al. 2007). *Ampelomyces sp.* is best known hyperparasite of powdery mildew pathogens and reported on over 65 species of the *Erysiphaceae*. *Ampelomyces* is a hyperparasite that infects mycelium, and harms conidial spores and ascocarps of powdery mildews agents (Altin & Gülcü, 2018;L Kiss et al., 2010). *Cladosporium sp.* also occur as a secondary invader of fungi. *C. exile*, *C. inversicolor*, *C. lycoperdinum*, *C. perangustum*, and *C. phyllactiniicola* are hyperparasite of *Phylactinia guttata* and these pathogens can be found in chasmothecia

of *Phyllactinia guttata* that infects leaves of *Corylus avellana* (Bensch et al., 2010). Hyperparasites are discussed in detail under the title of hyperparasites. *Colletotrichum sp.* cause a disease called gray necrosis on hazelnut flowers and nuts that result in early fruit drop (Belisario and Santori 2009). *C. gloeosporioides* and *C. acutatum* produce large circular lesions on leaf surface that are green-grey or dark grey with a distinct white margin that grow on hazelnuts (Mirhosseini and Taherzadeh 2007) (Sezer & Dolar, 2012). *Elsinoë coryli* is a plant pathogen that causes leaf spots and these pathogens infect various plant species including *Corylus avellana*. Pathogen infection symptoms are described as formation of cork-like necrotic tissues (Fan et al., 2017). *Gnomoniaceae* are identified by ascomata that are generally immersed, solitary and without a stroma, or aggregated with a rudimentary stroma. *Gnomoniaceae* can be detected on leaves, twigs or stems, but also in bark or wood. *Gnomonia sp.* is host on specific plants in *Betulaceae* family. *Ophiognomonia ischnostyla* also belongs to *Gnomoniaceae* genera and *Fagales* (*Betulaceae*, *Fagaceae*, *Juglandaceae*) are host to these pathogens (Sogonov et al., 2008). *Mamianiella coryli* are found in living leaves of *Corylus avellana* L, *C. californica*, *C. cornuta* and *C. americana*. The pattern of ascocarp development in *M. coryli* is like that found in *Gnomonia* species (Morgan-Jones, 1981). *Paraconiothyrium brasiliense* have been isolated from *C. avellana* (Salehi, 2019). *Phyllosticta coryli* cause leaf spot on *Corylus heterophylla*, starting as pinpoint brown spots, which enlarged and then developed into regular, dark brown lesions, 3 to 9 mm in diameter on both side of the leaf (Liu Z.H. et al. 2013). *Mycosphaerella s. str.* are proposed to be limited to asexual morphs for *Ramularia* species and remaining mycosphaerella-like species should be assign to other genera. *Ramularia vizellae* cause leaf spot on *Corylus sp.* and the symptoms of the disease are identified by small brown rectangular lesions, often surrounded by a yellow halo (Isabel et al., 2015). *Septoria sp.* is a biotrophic pathogen that cause leaf spot diseases on *Betulaceae* family. *Septoria ostryae* are located on *Corylus cornuta*, *Corylus americana*, *Septoria avellanae* are located on *Corylus avellana* L., and finally *Septoria coryli* are located on *Corylus avellana* L leaves. (Constantinescu et al., 1983). Finally, *Erysiphe corylacearum* and *Phyllactinia guttata* are two biotrophic pathogen that cause Powdery mildew disease on *Corylus species*. The disease can be identified by forming white powdery like patches and will be discussed in detail under next title.

**Table 2:** List of *Ascomycota* species that can be find on *Corylus sp.* leaves. Pathogen species, host species and GenBank accession number of known ITS sequences are recorded.

<b>Species</b>	<b>Host</b>	<b>Infected organ</b>	<b>GenBank accession ITS</b>
<i>Alternaria alternata</i>	<i>Corylus avellana</i>	leaf	KU986508.1
<i>Alternaria arborescens</i>	<i>Corylus avellana</i>	leaf	NR_135927.1
<i>Alternaria tenuissima</i>	<i>Corylus avellana</i>	leaf	AF229476.1
<i>Ampelomyces quisqualis</i> *	<i>Corylus avellana</i>	Leaf with powdery mildew infection	MH997723.1
<i>Cladosporium Exile</i> *	<i>Phyllactinia guttata</i>	Chasmothecia on leaves of <i>Corylus sp.</i>	HM148091.1
<i>Cladosporium inversicolor</i> *	<i>Phyllactinia guttata</i>	chasmothecia on leaves of <i>Corylus sp.</i>	HM148104.1
<i>Cladosporium lycoperdinum</i> *	<i>Phyllactinia guttata</i>	chasmothecia on leaves of <i>Corylus sp.</i>	HM148113.1
<i>Cladosporium macrocarpum</i> **	<i>Phyllactinia sp. on Corylus sp.</i>	chasmothecia on leaves of <i>Corylus sp.</i>	EF679373.1

<i>Cladosporium perangustum*</i>	<i>Phyllactinia guttata</i>	chasmothecia on leaves of <i>Corylus sp.</i>	HM148130.1
<i>Cladosporium phyllactiniicola*</i>	<i>Phyllactinia guttata</i>	chasmothecia on leaves of <i>Corylus sp.</i>	HM148150.1
<i>Cladosporium sphaerospermum*</i>	<i>Phyllactinia guttata on Corylus sp.</i>	chasmothecia on leaves of <i>Corylus sp.</i>	EU570254.1
<i>Cladosporium tenellum</i>	<i>Phyllactinia sp. on Corylus sp.</i>	chasmothecia on leaves of <i>Corylus sp.</i>	EF679399.1
<i>Colletotrichum acutatum</i>	<i>Corylus avellana (hazelnut)</i>	Leaf, husk and pedicel of the fruit	NR_144794.1
<i>Colletotrichum fioriniae</i>	<i>Corylus avellana (hazelnut)</i>	Leaf, husk and pedicel of the fruit	NR_111747.1
<i>Elsinoe coryli</i>	<i>Corylus avellana</i>	leaf spots	NR_148134.1
<i>Erysiphe corylacearum***</i>	<i>Corylus avellana</i>	leaf	
<i>Gnomonia amoena</i>	<i>Corylus sp.</i>	leaf	EU254769.1
<i>Gnomonia cf. Ischnostyla</i>	<i>Corylus avellana</i>	leaf	EU254895.1
<i>Gnomonia gnomon</i>	<i>Corylus avellana</i>	leaf	AY818954.1
<i>Gnomonia monodii</i>	<i>Corylus avellana</i>	leaf	EU254785.1

<i>Gnomonia neognomon</i>	<i>Corylus californica</i>	leaf	EU254786.1
<i>Gnomonia orcispora</i>	<i>Corylus californica</i>	leaf	EU254788.1
<i>Gnomonia ostryae</i>	<i>Corylus avellana</i>	leaf	EU254790.1
<i>Gnomonia pendulorum</i>	<i>Corylus californica</i>	leaf	EU254791.1
<i>Gnomonia pseudoamoena</i>	<i>Corylus avellana</i> and <i>Corylus californica</i>	leaf	EU254792.1
<i>Gnomonia skokomishica</i>	<i>Corylus californica</i>	leaf	EU254797.1
<i>Gnomonia virginiana</i>	<i>Corylus avellana</i>	leaf	EU254801.1
<i>Mamianiella coryli</i>	<i>Corylus californica</i> , <i>Corylus cornuta</i>	leaf	EU254862.1
<i>Ophiognomonia ischnostyla</i>	<i>Corylus avellana</i>	leaf	EU254890.1
<i>Paraconiothyrium brasiliense</i>	<i>Corylus avellana</i>	leaf	MG062777.1
<i>Phyllosticta coryli</i>	<i>Corylus heterophylla</i> and <i>Corylus avellana</i>	leaf	KC196068.1
<i>Phyllactinia guttata</i> ***	<i>Corylus avellana</i>	leaf	
<i>Ramularia vizellae</i>	<i>Corylus sp.</i>	leaf	KP894311.1

<i>Septoria</i>	<i>Corylus cornuta</i>	leaf	DQ019396.1
<i>ostryae</i>			

\* Hyperparasite of powdery mildews

\*\* Teleomorph: *Davidiella macrocarpa*

\*\*\*Powdery mildew

### 1.3.2 Powdery Mildew Disease

Powdery mildews are an agronomically important group of obligate biotrophic (can only grow and reproduce on living hosts) fungal plant pathogens distributed nearly worldwide, with the exception of the Antarctic region, and currently comprises around 900 species belonging to 18 genera , which infect a wide range of dicotyledonous and monocotyledonous host plants and cause serious diseases on numerous economically important cultivated plants, such as cereals, fruit trees and ornamental plants (Braun and Cook 2012). The pathogen is common for infecting adaxial of the leaves, but it can also attack the underside of the leaves or above-ground parts, including spikes, leaves and stems of a plant. Powdery mildews rarely kill their hosts but utilize their nutrients, reduce photosynthesis, increase respiration and transpiration, impair growth, and reduce yields, sometimes by as much as 20 to 40% (G. N. AGRIOS, 2005).

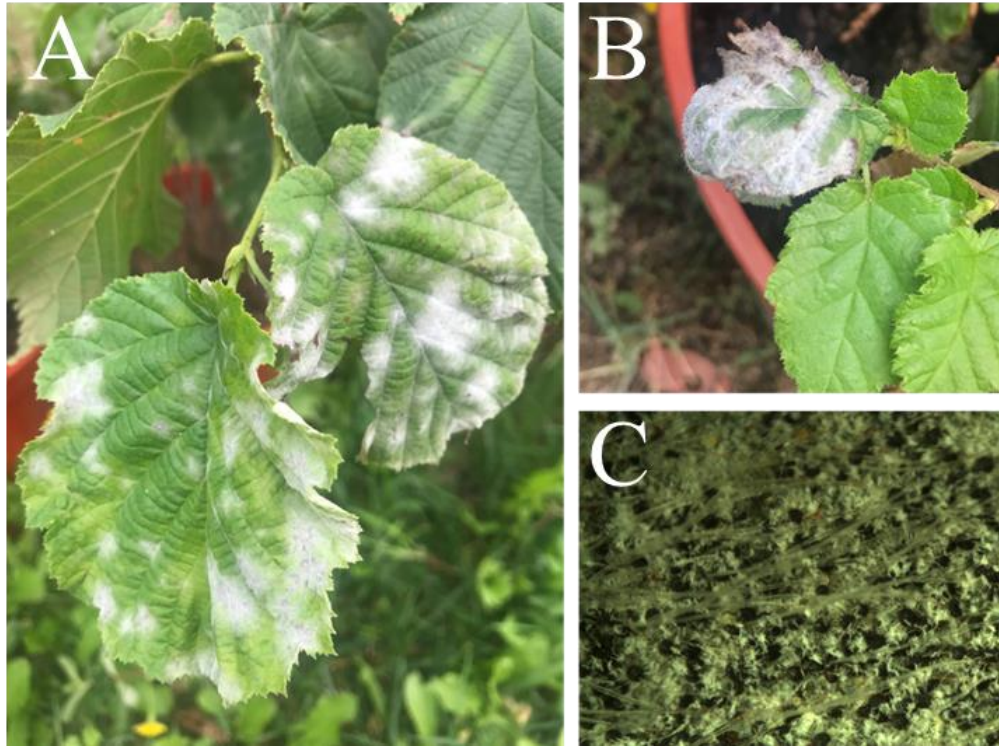


**Figure 4:** Powdery mildew infection. A) Two infected *C. avellana* cv. Tombul leaf. Characteristic structure of Powdery mildew white powdery patches. B) Healthy and powdery mildew infected leaf samples of *C. avellana* cv. Çakıldak. C) Closer look at the white powdery patches, chasmothecia as black circles.

The genus *Erysiphe* was first introduced for powdery mildew by their morphological characteristic as forming white powdery patches or spots appear as white to greyish color (Figure 4 A-B). *Erysiphe* is the largest genus in the *Erysiphaceae* family containing 450 of the 873 species, more than 50% of all species from the family. *Erysiphe* sp. is characterized by chasmothecia having multiple asci and mycelioid appendages that are mostly curved (Figure 4 C) (Braun & Cook 2012).

The genus *Phyllactinia* were reported to occur on about 700 species covering 69 plant families, and it is distributed worldwide, especially in the temperate regions of the Northern Hemisphere such as East Asia, Europe, and North America. This genus is mostly known to infect on broad range of hard-shelled fruit bearing woody plants (Susumu Takamatsu et al., 2008). *Phyllactinia* genus having unique morphological

characteristics of chasmothecia, which have two kinds of appendages. First type is characterized by a rigid, acicular appendage with a bulbous swelling at the base, arising from the equatorial area of the ascomata. Second type is known as penicillate cell, arises from the apical part of the ascomata and has apically digitated branches (Braun et al. 2002).

Conidia (asexual spores) are produced on plant surfaces during the growing season. Conidia are developed either independently or in chains on specialized hyphae called conidiophores. Conidiophores arise from the hyphae that penetrates the plant cell wall and emerge through leaf stomata and arrive to mesophyll cells. Then a feeding structure called haustorium is formed inside the host cell. The haustorium is surrounded by a modified membrane called extrahaustorial membrane which separates from the host cell cytoplasm. Haustoria plays an essential role in plant-fungus recognition and has a role in uptake of the nutrients into the fungus pathogen, also secretes effector proteins into host cell to develop a successful biotrophic relation between the pathogen and host cell (Qin et al., 2020). At the end of the growing season or when nutritional conditions become unfavorable, powdery mildew fungi produce sexual spores, ascospores, in a sac-like ascus enclosed in a fruiting body called a chasmothecium. The chasmothecium is generally spherical with no natural opening, but when a crack develops in the wall of the fruiting body the ascospores are released. On the surface of the chasmothecia sometimes a variety of appendages may occur. These appendages are most likely helping with attaching to the fruiting bodies of the host plant, particularly to the bark of woody plants, where they overwinter (Mori et al. 2000; Braun and Cook 2012) (Figure 5).

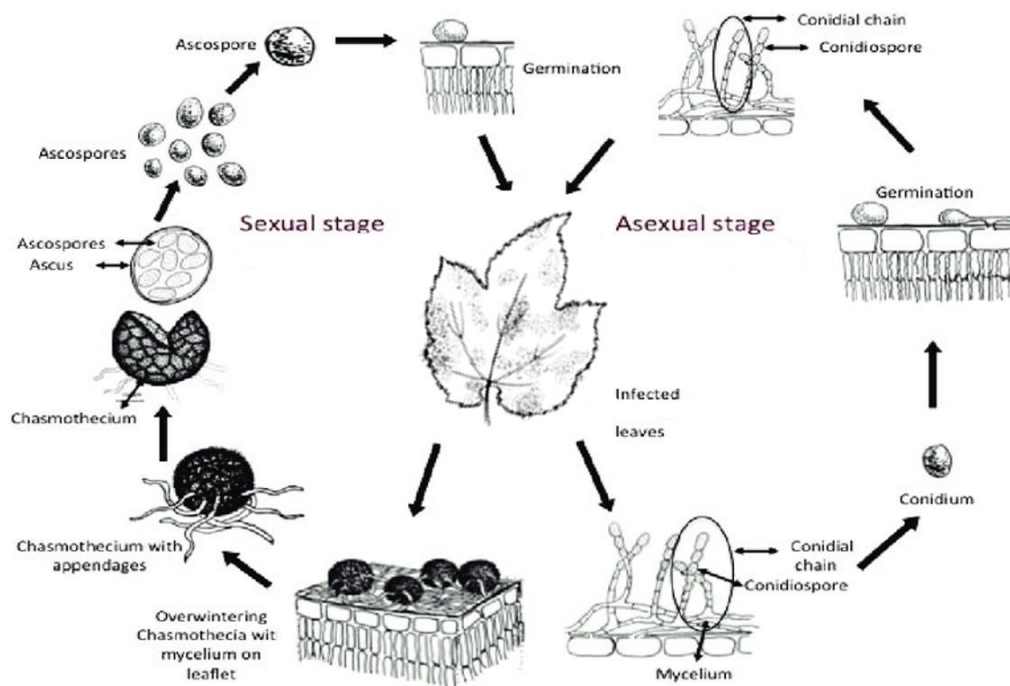


**Figure 5:** Schematic view of powdery mildew life cycle. Spores on the leaf surface form hyphae that covers and expand through surface of leaf. Haustorium is formed by conidiophores arise from the hyphae. Above the leaf conidial chain is form from the conidiospore. Conidia play a role in asexual reproduction of the pathogen. Fruiting body called a chasmothecium rise from hypha carrying sac-like Ascus. Ascospores are released from Ascus (Jin et al., 2013).

### 1.3.3 Powdery mildew Disease on *Corylus avellana*

*Erysiphe corylacearum* and *Phyllactinia guttata* are two pathogens that infect *Corylus avellana* L. In 2005 *Phyllactinia guttata* have been reported on hazelnuts in Washington, USA and there were previous reports of *P. guttata* occurring on *C. avellana* in Europe, Iran, and Canada (Hartney et al., 2005). The observations conclude that powdery mildew cause no significant damage to hazelnut scrubs and unlikely to threaten the long-term survival of infected scrubs.

For the commercial hazelnut orchards, the disease is usually left untreated because it is regarded as not sufficiently serious since it has little or no direct impact on nut development; fungal growth is detectable only on the underside of leaves late in the season. Between 2014 and 2015 *C. avellana* L. cultivation areas throughout the eastern

Black Sea region started to develop more critical effects on the hazelnut orchards due to Powdery Mildew disease. By 2016 all 16 provinces that are licensed for hazelnut cultivation were showing more destructive powdery mildew disease. This new destructive powdery mildew agent was analyzed for both morphological characteristics of asexual and sexual states and analyses of DNA sequences of the internal transcribed spacer (ITS) and 28S regions of the ribosomal DNA and determined to be *Erysiphe corylacearum* rather than *P. guttata*. *Erysiphe corylacearum* was previously observed in Asia and North America to affect various *Corylus* species (Sezer et al., 2017a). By 2017 in Iran (Arzanlou et al., 2018), 2018 in Azerbaijan (Abasova et al., 2018), and 2019 in Ukraine (Heluta et al., 2019), Switzerland and central Europe (Beenken et al., 2020) have reported new powdery mildew pathogen as *Erysiphe corlacearum*.

*Erysiphe corylacearum* and *Phylactinia guttata* can be differentiate by morphological characteristics and genetical analysis of Internal transcribed spacer (ITS) region.

#### 1.3.4 Powdery Mildew morphological identification

Powdery mildew disease in *C. avellana* species are caused by two pathogens; *Phyllactinia guttata* and *Erysiphe corylacearum*. Two pathogens morphological characteristics are as follow;

*Erysiphe corylacearum* morphological descriptions are as;

- Mycelium amphigenous, branched, forming dense, irregular patches, persistent,
- Hyphae 3–7  $\mu\text{m}$  wide, thin-walled and smooth, septate, branched, hyphal appressoria lobed, solitary,
- Conidia formed singly, ellipsoid-ovoid to doliiform, (25–)27–38  $\times$  14–21  $\mu\text{m}$ , length/width ratio 1.4–1.9(–2) and produced singly on the conidiophores,
- Chasmothecia scattered to gregarious, 81–101  $\mu\text{m}$  diam., appendages 5–11, equatorial, straight, 4–5 times dichotomously branched, tips recurved, 73–110  $\times$  6–11  $\mu\text{m}$ , walls rough, pigmented and enlarged towards the base, but thin above, aseptate, or single septum at the base,
- Asci 3–5, obovoid to broadly ellipsoid, saccate, 37–59  $\times$  24–40  $\mu\text{m}$  and sessile, 4–7-spored,
- Ascospores ellipsoid-ovoid, hyaline, 13–18  $\times$  8–11  $\mu\text{m}$ ,

- Appressoria solitary, lobed, 2–4  $\mu\text{m}$  in diam,
- Conidiophores arising from the adaxial surface of the mother cells, centrally or slightly lateral, 55–80  $\times$  5–10  $\mu\text{m}$ ,
- Foot cells erect, cylindrical to flexuous-sinuuous, followed by 1–2 shorter cells, 24–60  $\times$  5–9  $\mu\text{m}$ ,
- Appendages 6–15 per chasmothecium, equatorial, stiff, straight to curved, 0.75 to 1.34 times as long as the chasmothecial diam., 55–86  $\times$  45–7  $\mu\text{m}$ , stalk aseptate, wall smooth to rough, hyaline, thin in the upper half, thick towards the base, apex 3–5 times closely and regularly branched, tips recurved,
- Peridial cells polygonal to rounded, 13.3  $\pm$  0.3  $\mu\text{m}$  diam.

*Phylactinia guttata* morphological descriptions are as;

- Mycelium mostly hypophyllous, effuse or formed patches with color white to greyish
- Hyphae straight, branched, septate 2–6  $\mu\text{m}$
- Conidiophores arising from hyphae, straight, filiform
- Chasmothecia are globose, convex on the ventral side, and nearly plane on the dorsal side; each with a gelatinous mass of penicillate cells and acicular appendages, measurements are 185–215  $\mu\text{m}$  in diameter by 100–145  $\mu\text{m}$  high; appendage length was 360–545  $\mu\text{m}$ ; penicillate cell bases are 29–48  $\times$  7–20  $\mu\text{m}$
- Asci are short-stipitate, clavate to nearly spindle shaped, 70–90  $\times$  35–45  $\mu\text{m}$ , and contained two ascospores,
- Ascospores are ellipsoid-ovoid, yellowish-orange, highly guttulate, and 32–42  $\times$  19.5–24  $\mu\text{m}$ ,
- Appressoria unlobed or occasionally branched to moderately lobed, hooked, elongated or nipple shaped, and occur singly or frequently in opposite pairs

Under the light microscope these two pathogens can be differentiated by using number of asci/fruitlet body, ascocarp diameter, and form of appendages on chasmothecia. *P. guttata* ascocarps are often situated on the *C. avellana* leaf surface with appendages pointing away from the epidermis and the morphology of the appendages can be described as bulbous equatorial at the starting point and needle like at the tips. However, *E. corylacearum* chasmothecia appendages get branched and curved toward the tips (Figure

6). Unfortunately, these morphological identification methods are useful if chasmothecia is visual meaning late stages of the infection, so a genetic identification can detect the disease at the early stages.

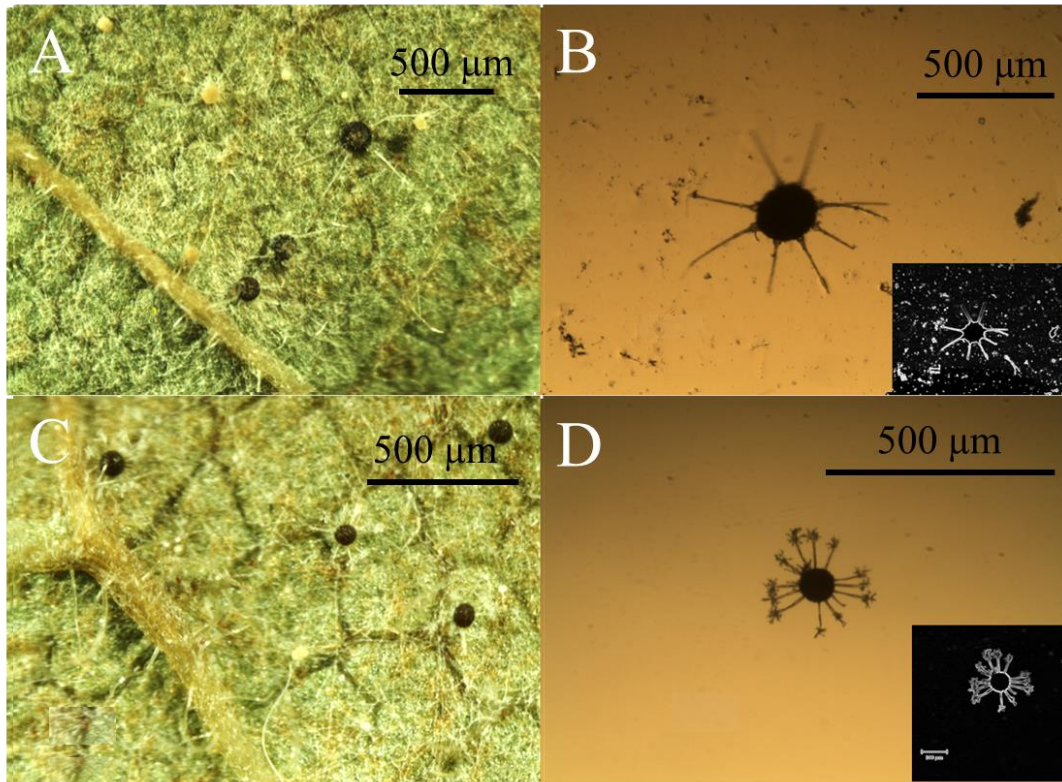


**Figure 6:** *P. guttata* and *E. corylacearum* morphology under light microscope **A)** *C. avellana* L. leaf with *P. guttata* infection, **B)** *P. guttata* chasmothecia, appendages bulbous at the starting point and needle like at the tips. Black and white threshold image of *P. guttata* chasmothecia is given at bottom right. **C)** *C. avellana* L. leaf with *E. corylacearum* infection. **D)** *E. corylacearum* chasmothecia, appendages are branched and curved at the tips. Black and white threshold image of *E. corylacearum* chasmothecia is given at bottom right.

### 1.3.5 Powdery mildew Genetic identification

#### 1.3.5.1 DNA Barcoding

DNA barcoding is a method used for species identification from a standardized short section sequences of specific gene or genes. Previously identified primers are used for

generating the sequence of the sample to be validated by available online barcode reference library of possible taxonomic groups. Eukaryotic rRNA gene consists of 18S, 5.8S, 28S and two internal transcribed region that transcribed by *RNA polymerase I* (Figure 7), after posttranscriptional processes the two internal transcribed spacers are removed. These two spacers between small subunit rRNA, including the 5.8S gene, are usually referred as the Internal transcribed spacer (ITS) region. By now more than 172,000 full-length fungal ITS sequences are accessible in GenBank, representing nearly 15,500 species and 2,500 genera (Begerow et al., 2010; Schoch et al., 2012).

Classification and identification of the *Erysiphales* was previously based on the morphology of the teleomorph (the cleistothecium) and anamorph stages of the fungi and their host range (Braun 1987). However, some species were difficult to identify based only on anamorph morphology and another problem is some species whose teleomorph stages have not been found or are rarely found so the lack of information usually let the identification of species until the genus level. The genera *Golovinomyces* and *Neoerysiphe* were treated as distinct from *Erysiphe s.st.* also, similarity between *Erysiphe s.str.* and the genera *Uncinula* and *Microsphaera* might cause misidentification and misclassification of the specimen. Later a technique is developed by amplification of ribosomal DNA (rDNA) and the direct sequencing of the PCR product help for phylogenetic identification of powdery mildew fungi. Universal ITS primers were designed (White et al. 1990) by DNA extracted from scrapings of dried anamorphic material, unfortunately this resulted in the amplification of other species such as plant, fungi, insect or even nematode. Since the powdery mildews are obligate parasites of plants that are unculturable on artificial media, extracted DNAs are usually collected from herbarium specimens or directly from fresh materials that are collected in the field. This results in frequent contamination of DNA by other fungi, plants, insects and nematodes that were present on the leaf or around the powdery mildew infection, and eventually cause to failure of analysis. However nested PCR designed provide enough stability to work on a wide range of powdery mildews and provide the elimination of other kingdoms from contaminating the specimen DNA by PCR (Hirata and Takamatsu 1996) (S. Takamatsu and Kano, 2001). Several adjustments have been made to the method that helped the use of both anamorph and teleomorph material and several primers have been designed for correct classification and identification of powdery mildew agents (Cunnington et al. 2003; Mori et al. 2000). Researchers can select the primers through the

location of the primers on the ITS region (Figure 7. Primers can be listed by the amplified region as 18S, 5.8S, 28S, ITS1 and ITS2, then select the forward and reverse primers (Table 3).

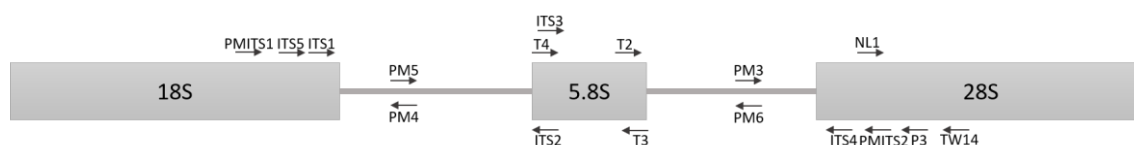


**Figure 7:** ITS region of fungi kingdom and universal ITS primers. 18S, 5.8S, and 28S rRNA genes are shown by grey rectangles and the two internal transcribed spacers are shown by grey lines, position of universal primers was labeled on ITS region. Forward primers are labelled at the top of the figure and Reverse primers are labelled at the bottom of the figure.

**Table 3:** List of universal ITS primer for fungi and powdery mildew agents. Primers are designed from 18S, 5.8S, 28S and two internal transcribed regions of ITS. Amplified region, primer name, direction of the primer (F: Forward, R: Reverse), primer sequences from 5' to 3' and the references are labelled.

Amplified Region	Primer name	Direction	Primer sequence	Reference
18S	ITS1	F	5'-TCCGTAGGTGAACCTGCGG-3'	White et al. 1990
	ITS5	F	5'-GGAAGTAAAAGTCGTAACAAGG-3'	
5.8S	ITS2	R	5'-GCTGCGTTCTTCATCGATGC-3'	
	ITS3	F	5'-GCATCGATGAAGAACGCAGC-3'	
28S	ITS4	R	5'-TCCTCCGCTTATTGATATGC-3'	
5.8S	T2	F	5'-GGGCATGCCTGTTCGAGCGT-3'	
	T3	R	5'-ACGCTCGAACAGGCATGCCC-3'	

	T4	F	5'-TCAACAACGGATCTCTTGGC-3'	Hirata 1996
18S	PMITS1	F	5'-TCGGACTGGCCAGGGAGA-3'	Cunnington et al. 2003
28S	PMITS2	R	5'-TCACTCGCCGTTACTGAGGT-3'	
ITS2	PM3	F	5'-GKGCTYTMCGCGTAGT-3	Takamatsu and Kano 2001
	PM6	R	5'-GYC RCYCTGTCGCGAG-3'	
ITS1	PM4	R	5',CCGGCCCCGCCAAAGCAAC-3'	
	PM5	F	5'-TTGCTTTGGCGGGCCGGG-3'	
18S	P3	R	5'-TTTTGTTGGTTTCTAGGACC-3'	Mori et al. 2000
	P5	R	5'-AACTTAAAGAAATTGACGGAA-3'	
28S	NL1	F	5'-AGTAACGGCGAGTGAAGCGG-3'	
	NL3	F	5'-AGACCGATAGCGAACAAGTA-3	
	NLP2	R	5'-GGTCCCAACAGCTATGCTCT-3'	
ITS2	PM3	F	5'-GKGCTYTMCGCGTAGT-3'	
28S	TW14	R	5'- GCTATCCTGAGGGAAACTTC-3'	

### 1.3.5.2 Loop Mediated Isothermal Amplification (LAMP)

In 2000 Notomi et al. developed a novel method called loop mediated isothermal amplification (LAMP) that can amplify few copies of DNA to  $10^9$  in less than an hour under isothermal conditions with great specificity (Notomi et al., 2000). Since now LAMP has undergone many adaptations and has been put into practice for the detection of pathogens in samples ranging from animals, plants, and humans.

LAMP is an isothermal nucleic acid amplification method that generally employs a set of four or six different primers, which specifically bind to complementary sequences on the molecular target. Primer sets for the LAMP assay include the forward outer primer (F3), the backward outer primer (B3), the forward inner primer (FIP), the backward inner

primer (BIP), and two other primers the forward loop primer (FLP) and the backward loop primer (BLP) designed to accelerate the amplification (Li et al., 2016).

During the initial stages of the LAMP reaction, the inner primers (FIP or BIP) anneal by Watson–Crick complementarity to regions F2c or B2c within the target region. The outer primers (F3 or B3) then hybridizes to region F3c or B3c on the target and initiates the formation of self-hybridizing loop structures by the invasion of strands of DNA sequences already extended from the inner primers, including FIP and BIP. This results in the formation of a dumbbell-shaped DNA, and the same dumbbell structure then becomes a seed for exponential amplification. The addition of loop primers (LF and LB) can accelerate the process for exponential amplification of the target sequence. The final products obtained are a mixture of cauliflower-like structures with multiple loops and concatemers of the DNA with various stem lengths (Figure 8).

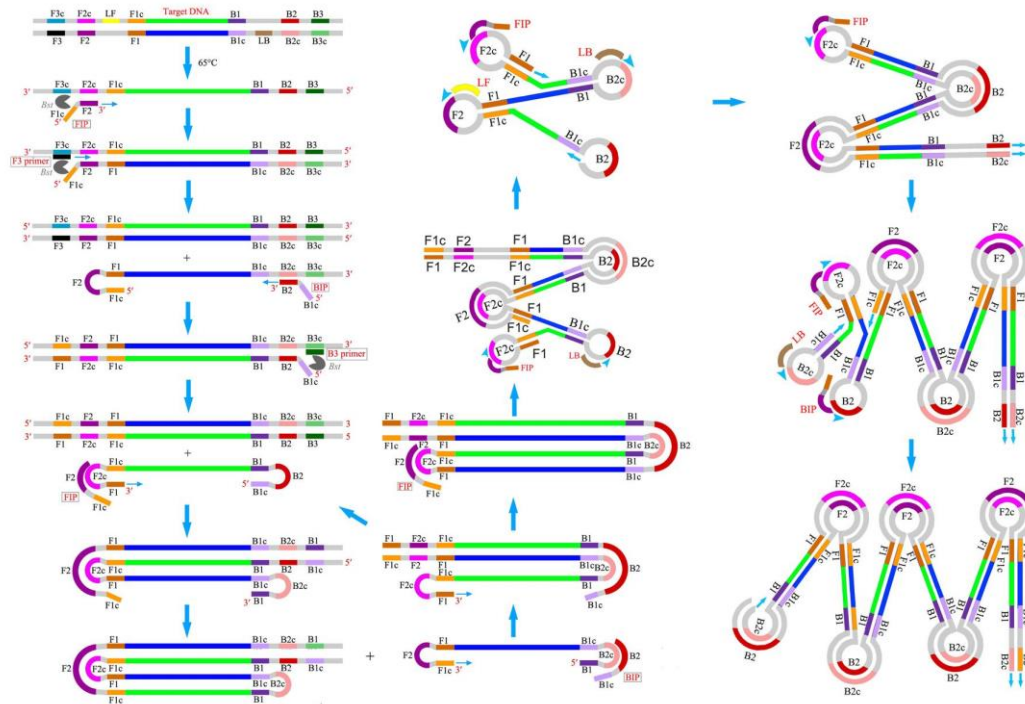


**Figure 8:** LAMP assay amplification creation and cauliflower structure formation (Li et al., 2016).

LAMP assay can be performed with simple and readily available incubation sources like a water bath or heating block for isothermal heating at a single-temperature incubation. The amplified products can be detected by naked eye (by color change), or

with real-time measurement and high-throughput instruments like UV light irradiation, real-time fluorescence, gel electrophoresis, smartphone camera, and dsDNA binding dyes (da Silva Zatti et al., 2020).

## **1.4 Powdery mildew disease intervention**

### **1.4.1 Fungicide**

Fungicides are widely used in developed agricultural systems to control fungal disease and safeguard crop yield and quality of harvest. Currently there are several fungicides available to control powdery mildew that provides good disease control at very low dose rates, such as benzimidazoles, 2-amino-pyrimidines, quinone outside inhibitors (QoIs), and demethylation inhibitors (DMIs) (De Miccolis Angelini, R. M. et al. 2015). These fungicides disrupt cellular processes and bind to specific protein targets. Methyl benzimidazoles (MBCs) affect cytoskeleton by targeting  $\beta$ -tubulin, demethylation inhibitors (DMIs) targets an enzyme Sterol 14 $\alpha$ -demethylase (CYP51) that mediate membrane permeability for fungi, Quinone outside inhibitors (QoIs) and Succinate dehydrogenase inhibitors (SDHIs) both affect respiration by targeting mitochondrial cytochrome b and succinate dehydrogenase respectively. Fungicide application cause majority of pathogen population to detached from the infected area or inhibit the completion of their life cycle but the remaining pathogens result in strong selection for any resistant individuals and create fungicide resistance. It is reported that powdery mildew resistance to these fungicides appears within 2 to 7 years after a launch (Lucas et al., 2015).

Quinone outside inhibitors (QoIs) inhibit mitochondrial respiration by binding to the Qo site (the outer, quinone oxidizing pocket) of the cytochrome bc1 enzyme complex, result in the blocking of electron transfer in the respiration pathway and lead to an energy deficiency due to a lack of ATP (Becker et al., 1981). In 1996 Quinone outside inhibitors (QoIs) were introduced to field and started to be used commercially, but shortly after resistant isolates were discovered. Resistance to the fungicide is caused by a point mutation in the mitochondrial cytochrome b (cyt b) gene leading to an amino acid change from glycine to alanine at position 143 (G143A) (Gisi et al., 2002). Studies about the powdery mildew resistant show that different species show different levels of resistance to the fungicide, but it has been shown that QoI target cytochrome b protein is encoded

by mitochondrial DNA and there is a higher frequency of point mutation occurring than the nuclear DNA. Ultimately the usage of QoIs should be removed, or temporarily cast away from the management strategies against cucurbit powdery mildew (Fernández-Ortuño et al., 2006; Miles et al., 2012; Mosquera et al., 2019).

By 1960s Methyl benzimidazoles (MBCs) are introduced to control many plant diseases such as g gray mold, leaf blight, leaf scorch, leaf spot, and powdery mildew. Methyl benzimidazoles (MBCs) target cytoskeleton by binding to  $\beta$ -tubulin that inhibit the production of microtubules. MBC resistance occurs due to a point mutation in the gene encoding  $\beta$ -tubulin by several positions: glutamic acid to alanine at position 198 (E198A), valine or glycine at position 198 (V198G) and phenylalanine with tyrosine at position 200 (F200Y) (Vielba-Fernández et al., 2019; Vela-Corcía et al., 2018).

Demethylation inhibitors (DMIs) are used as a control of fungal pathogens of humans, animals and plants. DMIs are the largest member of the group of sterol biosynthesis inhibitors, sterol biosynthesis is very important for fungal cell membranes for regulating their stability and permeability. DMI fungicides interfere with the fungal sterol biosynthesis pathway. DMI resistance occurs by a variety of mechanisms; by survival of mutated cells with abnormal C14-methyl sterols in their plasma membranes, target-site modifications in the C14-demethylase (CYP51) gene or structure change in C14-demethylase, overexpression of the target gene during ergosterol formation (Tucker et al., 2020; Pirondi et al., 2014; Délye et al., 1997).

Succinate dehydrogenase inhibitors (SDHIs) inhibit the activity of the enzyme succinate dehydrogenase (SDH), also known as succinate ubiquinone reductase or complex II in the mitochondrial electron transport chain, which is composed of four nucleus encoded subunit proteins (SdhA, SdhB, SdhC and SdhD). SDHI fungicides target the ubiquinone-binding pocket of the enzyme and block the ubiquinone binding site of the enzyme. Fungicide resistance is created by the mutations within SdhB, SdhC and SdhD subunits that lead to amino acid substitutions (Cherrad et al., 2018; Yan et al., 2019; J. A. Lucas et al., 2015).

The cost and difficulty of discovery and registration of new fungicides combined with the public attitude and environmental concerns towards the use of pesticides, as well as the development of powdery mildew strains resistant to different fungicides have reduced the appeal of chemicals. Moreover, in some countries a number of fungicides effective

against powdery mildews are no longer registered for greenhouse production, due to restrictions in pesticide usage (Lucas et al., 2015).

#### 1.4.2 Fungal Hyperparasites

The importance of developing a biological control mechanism is essential since the usage of chemicals for plant disease control raises concerns about the human health, environment and emergence of fungicide resistance. One of the biological control mechanisms of powdery mildew can be achieved by hyperparasite fungi. These hyperparasites are mostly well-known natural antagonists of powdery mildews. *Ampelomyces spp*, *Tilletiopsis spp*, *Cephalosporium spp*, *Cladosporium spp* and *Trichothecium* were frequently isolated from plants infected with powdery mildew worldwide (Levente Kiss, 2003). *Ampelomyces spp* is one of the mostly studied hyperparasite and turned into a product. The degree of development of these hyperparasites depends on the species of powdery mildew fungus, that of the plant host, and environmental conditions.

Fungi of the genus *Ampelomyces* are naturally occurring well known hyperparasite of powdery mildew that infect more than 65 species (Levente Kiss, 1998). *Ampelomyces* can exist both at anamorphic and teleomorph stages of powdery mildew agents by infecting hyphae, conidiophores, conidia, and cleistothecia. *Ampelomyces* have an important role in reducing the development and distribution of powdery mildew pathogens. Infected colonies of powdery mildew are less powdery due to reduced or curtailed production of conidia. *Ampelomyces* have been recorded to reduce sporulation and production of cleistothecia by infecting at conidium stage; infected powdery mildew agent usually does not form cleistothecia, and if cleistothecia form asci are not grow in them (Angeli et al., 2009). *Ampelomyces* overwinters in the form of conidia and pycnidia (asexual fruiting body) in cleistothecia of the fungal host. Conidia of *Ampelomyces* are dispersed by wind, raindrops and attached host conidia in the course of the growing season after overwintering. *Ampelomyces* hyperparasites, are observed to lessen their development by the second half of July and in August. the increase of humidity at the end of August and beginning of September, infection of the majority of species of powdery mildew fungi with *Ampelomyces* intensifies and remains steady until the end of the growing season (Rankovic, 1997; Levente Kiss, 2003). *Ampelomyces spp*. are successful candidate by the

positive results on the tested crops and not being hazard for human health. One of *Ampelomyces* strain has been formulated, registered and commercialized in some countries by Ecogen, Inc. (Langhorne, PA, USA) as a product under the trade name AQ10TM Biofungicide (Hofstein et al., 1996; Arena et al., 2017). *Lasiodiplodia theobromae* the asexual state of *Botryosphaeria rhodiana* has been reported as pathogenic to the powdery mildew agents but further investigation should be done to use for biocontrol agent (Sreerama Kumar & Singh, 2009). *Acremonium alternatum* is another mycoparasitic fungi to be used in the biocontrol of cucurbit powdery mildew (*Sphaerotheca fusca*) in melon greenhouses. *Acremonium alternatum* shown to control the disease to some extent and improved considerably the photosynthetic status of infected leaves (Romero et al., 2003). *Lecanicillium lecanii* is another hyperparasite to reduce the powdery mildew disease by suppressing the growth and spore production of the causal agent of cucumber powdery mildew. and help with maintaining the integrity of the photosynthetic apparatus almost intact for infected melon leaves (Romero et al., 2003; Goettel et al., 2008).

Disease control with hyperparasites are still a controversial topic, for crops especially grown in green houses development of non-chemical control method is crucial, but in the nature the effect of hyperparasites are still needed to prove the efficiency. Some experiments achieved control over the powdery mildew disease by using conidial suspensions other trials showed that the biocontrol was ineffective. In order to maintain control with biocontrol agent hyperparasites a certain level of disease should be tolerated, as only an already established infection can be attacked by hyperparasite. Also, the growth, sporulation and spread of their fungal hosts must be slower than hyperparasite thus they can only follow the spread of the disease, reducing its severity and its damaging effects on the infected plants. Most of the hyperparasite are not observed until late in the growing season on many crops. Thus, powdery mildew epidemics usually reach damaging levels before their growth and sporulation are arrested by hyperparasite. Since the early dispersal and establishment of the mycoparasite onto the first formed mildew colonies is the most important factor in the degree of suppression of powdery mildew on leaves and fruit, application must be targeted to ensure earlier infection of the powdery mildew pathogens. Hyperparasites should be spread to infected plants and repeated several times during the season to ensure a high level of control (L Kiss et al., 2004).

## 1.5 Issue to Address

Powdery mildew pathogen anamorph and teleomorph morphology is identified for multiple powdery mildew species. Infecting fungal pathogen identification are done by morphological analysis, followed by genetic validation. Internal transcribed spacer (ITS) region are used for genetic validation of fungal pathogens. Previously defined universal ITS primers are used for Polymerase chain reaction (PCR) for creating amplicons which are sequenced and blast with known fungal ITS sequences to identify the infecting pathogen. More than 172,000 full-length fungal ITS sequences are accessible in GenBank.

Several disadvantages are countable for genetic validation by PCR with universal ITS primers. Firstly, Universal ITS primers are designed to detect fungal pathogen rather than a specific species, so amplified ITS regions can be target pathogen, an opportunistic fungal pathogen, hyperparasite of target pathogen or even an unstudied fungal pathogen. Sequencing of amplified ITS region is another issue since not all research centers and universities own sequencing machines these institutions are dependent of sequencing companies which raise another issue of time expansion and extra cost. Early detection of powdery mildew pathogen is crucial for isolating infected hazelnut scrubs and developing a disease management strategy.

An advance identification method should be developed. That is specific for powdery mildew pathogen especially *E. corylacearum* since it is more destructive and harms the harvest most. Also, the developed method should be cost-effective, sensitive, fast, simple and adaptable for direct analyses applied on the field or orchards. Finally, a limit of detection should be described for early diagnosis of *E. corylacearum* that helps to identify powdery mildew infection levels.

Powdery mildew resistant genes especially MLO family are identified in several species however there are no studies for hazelnut powdery mildew resistant genes.

## 1.6 Proposed Approach

*Corylus avellana* powdery mildew infection are firstly done with morphological analysis which must be validated with genetic analysis. In this thesis an enhanced methods have been developed for genetic identifications. Destructive powdery mildew

agent *E. corylacearum* specific primers are designed for fungal pathogen identification. Eliminating steps of sequencing and blast analysis that are needed for universal ITS primers. *E. corylacearum* specific primer design shorten the time needed for pathogen identification and lower the cost. *E. corylacearum* primers are also adaptable for qPCR analysis to calculate copy number for determining the infection level by limit of detection. *E. corylacearum* specific 28S LAMP primers are also develop that are adaptable for colorimetric detection of pathogen identification. Lastly *P. guttata* specific primers are also develop for determining less destructive powdery mildew agent.

*Corylus avellana* cv. Tombul genome is finally sequenced by our group. The genome carries 27,316 high-confidence protein-coding genes, and over 20,000 were functionally annotated to known plant proteins Powdery mildew resistant gene family MLO is identified and consist of five genes.

## **2.MATERIALS AND METHODS:**

### **2.1 Orchards selection and weather station locations**

Locations of orchards from which hazelnut leaf samples were collected are portrayed in figure 9a whereas available weather stations close to these orchards are portrayed in figures 9b, 9c, and 9d respectively for Düzce, Sakarya, Ordu and Giresun regions. Details about the orchard locations is given in detail in Appendix A.

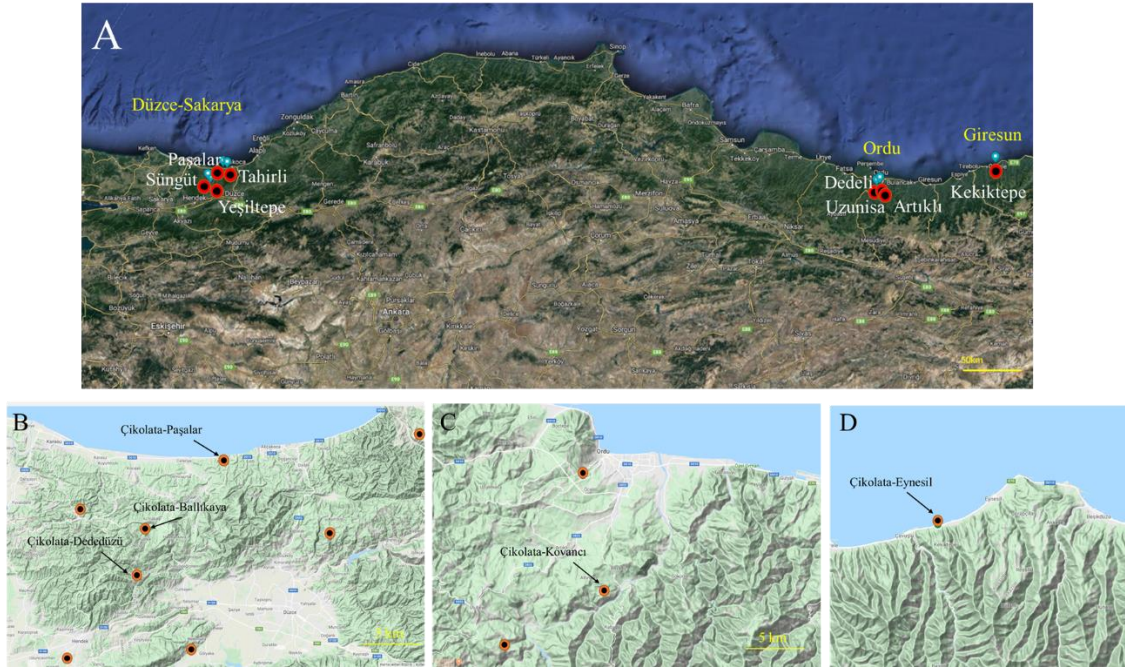


**Figure 9:** Locations of A) Hazelnut orchards and weather stations in B) Düzce-Sakarya C) Ordu D) Giresun regions

Selected weather stations record hourly measurement of air pressure (hPa), temperature (°C), highest and lowest temperature (°C), humidity (%), dew point temperature (°C), wind speed (km/h), wind run (km), High wind speed (km/h), wind chill (°C), Heat index (°C), THW index (°C), THSW index (°C), rain (mm), rain rate (mm/h), solar radiation (W/m<sup>2</sup>), solar energy (Ly), high solar radiation (W/m<sup>2</sup>), ET (mm), heating degree days and cooling degree days. These recorded data are accessible from website (<https://www.weatherlink.com/>).

## 2.2 Pathogen Diagnosis Algorithm

Aim of experimentation throughout the thesis is to classify collected samples as healthy, infected by *E. corylacearum* or infected by other pathogens. An experimental algorithm depicted in figure 11 is followed.

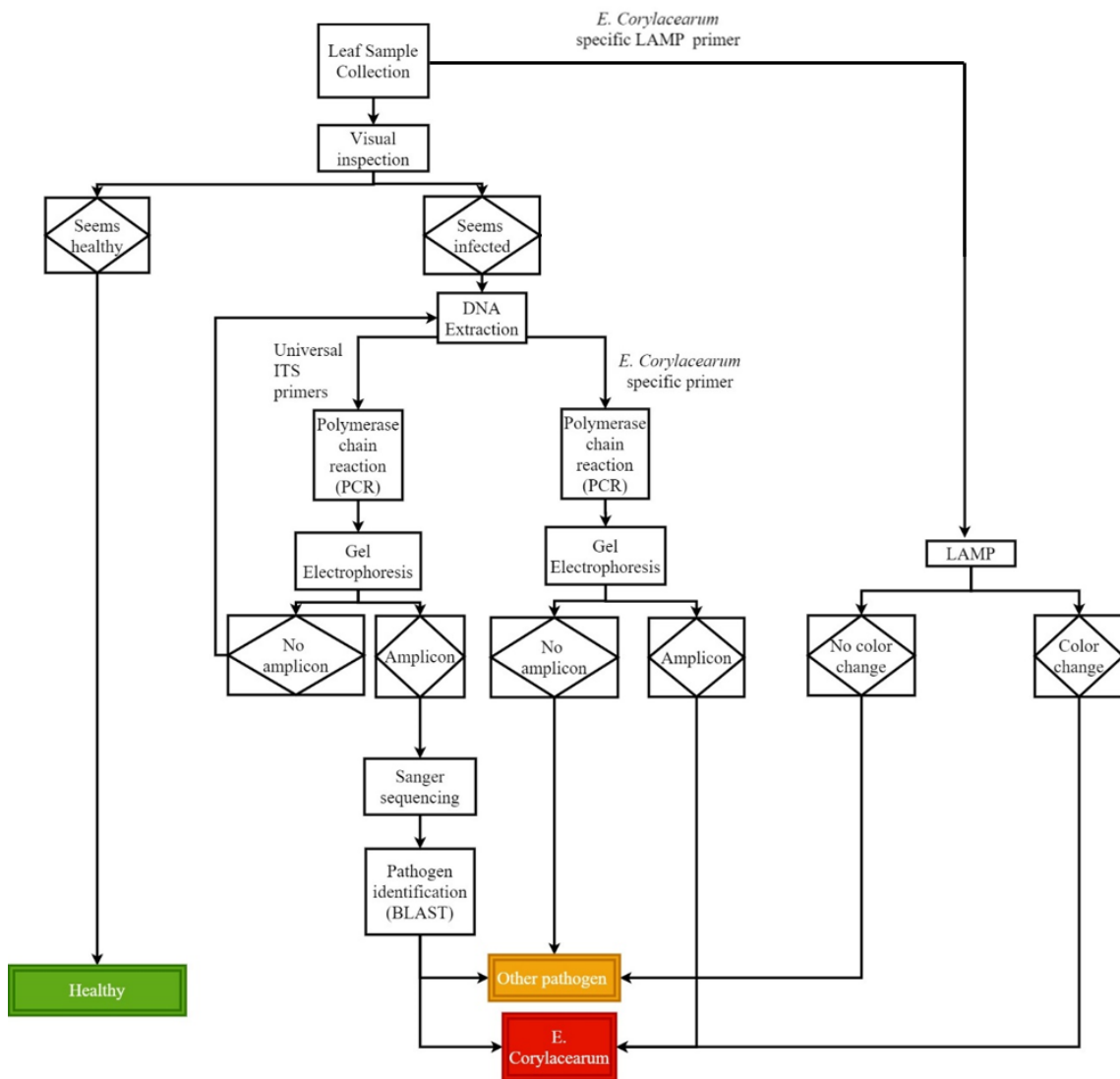


Figure 10: Algorithm for pathogen diagnosis workflow.

### 2.3 Leaf sample collection

Hazelnut leaf samples are collected from selected hazelnut orchards (Figure 10a). In addition to the collected sample a field trip to Düzce was made. This trip was made to observe fungal contamination on the field and analyzed the hazelnut shrub distribution for fungal contamination propagation. Several leaf samples with powdery mildew infection are collected for further examination.

Important points for hazelnut leaf samples collection from selected orchards are summarized. Leaf samples are chosen randomly from different locations in hazelnut orchards. Some important points have been listed below for collection;

- Three randomly chosen leaves on the ground that were fallen from the previous season,
- Three buds,
- Three fresh leaves,
- Until the powdery mildew disease symptoms occur the orchards were observed;
  - If there are no powdery mildew infection symptoms occurs, then randomly chosen three leaves were collected for analysis
  - If there are any powdery mildew infection symptoms occurs, then every two week three infected and three healthy leaves (no symptoms of white powdery patches) were collected until the end of the season.

Collected leaves samples have been wrapped with tissues and stored in an envelope with silica gel added to prevent humidity that might cause another pathogen occurrence. Then these envelopes were posted to Sabancı University Nanotechnology Research and Application Center (SUNUM) for further analysis. Envelopes arrived to SUNUM were firstly recorded by collection date and collected orchard. Leaf samples were stored in desiccator over night for complete leaf dry with exception of stopping the fungal growth. Detailed list of analyzed samples are summarized in APPENDIX B.

## 2.4 Initial Inspection by Microscopy

All received leaf samples are initially subjected to visual inspection by naked eye. If powdery mildew infection cannot be identified second inspection was done by stereo microscope (Nikon eclipse me 600). If powdery mildew infection cannot be identified by stereo microscope last visualization is done by light microscope (Nikon Eclipse ME 600). Disease observation for leaf samples were recorded. Detailed list of analyzed samples are summarized in APPENDIX B. Cleistothecium of *E. corylacearum* and *P. guttata* were collected by tweezer and stick on to carbon tape. Samples were coated (Cressington Sputter Coater) with Au/Pb at 30mA for 40sec. Coated pathogen samples were observed with Scanning Electron Microscope (SEM) (Zeiss LEO Supra 35VP FESEM). An electron gun voltage of 3kV was employed throughout the analyses.

## 2.5 DNA extraction

Whether infected or not, all collected leaf samples that are going to be extracted are measured for weight and recorded. Measured leaf samples are used for DNA extraction using the Nucleospin Plant II kit (Macherey-Nagal) following the manufacturer's protocol for fungal material. For the final step each sample is dissolved in 60 $\mu$ l of elution buffer PE. Extracted DNA were measured for nucleic acid concentration (ng/ $\mu$ l) by Nanodrop 2000c (Thermo Scientific). Firstly, 1 $\mu$ l of PE that were used for dissolving DNA samples were loaded to nanodrop to set as blank. Blank was used for eliminating concentration of PE buffer. 1 $\mu$ l of samples were loaded to nanodrop and nucleic acid concentration (ng/ $\mu$ l), A260, A280, 260/280 and 260/230 were recorded. DNA extracts are then analyzed by agarose gel electrophoresis for contamination of RNA and integrity. Agarose gel was prepared as 1% and Gelred Nucleic acid Stain (BIOTIUM) is added with 1:50 ratio. Extracted DNA were mixed with loading dye (1:5) and loaded to gel. The gel was run at 100V for 30 minutes. Then it was visualized by Gel Doc EZ Imager (BIO-RAD).

## 2.6 Polymerase Chain Reaction (PCR) Analysis

The internal transcribed spacer region (ITS1-5.8S- ITS2) of ribosomal DNA (rDNA) was amplified using universal primers NL1, TW14, PM3, PMITS1, PMITS2, ITS4 and ITS5. Universal primers PM3 (5'-GKGCTYTMCGCGTAGT-3') and TW14 (5'-GCTATCCTGAGGGAACTTC-3') were used for outer 28S amplification then second PCR was done with primers NL1 (5'-AGTAACGGCGAGTGAAGCGG-3') and TW14 to amplify inner 28S. PMITS1 (5'-TCGGACTGGCCCAGGGAGA-3'), PMITS2 (5'-TCACTCGCCGTTACTGAGGT-3') were used for outer amplification. Inner amplification was done with primers ITS4 (5'-TCCTCCGCTTATTGATATGC-3') and ITS5 (5'-GGAAGTAAAAGTCGTAACAAGG-3'). PCR amplification was carried out using Maximo Taq polymerase (GeneON,) in Mastercycler gradient (Eppendorf). Using the following amplification conditions for: initial denaturation at 95 °C for 5 min; denaturation at 95 °C for 15s, annealing for 15s at various temperature depending on the primers which is summarized at table, extension 72 °C for 30s ; final extension at 72 °C for 5min. Denaturation, annealing and extension are run for 35 cycles.

Primers	Annealing Temperature
PM3-TW14	54°C
NL1-TW14	54°C
PMITS1-PMITS2	59°C
ITS4-ITS5	57°C
Ec_F1-R1	58°C
Ec_F1-R2	58°C
Ec_F1-R3	58°C
Ec_F2-R1	58°C
Ec_F2-R2	58°C
Ec_F2-R3	58°C

Pg_F1-R1	54°C
Pg_F2-R2	54°C
MLO2	52°C
MLO7-21	52°C
MLO7-70	52°C
MLO7-90	52°C
MLO10	52°C

**Table 4:** Annealing temperature of selected primers.

PCR products are analyzed by 1% agarose gel electrophoresis in 0.5× TBE buffer (45 mM Tris-borate, 1 mM EDTA). Gel run at 50V for 45 min. Agarose gel are screen by BIO-RAD Gel Doc EZ Imager through imaging program.

## 2.7 Sanger Sequencing

Selected leaf samples with positive results from PM3-NL1-TW14 and ITS4-ITS5-PMITS1-PMITS2 nested PCR amplicons were sent to BMLabosis (BM Lab. Sist. Ltd.) for Sanger sequencing. Received sequencing chromatograms were visualized. Low quality bases were trimmed. Forward and reverse reads were combined using SeqTrace software (Stucky, 2012). Sequences were compared with known fungal rDNA sequences in Unite blast server (<https://unite.ut.ee/analysis.php>). Sequences were also compared with ITS sequences of fungal leaf diseases that use *Corylus sp.* as host (Table 2). Multiple sequence alignment and phylogenetic tree construction were carried out using MEGAX software with default parameters (Kumar et al., 2018) for pathogen identification.

## 2.8 Specific PCR primer design

Primers were design by NBCI primer design website (<https://www.ncbi.nlm.nih.gov/tools/primer-blast/index.cgi>). Designed primer are kept between 18-24 bp. G/C content is kept between 40-60%. Melting temperature (T<sub>m</sub>) were

arranged to be between 50-60°C. All designed primers are blasted with hazelnut leaf infecting pathogen ITS sequences and *C. avellana* genome.

## 2.9 Quantitative-PCR (qPCR) Analysis

Quantative-PCR analysis sample collection was done by a cookie cutter with 2cm diameter to cover the same amount of area for each sample.



**Figure 11:** Sample collection with cookie cutter for covering same for each sample.

DNA extracted from collected samples. Powdery mildew infection quantification is done by quantitative polymerase chain reaction technique (qPCR) (LightCycler® 480 Instrument II, Roche). qPCR mixture is prepared by 10µm 2X master mix (LightCycler® 480 SYBR Green I Master), 0,8 µl forward primer, 0,8 µL reverse primer, 1µl DNA and 7,4µL H<sub>2</sub>O. All samples were amplified and measured in triplicate. Ec\_F1-R3 primers are used for qPCR analysis. The melting temperature of the primary PCR product (“Tm2”) was used for confirmation specific amplification (should be within ±0.5°C of the PCR standard).

## 2.10 Loop Mediated Isothermal Amplification (LAMP) assay

LAMP primers were designed by PrimerExplorer V5 and confirmed by BLAST with *C. avellana* genome and hazelnut leaf fungal pathogen ITS sequences (Table 2) to prevent

misamplifications. Total volume of the LAMP reaction mixture was 25  $\mu\text{L}$  containing 10X Isothermal Amplification buffer (2,5  $\mu\text{L}$ ), 100mM  $\text{MgSO}_4$  (1.5  $\mu\text{L}$ ), 10 mM dNTPS (3,5  $\mu\text{L}$ ), 10X primers (2.5  $\mu\text{L}$  (1.6  $\mu\text{M}$  FIP/BIP, 0.2  $\mu\text{M}$  F3/B3, 0.4  $\mu\text{M}$  LoopF/B), DNA template (1  $\mu\text{L}$ ),  $\text{H}_2\text{O}$  (13  $\mu\text{L}$ ) and 1  $\mu\text{L}$  (0.32 U/ $\mu\text{L}$ ) of Bst Polymerase 2.0 (8,000 U/mL). The LAMP solution was incubated for one hour at 65°C in Mastercycler gradient (Eppendorf).

LAMP amplicons were analyzed by 2% agarose gel electrophoresis in 0.5 $\times$  TBE buffer (45 mM Tris-borate, 1 mM EDTA). Agarose gel were screen by BIO-RAD Gel Doc EZ Imager through imaging program.

Eriochrome Black T (EBT) is a metal indicator depending on the concentration of  $\text{Mg}^{2+}$  solution changes color. EBT is used for colorimetric detection of LAMP amplication, during the LAMP reactions  $\text{Mg}^{2+}$  concentration decreases and initial purple color of solution change to sky blue (Oh et al., 2016). LAMP assay with 28S-LAMP primers can be adapted to visual detection by color change observation. LAMP assays are efficient than PCR analysis because amplification can be done with a water bath or heating block. Many pathogen identification are done with LAMP (da Silva Zatti et al., 2020).

## **2.11 RNA extraction**

RNA extraction was done by CTAB nucleic acid extraction protocol (Doyle, 1987; Saghai-Marooif et al., 1984) by adapting it to RNA extraction. Extracted RNA were measured by Nanodrop 2000c (Thermo Scientific). Firstly, by loading 1 $\mu\text{l}$  of TE as blank to limit the background noise then 1 $\mu\text{l}$  of samples were loaded and nucleic acid concentration (ng/ $\mu\text{l}$ ), A260, A280, 260/280 and 260/230 values were recorded. RNA extracts were analyzed by agarose gel electrophoresis. Agarose gel were prepared as 1% and Gelred Nucleic acid Stain (BIOTIUM) was added with 1:50 ratio. Extracted DNA were mixed with loading dye (1:5) and loaded to gel. The gel was run at 100V for 30 minutes. Then it was visualized by Gel Doc EZ Imager (BIO-RAD). Extracted RNA samples were treated with DNase to eliminate DNA contamination. DNase treated RNA samples were measured by Nanodrop 2000c (Thermo Scientific). Firstly, by loading 1 $\mu\text{l}$  of nuclease-free water as blank to limit the background noise then 1 $\mu\text{l}$  of samples were loaded and nucleic acid concentration (ng/ $\mu\text{l}$ ), A260, A280, 260/280 and 260/230 values were recorded. DNase treated RNA samples were denatured at 65 °C for 5 min before

analyzed by agarose gel electrophoresis. Agarose gel was prepared as 2% and Gelred Nucleic acid Stain (BIOTIUM) was added with 1:50 ratio. DNase treated RNA samples were mixed with loading dye (1:5) and loaded to gel. The gel was run at 100V for 30 minutes. Then it was visualized by Gel Doc EZ Imager (BIO-RAD).

### **3. RESULTS AND DISCUSSION**

#### **3.1. Hazelnut orchards and Environmental factors**

Environmental factors affecting the disease growth were studied by determining the weather stations near each selected orchard. Details about the selected weather station are listed at Appendix A. Fresh leaves of hazelnut scrubs usually start to grow on March and around November leaves start to fall off, hourly data is collected from each weather station for nine-month period. Considering the previous studies about the environmental five factors are selected for further analysis. Weather data of temperature, humidity, wind speed, rain and solar radiation are calculated for daily average, and for lowest and highest temperature daily minimum and maximum temperature is recorded.

Optimum conditions for powdery mildew pathogen germinations were temperature between 15 °C to 25°C, humidity between 75% - 95% RH, low sunlight, low rain (Husain & Akram, 1995; Sugai et al., 2020) Optimum conditions for powdery mildew pathogen propagation were temperature around 20 °C, humidity between 75% - 95% RH, high rain, high wind (Carver et al., 1994; Sugai et al., 2020).

Pasalar orchard weather analysis for 2018; are around middle of May average temperatures reaches to 20 °C (Figure 9B) and humidity was around 80% RH (Figure 9C) and total rain (Figure 9E) is very low which was optimum for powdery mildew pathogen germination. From June to October average temperature was around 20 °C which is optimum for powdery mildew propagation, but humidity (Figure 9C) and wind speed was very low (Figure 9D). In 2019 by May temperature reaches 15 °C (Figure 10B), humidity was around 80% RH (Figure 10C) but weather was rainy (Figure 10E) and high in solar radiation (Figure 10G). By August wind speed (Figure 10D), temperature (10B) and humidity (Figure 10C) were optimal for propagation.

### Pasalar 2018

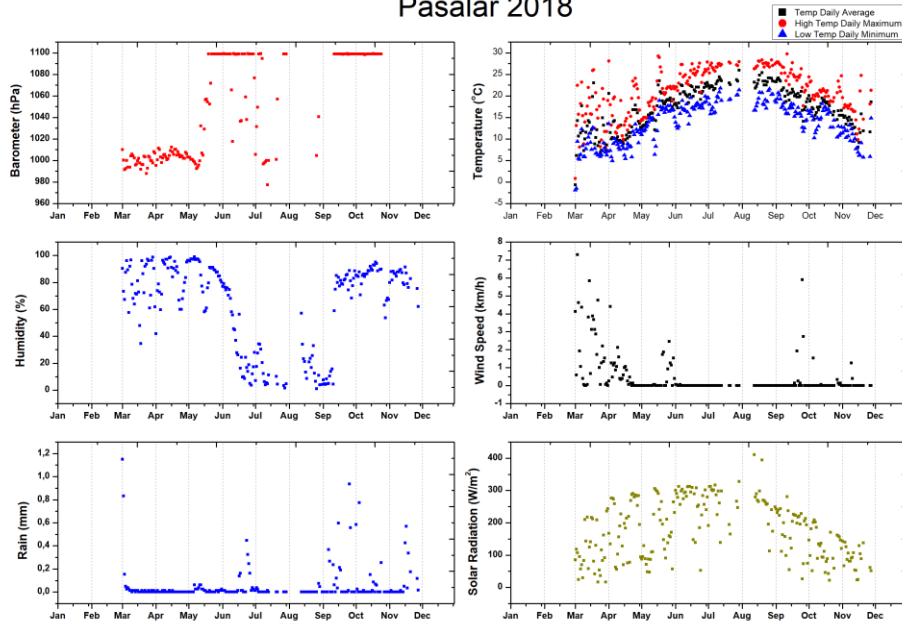


**Figure 12:** The graphs are 2018 data from Pasalar station. Each scatter point shows the daily average of the recorded value. A) Air pressure (hPa), B) Temperature (°C), highest and lowest temperature (°C), C) Humidity (%), D) Rain (mm), E) Solar radiation (W/m<sup>2</sup>).

### Pasalar 2019

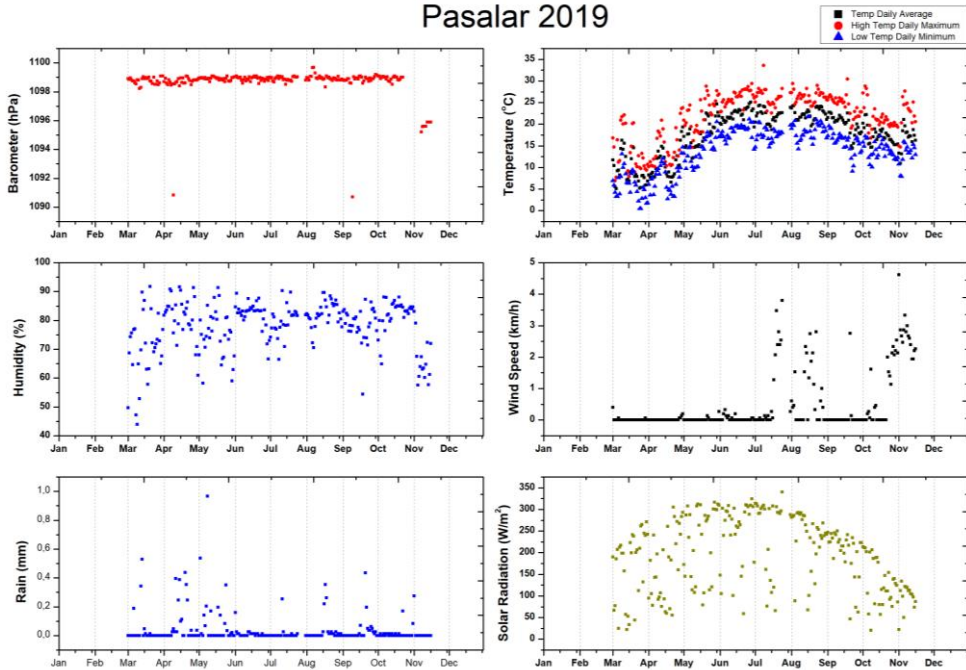


**Figure 13:** The graphs are 2019 data from Pasalar station. Each scatter point shows the daily average of the recorded value. A) Air pressure (hPa), B) Temperature (°C), highest and lowest temperature (°C), C) Humidity (%), D) Rain (mm), E) Solar radiation (W/m<sup>2</sup>).

Ballıkaya orchard weather analysis for 2018; starting from April temperature reached to 15 °C (Figure 11B) but humidity was inconsistent with multiple point reaching to 75% RH (Figure 11C). Temperature around 20 °C (Figure 11B) for most of the season with high humidity (Figure 11C) also by September wind speed (Figure 11D) starts to increase. However, for 2019 both humidity (Figure 12C) and temperature (Figure 12B) were below optimum levels.

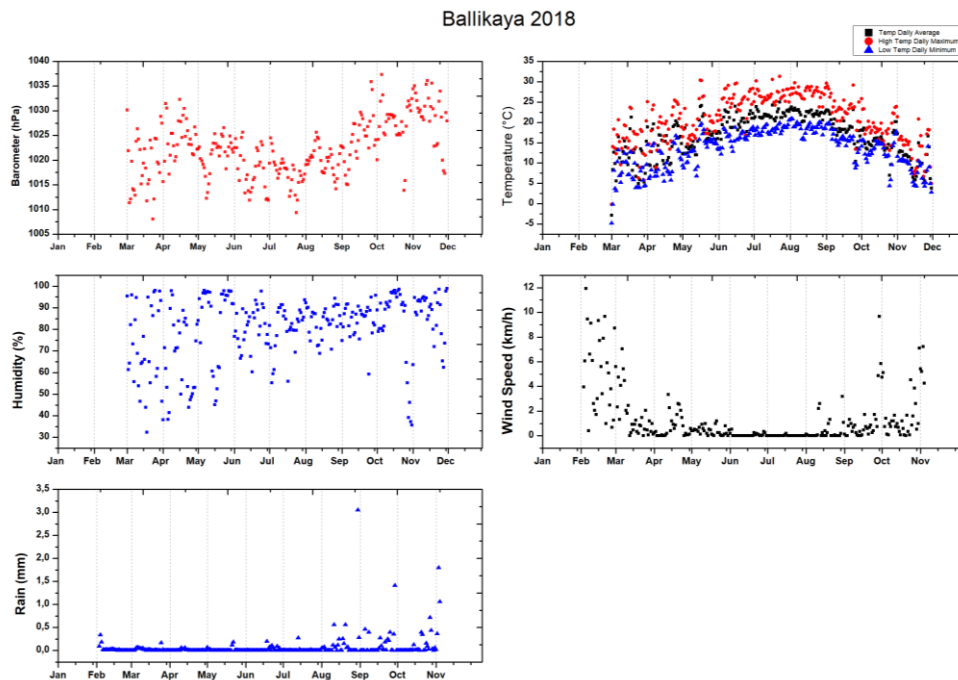


**Figure 14:** The graphs are 2018 data from Ballıkaya station. Each scatter point shows the daily average of the recorded value. A) Air pressure (hPa), B) Temperature (°C), highest and lowest temperature (°C), C) Humidity (%), D) Rain (mm).

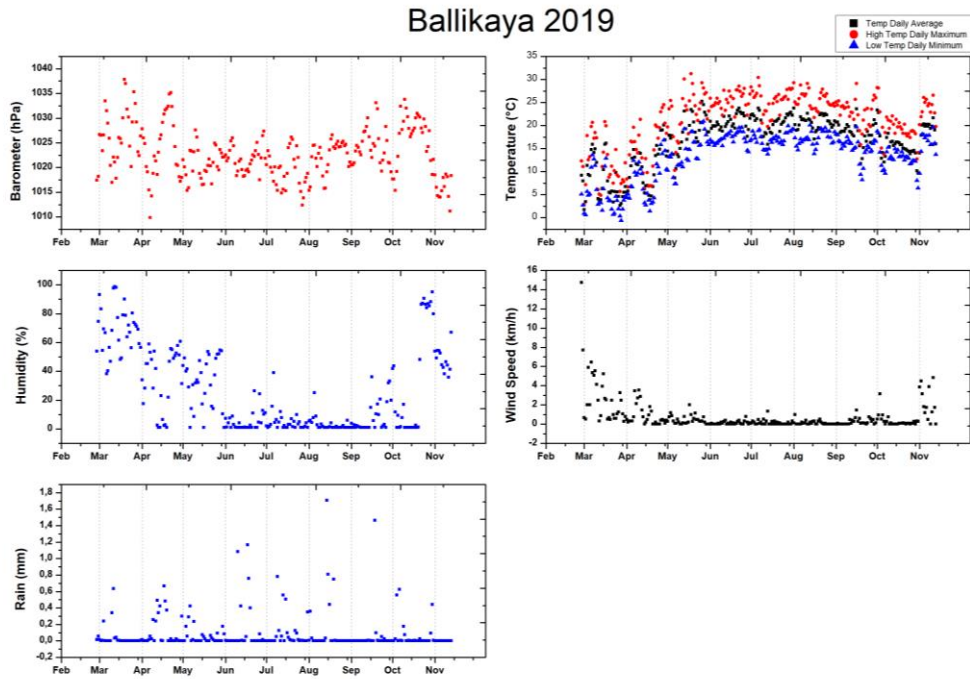


**Figure 15:** The graphs are 2019 data from Ballıkaya station. Each scatter point shows the daily average of the recorded value A) Air pressure (hPa), B) Temperature (°C), highest and lowest temperature (°C), C) Humidity (%), D) Rain (mm).

Kovancı orchard weather analysis for 2018; by May temperature reaches to 15 °C (Figure 13B), humidity is inconsistent with multiple point reaching to 75% RH (Figure 13C) and higher, but solar radiation (Figure 13F) in high levels.

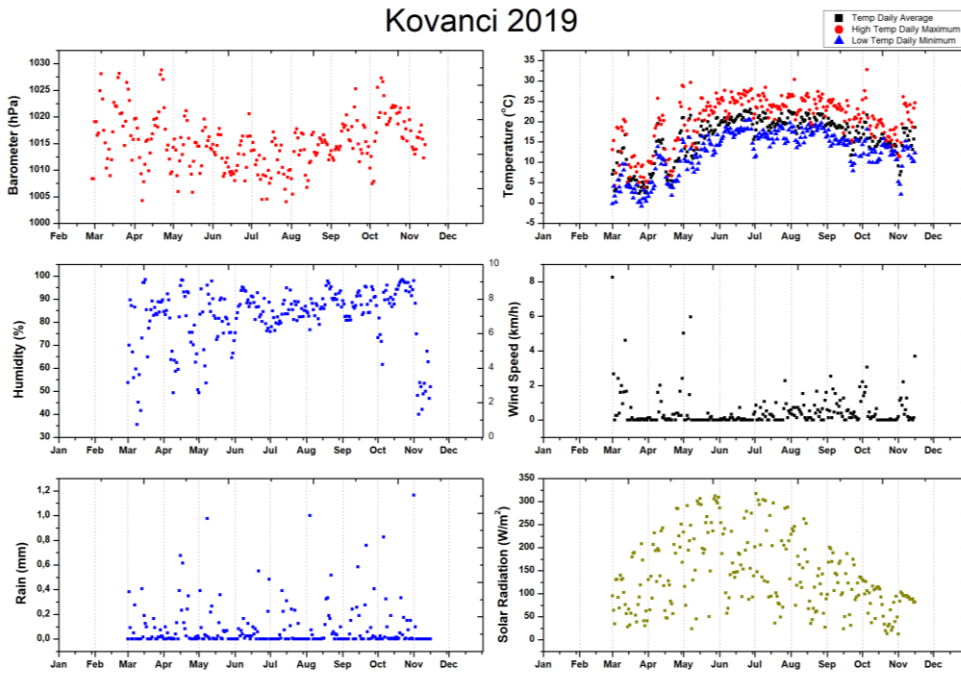


**Figure 16:** The graphs are 2019 data from Kovanci station. Each scatter point shows the daily average of the recorded value A) Air pressure (hPa), B) Temperature (°C), highest and lowest temperature (°C), C) Humidity (%), D) Rain (mm), E) Solar radiation (W/m<sup>2</sup>).

Eynesil orchard weather analysis for 2019; by June both temperature (Figure 14B) and humidity (Figure 14C) reach to optimum levels for powdery mildew germination. High wind speed (Figure 14D) throughout whole season, from June to September temperature around 25 °C and humidity around 80% RH and more.

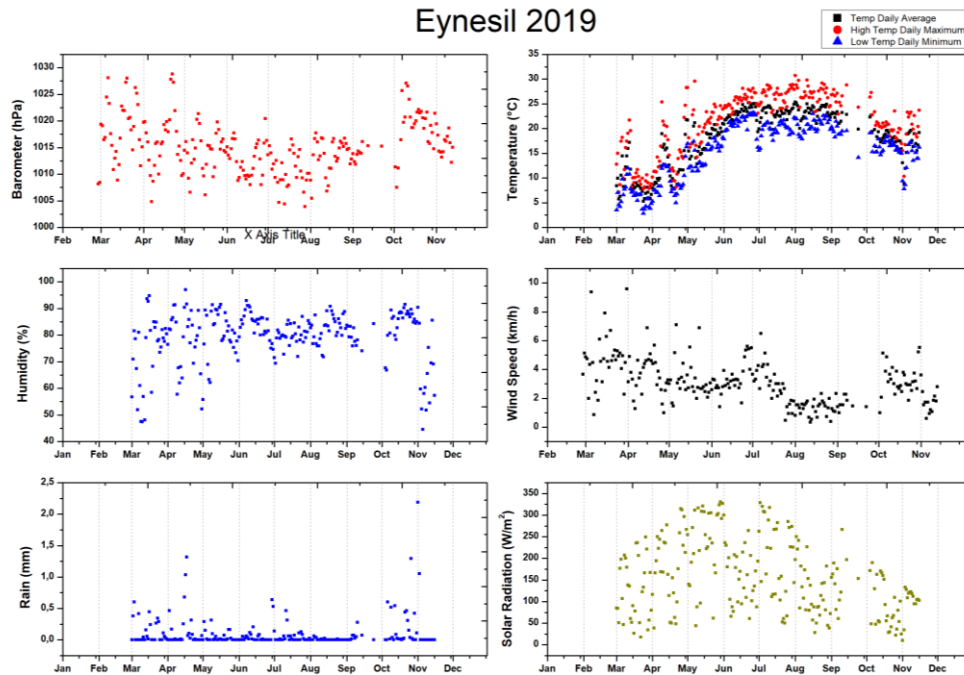


**Figure 17:** The graphs are 2019 data from Eynesil station. Each scatter point shows the daily average of the recorded value A) Air pressure (hPa), B) Temperature (°C), highest and lowest temperature (°C), C) Humidity (%), D) Rain (mm), E) Solar radiation ( $W/m^2$ ).

Powdery mildew pathogens spend their entire life on the green tissue of their host. Powdery mildew pathogens were expected to affect by the surrounding conditions of infected leaves (e.g., humidity, temperature, sunlight and wind speed). Effects of climatic factors on powdery mildew is studied in several crops such as barley (Sugai et al., 2020), strawberry (Amsalem et al., 2006) and sunflower (Husain & Akram, 1995).

Various studies about the weather conditions can be summarized as; temperatures allowing for disease development have been shown to range from 15 °C to 25 °C, with an optimum of approximately 20 °C (Celio and Hausbeck, 1998; Husain and Akram, 1995). Powdery mildew conidia are viable for short period of time and for germination they need 4 to 6 hours of optimum humidity and temperature. Conidial germination and germ tube elongation of strawberry powdery mildew agent *Sphaerotheca macularis* f. sp. *fragariae*, was studied in wide range of temperature (5 °C - 35 °C) and highest result occur between 15 °C to 25°C (Miller et al., 2003).

Effect of humidity in conidial germination was also analyzed and found that germination rate was highest at 97% - 100% relative humidity (RH), while at 75% RH a significant increase was observed. On the other hand, conidia production is significantly decreased above 95% RH (Amsalem et al., 2006). Powdery mildew growth and effects of humidity for disease expansion is studied in *Blumeria graminis* f. sp. *hordei*, the fungal pathogen of barley. Barley leaves that were exposed to high humidity (more than 95% relative humidity (RH)) was shown that the infection was considerably suppressed due to the fail of secondary hyphae formation and penetration rate. *Blumeria graminis* f. sp. *hordei* secrete various proteins like cell wall degrading enzymes and effector proteins to suppress the penetration resistance of host plants when attempting to penetrate host cells. At high humidity levels these substances do not occur due to the failure of appressorium formation. On the other hand, *Blumeria graminis* f. sp. *hordei* successfully penetrated to barley epidermal cell wall under the low humidity (70% relative humidity) condition (Sugai et al., 2020).

Highest conidial germination rates and germ tube lengths were recorded under complete darkness, assuming powdery mildew pathogens survive and proliferate well under shaded conditions, indicating that the conidia might be sensitive to direct sunlight and UV radiation (Amsalem et al., 2006). Effects of sunlight is analyzed in *Erysiphe graminis* f. sp. *avenae* and found that when the pathogen is exposed to light during their development, the formation of haustoria is delayed. However light exposure have no effect on germination and formation of appressorial lobe (Carver et al., 1994).

In addition to temperature and humidity, effect of free water is also studied and found that different species respond differently in their ability to germinate on and in water. However if conidia lose cytoplasmic integrity then it cannot germinate (Sivapalan, 1993). However rain has a crucial effect on expansion of the disease by physically removing the conidia from leaf surface, especially when rain occurs after dry weather (PERIES, 1962).

Optimal RH for disease severity ranged from 80 to 100% depending on the pathogen and host. Rainfall and temperature are likely to be the primary factors which control the growth of mildew, and dry weather and temperatures between 15 °C to 25°C being favorable for the spread of the disease. Conflicting reports from different researchers may explained by age of conidia, isolate and population variability, and/or interaction between different cultivars and the pathogen.

Weather analysis of Paşalar 2018 show that powdery mildew pathogen germination is expected to start by middle of May with average temperatures around 20 °C (Figure 9B) and humidity around 80% RH (Figure 9C). Also, total rain (Figure 9E) is very low which was optimum for powdery mildew pathogen germination. So powdery mildew disease is expected to occur in hazelnut scrubs. From June to October average temperature was optimum for powdery mildew propagation, however humidity (Figure 9C) and wind speed was very low (Figure 9D) which might cause low levels of disease propagation. In 2019 powdery mildew germination were expected to be shift to mid-June since the temperature reaches 20 °C (Figure 10B), humidity was around 80% RH (Figure 10C) and low in rain (Figure 10E) and high in solar radiation (Figure 10G). By August wind speed (Figure 10D), temperature (10B) and humidity (Figure 10C) were optimal for propagation. For 2020 powdery mildew disease were expected to increase because weather conditions were optimum for powdery mildew propagation.

Ballıkaya orchard 2018 weather analysis were starting from April temperature reached to 15 °C (Figure 11B) but humidity was inconsistent with multiple point reaching to 75% RH (Figure 11C) so early germination was expected for powdery mildew. Also, Ballıkaya orchards powdery mildew infection were expected to develop disease for longer period since weather conditions were optimum for several months. Temperature are optimum (Figure 11B) for most of the season with high humidity (Figure 11C) which was in favor for powdery mildew propagation. By September wind speed (Figure 11D) starts to increase which was helpful for disease propagation. However, for 2019 both humidity (Figure 12C) and temperature (Figure 12B) were below optimum levels so there might be a decrease in powdery mildew infection. Weather analysis prediction showed that in 2019 powdery mildew disease occurrence will be lower than 2018 incidents.

Kovancı orchard 2018 weather analysis showed that by May temperature reaches to 15 °C (Figure 13B), humidity was inconsistent with multiple point reaching to 75% RH (Figure 13C) and higher, but solar radiation (Figure 13F) was in high levels. Powdery mildew germination was expected to be at average levels. Also, for 2019 humidity and temperature were optimal for disease germination. In 2019 powdery mildew occurrence was expected to be higher than 2018 because the amount of rain and wind are higher than 2018. Rain and wind are two factors that are crucial for disease propagation with physical impacts.

Eynesil orchard weather analysis for 2019 showed that; by June both temperature (Figure 14B) and humidity (Figure 14C) reach to optimum levels for powdery mildew germination. Powdery mildew propagation was expected to be in high levels for Eynesil orchards. High wind speed (Figure 14D) were observed throughout the whole season and from June to September temperature around 25 °C and humidity around 80% RH and higher which are in favor of propagation.

Expectations about powdery mildew disease germination and propagation related to weather conditions are discussed above however amount of collected leaf samples and collected time points were not enough to correlate any relation between the disease development and atmospheric conditions.

### **3.2 Visual Analysis of Collected Leaf Samples**

Powdery mildew infection can be identified by the formation of white powdery patches on both side of the leaf. These patches are created by hyphal expansion of pathogens and in the late stage of infection these patches enlarge by covered area which can be detected by naked eye. In some cases, powdery mildew covers the whole surface of leaf. Analyzed leaf samples were mostly at the hyphal expansion stage (formation of white, fiber-like networks) but some leaves contain cleistothecia (black spherical fruiting bodies). Visual analysis of each leaf sample is recorded in Appendix B. General observation about powdery mildew infected leaf samples are summarized as follows.

*Corylus avellana* cv. Tombul leaf samples collected from Sabancı University garden were highly infected with powdery mildew that can be identified by even naked eye. Sabancı leaves powdery mildew infection were formed of conidial chains, conidiospores and hyphae (Figure 15). Further analysis under stereo microscope were used for observation of chasmothecia with different colors as black, brown or yellowish (immature chasmothecia) within the hyphae suggesting different stages of sexual reproduction.

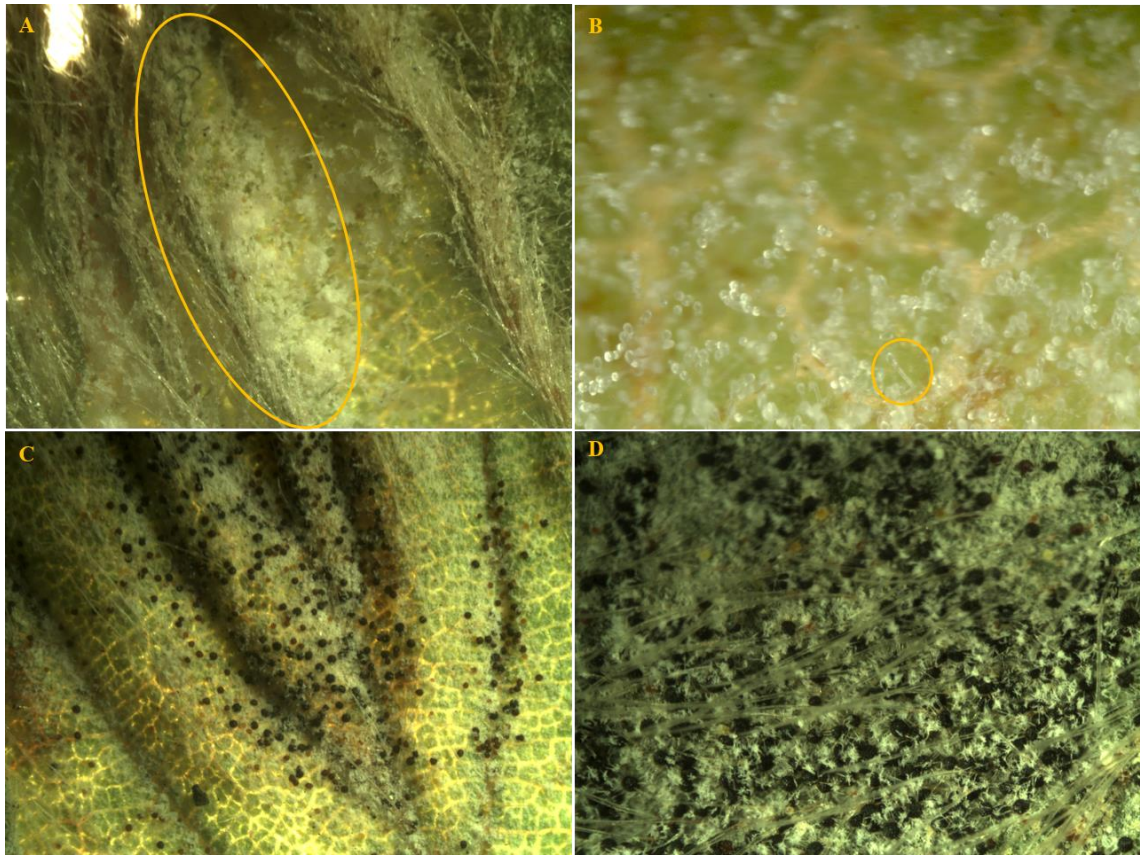


**Figure 18:** *C. avellana* leaf collected from Sabancı University. A) Mycelia of powdery mildew infection, there was no cleistothecium formation so fungal growth was at vegetative stage or hyphal expansion stage, B) Leaves covered with conidia, Orange circle highlighting conidia risen from hypha C) Cleistothecium were formed on the leaf surface fungal growth was at sexual phase D) Extreme cleistothecium formation.

At the beginning of the season collected leaf samples from each selected orchard were not showing powdery mildew infection. As the middle of the season samples started to show powdery mildew infection in low levels. Near the end of the season powdery mildew infections were detectable by naked eye. For each orchard powdery mildew infected leaf sample are presented as followed;

Leaf samples of Sakarya orchards, from mid-season and late season. White patches are not formed yet but hyphae are distributed on the surface of the leaf (Figure 16A). Powdery mildew covering the whole surface of leaf, white patches are united (Figure 16B). Both leaves are at hyphal expansion stage.

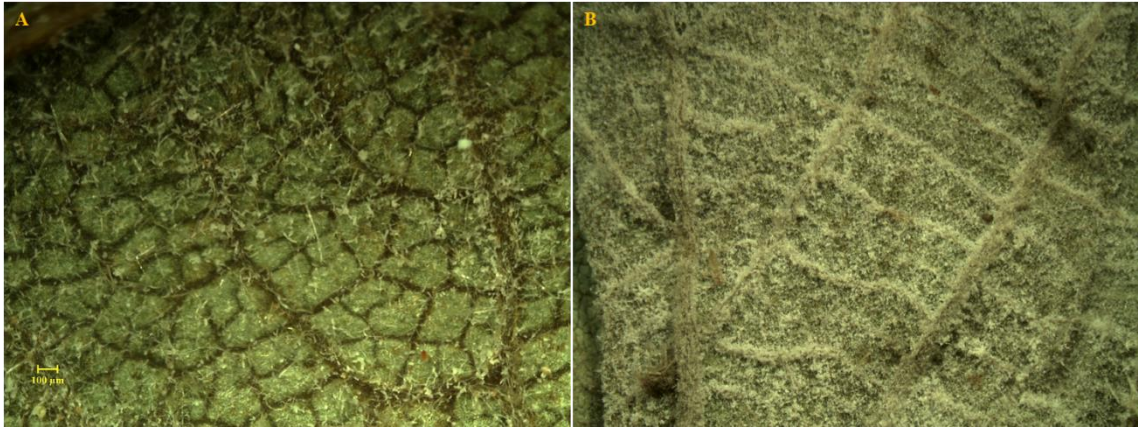


**Figure 19:** Sakarya infected leaf samples A) Powdery mildew infected leaf sample from mid-season. Hyphae were detectable by stereo microscope B) Powdery mildew infected leaf sample from mid-season. Hyphae are detectable by naked eye.

Düzce leaf samples were mostly at hyphal expansion stage but significant amount of chasmothecia were detectable by late season. Hyphae and conidia formation recorded for leaf samples like spider web networks (Figure 17A). Powdery mildew infection can be visualized as white patches (Figure 17B). Samples collected from Düzce field trip will be discussed in detail under the topic morphology of powdery mildew pathogen observed on leaf samples.

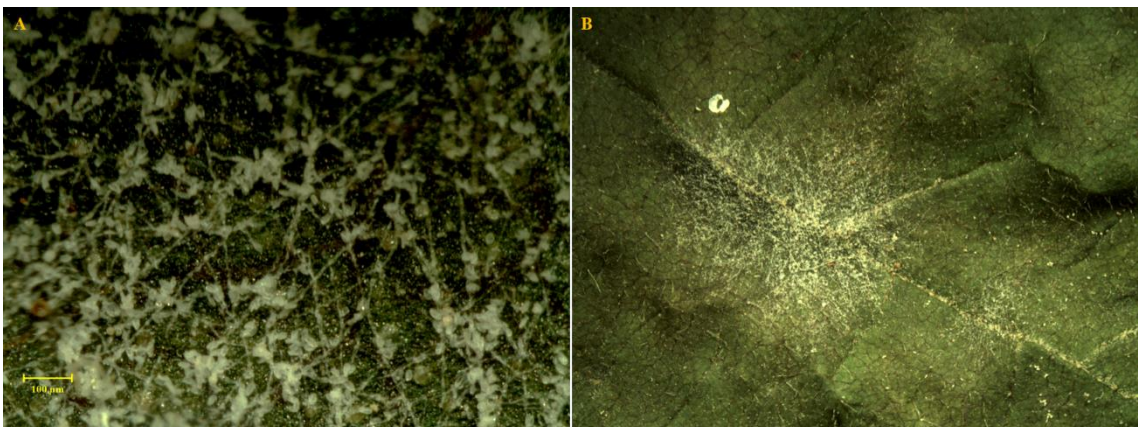


**Figure 20:** Düzce leaf samples A) Hyphae and conidia formed on the surface of leaf B) Powdery mildew characteristic appearance of white powdery patch are observed.

Ordu leaf samples with powdery mildew infection were also mostly in vegetative stage with hyphal expansions. Powdery patches are started to occur by mid-season in various sizes (Figure 18A). By late season powdery mildew effects increased and cleistothecium are observed.

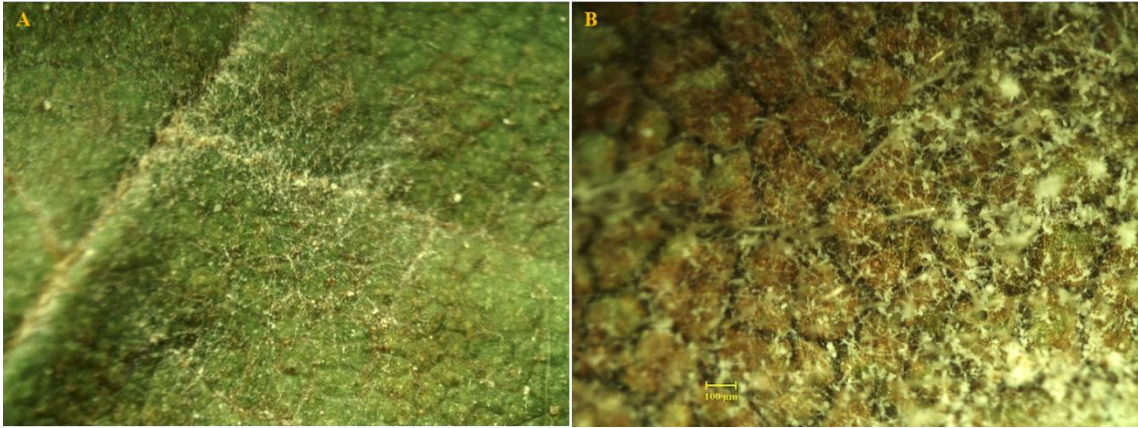


**Figure 21:** Ordu leaf samples. A) Slightly occurrence of powdery mildew patches, B) Hyphal expansions of powdery mildew.

Lastly leaf samples mailed from Giresun at hyphal expansion but powdery patches are started to occur (Figure 19A) also by mid-season few chasmothecia were detected (Figure19B).

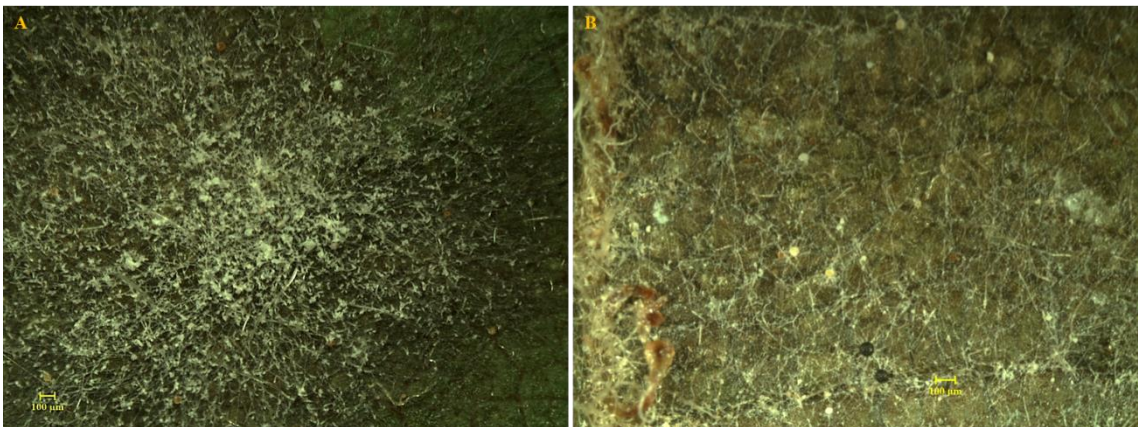


**Figure 22:** Giresun leaf samples A) Powdery mildew as white patches B) Chasmothecium occur on the surface of the leaf

Powdery mildew in hazelnuts was previously observed in Turkey. The disease was described as circular to irregular white patches formed by mycelium and conidia. Powdery mildew colonies were observed in abaxial and adaxial meaning both side of the leaves. Powdery mildew infected areas were differentiated by the appearance of color change from green to yellow and eventually turned to brown lesions. The disease was developed in early spring, with symptoms observed on leaves, young shoots and immature nut clusters (Sezer et al., 2017b). Similar to our observations powdery mildew infection started to occur by mid-season with the appearance of white smear patches. White patches were formed by hyphae formation causing mycelium development. By the end of the season white patches were dense. Collected leaf samples from Sakarya orchards were covered with powdery mildew infection. Leaf samples collected from Ordu and Giresun orchards were observed to contain mature chasmothecia. Further morphological examinations were done by microscope analysis.

### **3.3 Morphology of Powdery mildew pathogen observed on leaf samples**

Visual analysis of powdery mildew infecting agent is summarized as;

1. Mycelia of the infected leaves are white and composed of light to dense patches (Figure 20A)
2. Conidiospore are shaped as ellipsoid-ovoid and rise from hyphae (Figure 20B).
3. Chasmothecium are 80-120 $\mu$ m in diameter and appendages straight, 4–5 times dichotomously branched (Figure 20C-D), and tips are curved (Figure 20E)
4. Asci are broad ellipsoid ovoid (Figure 20F-G).

Morphological analysis can be concluded as collected leaf samples from selected orchards and samples collected from Sabancı University are all infected with powdery mildew disease and the infecting agent is defined as *Erysiphe corylacearum*.

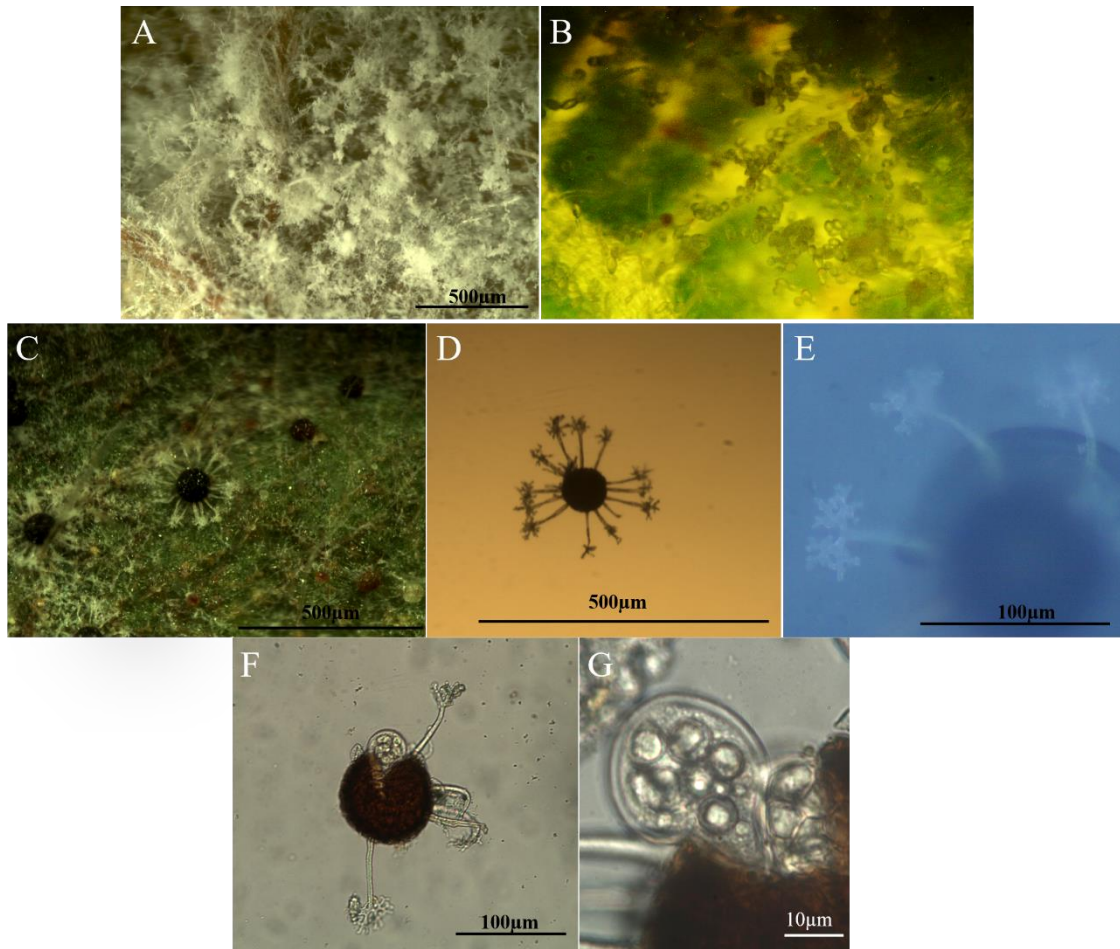


**Figure 23:** Powdery mildew agent *E. corylacearum* collected from hazelnut orchards. A) *E. corylacearum* powdery patch formed by hyphae and conidia B) Conidia C) Chasmothecium and hyphal network on the surface of the leaf, D) Chasmothecium, E) Appendages of the chasmothecium, F) Chasmothecium releasing asci G) Ascospores inside asci.

However, stereo microscope observation of leaf samples collected from Düzce field trip on 21.11.18 are showing both same and different symptoms from previously collected leaf samples. Especially underside of leaf samples two different type of chasmothecium are observed. These leaves might be infected with both *P. guttata* and *E. corylacearum* pathogens (Figure 21).

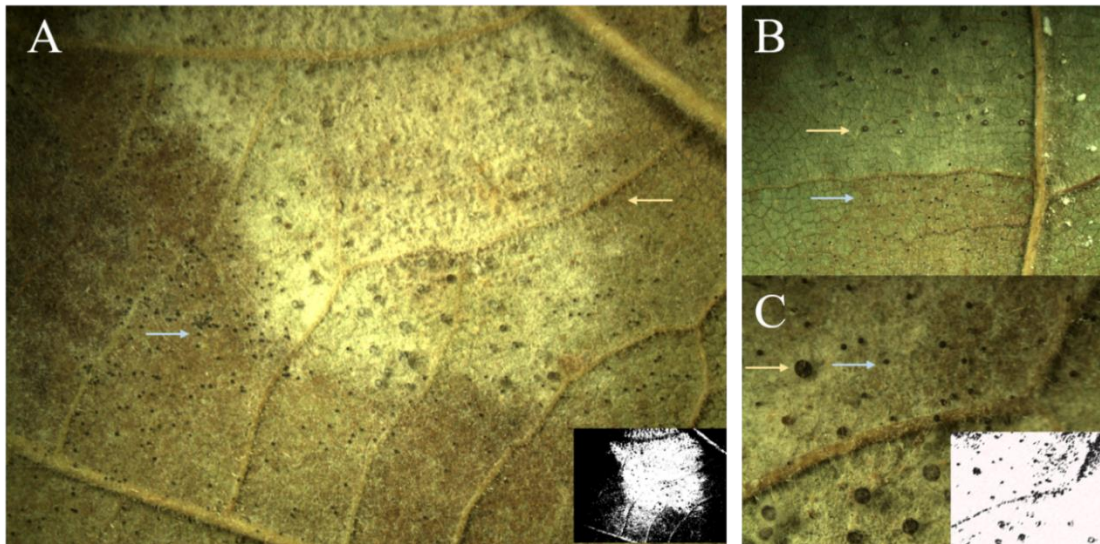


**Figure 24:** Powdery mildew infected leaf sample collected from Düzce field trip. Blue arrow pointing larger chasmothecium and yellow arrow pointing smaller chasmothecium. A) Powdery mildew infected area contains two different sized chasmothecium and white powdery patches formed by hyphae (corner: thresholded infection distribution total infected area fraction: 62%) B) Infected hazelnut leaf surface, C) Portion of the leaf (corner: thresholded chasmothecium distribution chasmothecium fraction over infected area: 8%).

Chasmothecium of each pathogen were observed with SEM. *E. corylacearum* chasmothecium of 10 samples were measured and average diameter is between 80-100  $\mu\text{m}$  (Figure 22A), appendices up to 14 and containing multiple dichotomously branched tips (Figure 22B). *P. guttata* chasmothecium are larger in diameter around 130-185  $\mu\text{m}$  (Figure 22C), appendices up to 10 and bulbous swelling at the base and straight to the tip (Figure 22D). The bulbous appendages are firstly formed towards the air and then appendages point downward towards the mycelium to free the mature ascocarp from the leaf surface.

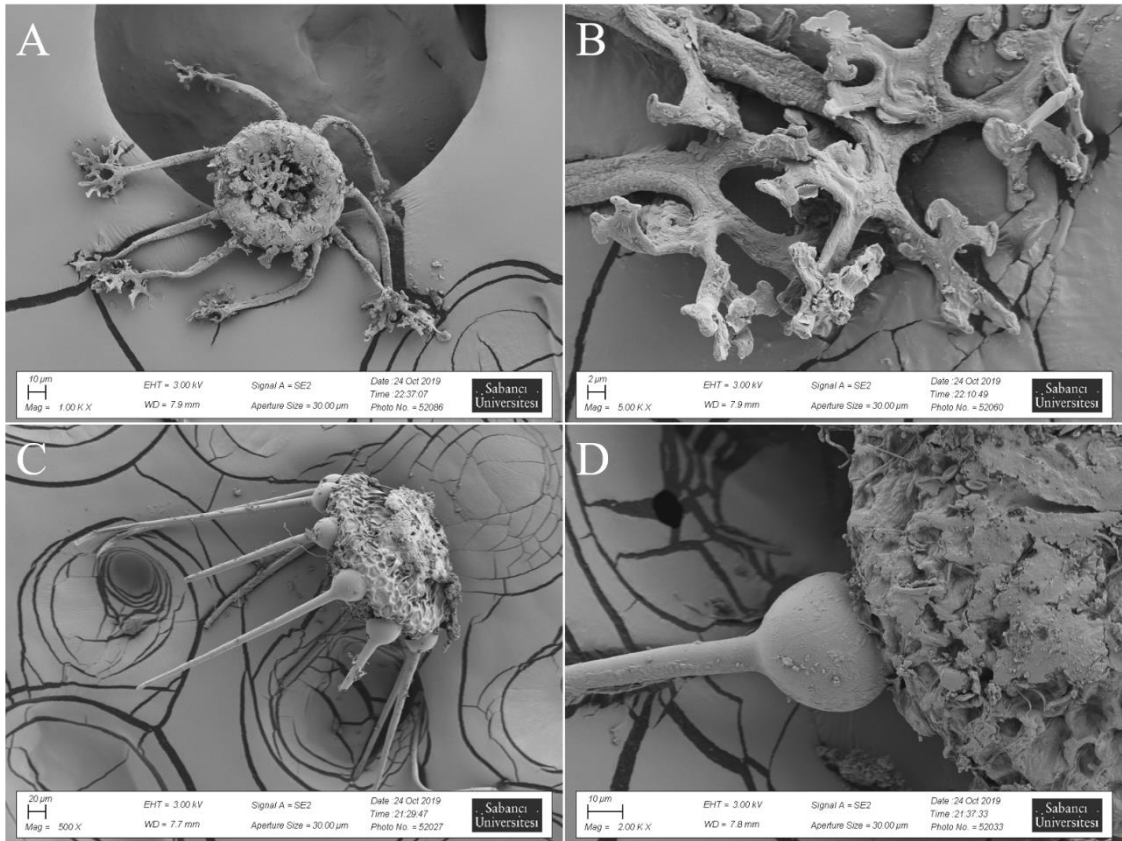


**Figure 25:** SEM image of chasmothecium of powdery mildew pathogens. A) *E. corylacearum* chasmothecium average size around 120 $\mu$ m, B) *E. corylacearum* chasmothecium containing multiple dichotomously branched tips C) *P. guttata* chasmothecium average size around 90  $\mu$ m, D) *P. guttata* chasmothecium appendices were bulbous swelling at the base and straight to the tip.

Visual analysis of powdery mildew pathogen observed on *Corylus sp.* leaf samples collected from selected orchards were summarized. Mycelium observations were described as branched, forming irregular dense patches and increase in size by growing at any direction. Hyphae are noted to be smooth, divided and branched. Conidia are formed singly rising from hyphae, shape can be described as ellipsoid ovoid. Conidiophores are produced singly from conidia. Chasmothecia are dispersed gregariously with diameter around 80 to 110  $\mu$ m. Appendages are positioned equatorial and developed straight. Towards the tip appendages are 4 to 5 times dichotomously branched and tips are recurved. Asci are obovoid to broadly ellipsoid, can be defined as sac, size between 40 to 60  $\mu$ m. Asci containing 4-6 ascospores positioned as sessile. Finally, ascospores are hyaline with shape of ellipsoid ovoid. These morphological

structures are matching with the powdery mildew agent *E. corylacearum* which was previously described in Braun and Cook (2012).

Morphology and size of mycelia, conidiophores, conidia, ascocarps, and ascocarp appendages were used for powdery mildew pathogens classification. In this study microscope analysis were focused on the morphology of chasmothecium for *Corylus avellana* powdery pathogen identification because *E. corylacearum* and *P. guttata* were very different from each other. The bulbous appendages were easy to recognize and identify the pathogen as *P. guttata* and dichotomously branched and curved tips were characteristic morphology of *E. corylacearum*.

### **3.4 Fungal pathogen identification by PCR analysis using Universal ITS primers**

Internal transcribed spacer (ITS) region were used for pathogen species identification. Each species ITS regions have unique and common areas. Universal primers identified the ITS region from these common areas and species are identified from their unique regions. Previously described universal ITS primers PM3, NL1 and TW14 are selected for PCR analysis. Unfortunately, these amplicons can occur in any fungal contamination. To verify the infecting species these amplicons should be sequenced, and the sequencing result should be match with the targeted pathogen.

DNA are extracted from fresh young leaf, bud and fallen leaf samples from Ordu (20.03.2018), Düzce and Sakarya (21.03.2018) for fungal pathogen identification. Universal ITS primers NL1-TW14-PM3 are used for nested PCR analysis. Formation of PCR amplicons can be commented as presence of fungal pathogen rather than concluding the infecting agent as *E. corylacearum*. PCR amplicons are expected to be 840bp in size.

Gel analysis of all fallen leaf samples (7, 17, 35, 66, 50 and 58 which were summarized in Appendix B) are positive for amplification. Bud samples from Duzce-Pasalar (18), Sakarya-Sungut (36), Ordu-Artikli (51) and Ordu-Dedeli (59) samples are also positive for amplification. Lastly fresh leaf samples of Duzce-Pasalar (19), Ordu-Artikli (52) and Ordu-Dedeli (60) are also produced amplicons. Gel electrophoresis results show that these samples are contaminated with fungal infection. Ten samples were selected to be sequenced to identify the infecting pathogen These samples are from selected from each orchard of Yesiltepe (7), Pasalar (17, 18), Sungut (35, 36), Uzunisa (66), Artikli (50, 51)

and Dedeli (58,59). Selected samples are labelled with red arrow on the gel electrophoresis image (Figure 23).

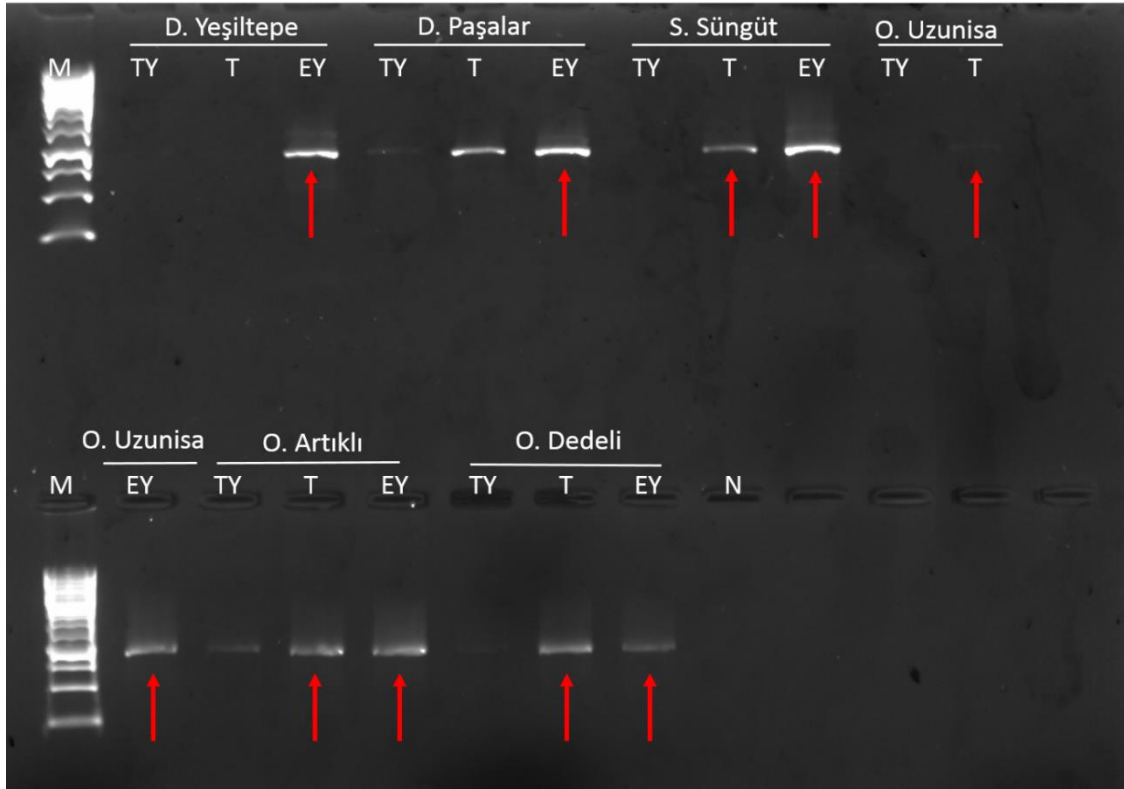


**Figure 26:** 28S rRNA gene isolated from the collected samples. TY: fresh young leaf, T: bud, EY: fallen old leaf samples, M: Ladder. Amplification seen as white lines represent the fungal contamination expected amplicon size for *E. corylacearum* is 840bp. Samples with red arrow are selected for sequencing.

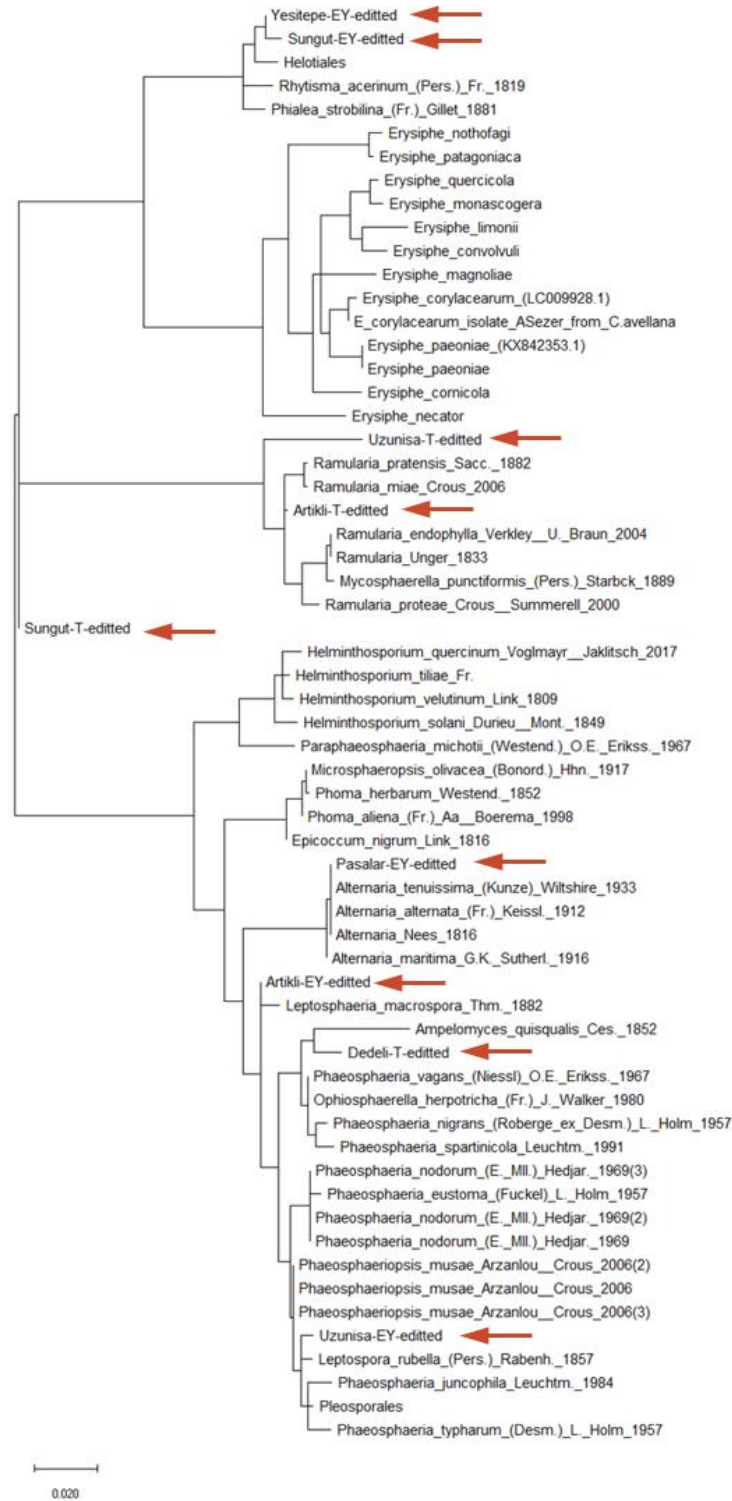


**Figure 27:** Phylogenetic tree analysis with sequenced samples EY-Yesiltepe, T-Pasalar, EY-Pasalar, T-Sungut, EY-Sungut, EY-Uzunisa, T-Artikli, EY-Artikli, T-Dedeli, EY-Dedeli samples and fungal rDNA sequences. Sequenced samples are labelled with red arrow.

Quality of sequences 7, 35 and 36 was inconsistent and none of the sequenced samples were matched with hazelnut leaf fungal pathogens. Samples 51 and 67 were match to *Ramularia spp.* Sample 17 match to *Alternaria spp.* Samples 59 and 66 matches to *Phaeosphaeriopsis spp.* Lastly sample 50 matches to *Leptospora spp.* (Figure 24).

Leaf samples that were collected from orchards in nature can be infected by several other fungal pathogens. Previous analysis for *E. corylacearum* identification universal ITS primers were used for nested PCR analysis. PM3-TW14 were used for 28S outer region amplification and NL1-TW14 for inner 28S region. Nested PCR were done for elimination of opportunistic fungal pathogen elimination (Sezer et al., 2017). Same ITS primers were used for pathogen identification. Nested PCR with universal ITS primer amplicons were sent for sequencing were not identified as powdery mildew agents. These leaves are infected with other opportunistic fungal pathogens of *Alternaria spp.*, *Ramularia spp.*, *Phaeosphaeriopsis spp.* and *Leptospora spp.* that are found commonly in nature. Even though aim of the nested PCR was to eliminate opportunistic fungal pathogen identification, still these pathogens were selected with primers. Visual analysis of selected samples was concluded as powdery mildew infection however powdery mildew infection cannot be determined by PCR with universal ITS primers. Reason behind this might be other fungal contaminants were dominant than *E. corylacearum* infection or *E. corylacearum* infection were in minor levels to be detected by universal ITS primers. Next step for powdery mildew pathogen identification will be starting freshly with new DNA extraction. On the other hand, processes of extracting DNA, doing nested PCR amplification, sequencing and analyzing sequenced samples nearly take 10 days to complete. So rather than starting from the beginning *Erysiphe corylacearum* specific primers will be designed to eliminate the time and money lost. Before designing *E. corylacearum* primers powdery mildew infected leaf samples should be identified to eliminate other fungal pathogen contamination.

### **3.5 PCR analysis using Universal ITS primers with *E. corylacearum* infected leaf sample**

In Sabancı University *C. avellana* cv. Tombul and Çakıldak have been planted previously to run observations about hazelnut growth. These scrubs show effects of

powdery mildew infection. Powdery mildew infected hazelnut leaf samples are selected to design *Erysiphe* specific primers. Infected (showing white patches) and healthy (showing no white patches or other infection marks) leaf samples (sample collection on 26.09.2018 in Appendix B) of each *C. avellana* cv. Tombul and Çakıldak are collected from two different locations of Sabancı University. Collected leaf samples have been photographed and examined visually for traces of powdery mildew infection (Figure 25-26). Powdery mildew infection in selected leaves are defined more aggressive in adaxial of the leaves than underside of the leaves. *C. avellana* cv. Tombul leaf samples show more infection than *C. avellana* cv. Çakıldak leaf samples. *C. avellana* cv. Tombul leaf sample can be identified by naked eye. *C. avellana* cv. Çakıldak powdery mildew infection for lower garden can also be identified by naked eye but for Higher garden powdery mildew infection is diagnosed by microscope analysis.

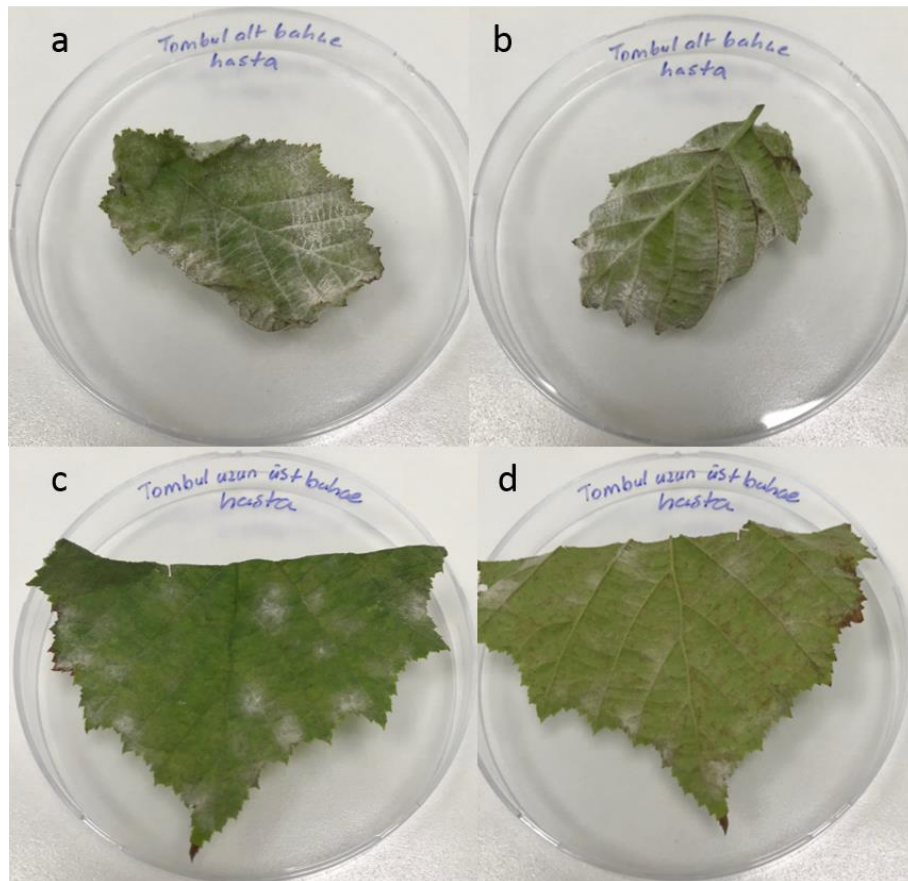


**Figure 28:** *C. avellana* cv. Tombul leaf samples. Effects of powdery mildew are white, persistent dense patches. Powdery mildew infection is more aggressive in adaxial of leaf than underside of the leaf. A) Adaxial of Powdery mildew infected leaf sample collected

from lower garden, B) Abaxial of Powdery mildew infected leaf sample collected from lower garden, C) Adaxial of Powdery mildew infected leaf sample collected from higher garden, D) Abaxial of Powdery mildew infected leaf sample collected from higher garden.

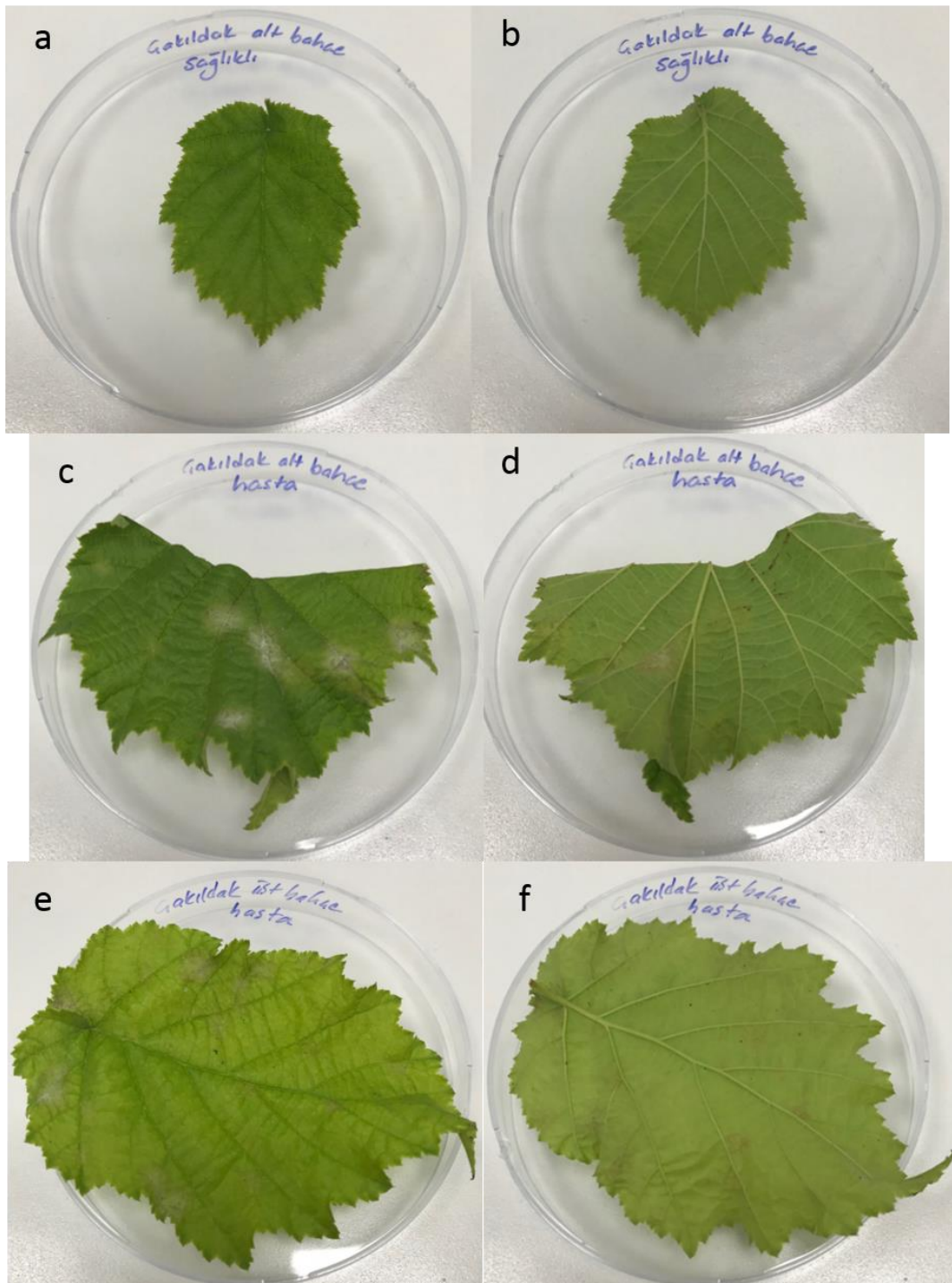


**Figure 29:** *C. avellana* cv. Çakıldak leaf samples. A) Adaxial of healthy leaf sample collected from lower garden, B) Abaxial of healthy leaf sample collected from lower garden, C) Adaxial of Powdery mildew infected leaf sample collected from lower garden, D) Abaxial of Powdery mildew infected leaf sample collected from lower garden, E) Adaxial of Powdery mildew infected leaf sample collected from higher garden, D) Abaxial of Powdery mildew infected leaf sample collected from higher garden.

DNA are extracted from collected leaf samples. Nested PCR are run with universal primers PM3-TW14-NL1 and expected amplicon size is 840bp. Agarose gel image display amplification for infected *C. avellana* cv. Tombul samples and healthy leaf sample meaning a fungal contamination is identified. *C. avellana* cv. Çakıldak infected leaf samples also produce amplicon, no amplicon is produced for healthy Çakıldak leaf sample meaning healthy leaf is not contaminated with any fungal pathogen (Figure 27).

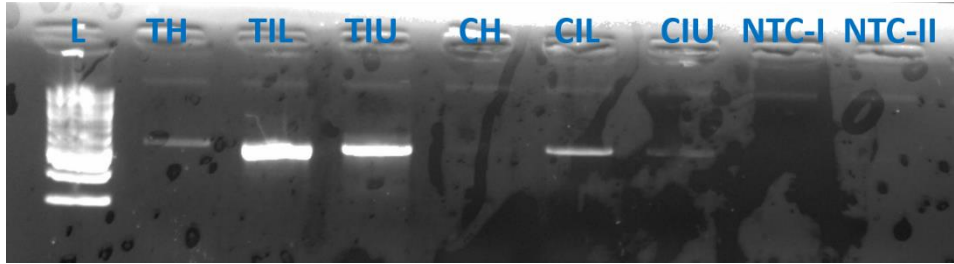


**Figure 30:** Sabancı University *C. avellana* cv. Tombul and Çakıldak healthy and infected leaf samples agarose gel electrophoresis. Expected amplicon size is 840bp. L: 1kb Ladder, TH: sample 1, TIL: Sample 2, TIU: Sample 3, CH: Sample 4, CIL: Sample 5, CIU: Sample 6, NTC-I: No template for PCR with primers PM3-TW14, NTC-II: No template for PCR with primers NL1-TW14.

Blast analysis showed the sequences matches to *Erysiphe* family members. *Erysiphe corylacearum* (isolate A. Sezer KX279887.1 and LC009928.1), *Erysiphe magnoliae* (KFMH1061), *Erysiphe necator* (MVAP06370315), *Erysiphe patagoniaca* (AB378745.1), *Erysiphe nothofagi* (AB378746.1), *Erysiphe corcicola* (LC228567.1), *Erysiphe convolvuli* (AB104518.1), *Erysiphe limonii* (LC010038.1), *Erysiphe monascogera* (AB331647.1), *Erysiphe quercicola* (LC128429.1), *Erysiphe paeoniae*

(AB257438.1) are the *Erysiphe* species and the GenBank accession number that were used for phylogenetic tree construction (Figure 28). Phylogenetic tree analysis and blast result show that selected samples were infected with powdery mildew pathogen *Erysiphe corylacearum*.

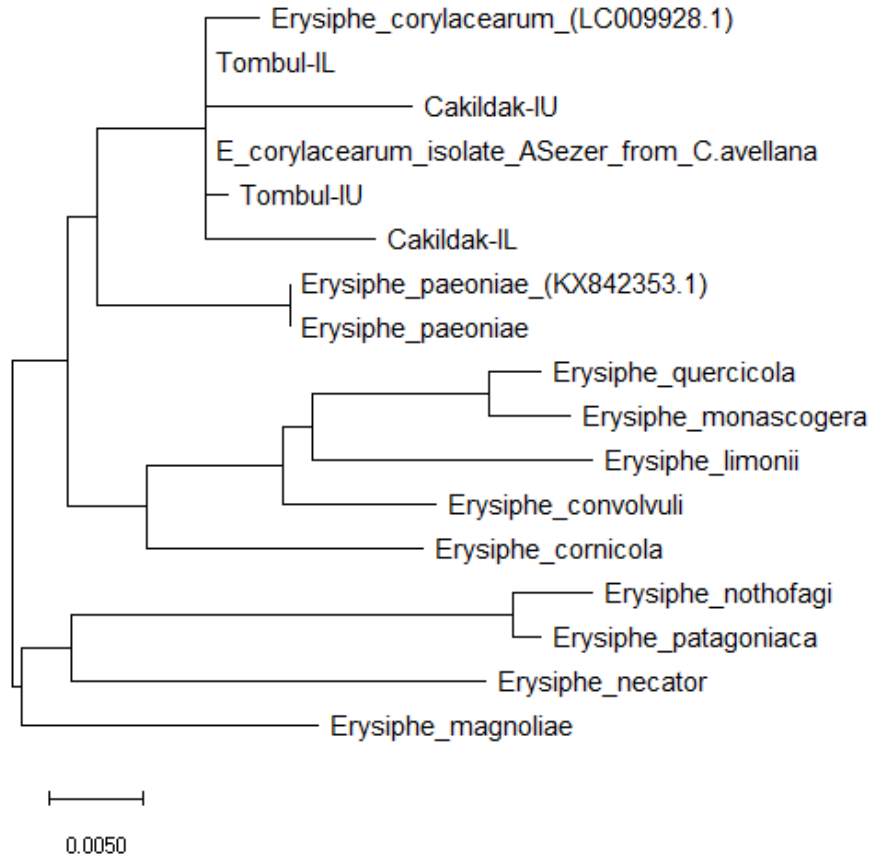


**Figure 31:** Phylogenetic tree of sequenced samples and *Erysiphe spp.*

Sabancı University powdery mildew infected *Corylus avellana* cv. Tombul and *Corylus avellana* cv. Çakıldak sample pathogens are identified as *E. corylacearum*. Other opportunistic fungal pathogens are not identified in any leaf sample. These leaf samples are perfect candidate to test the *E. corylacearum* specific primers since no fungal pathogen will encounter our analysis.

### 3.6 Designing *Erysiphe corylacearum* specific primers

*Ramularia* spp., *Alternaria* spp., *Phaeosphaeriopsis* spp. and *Leptospora* spp. species are previously encountered fungal pathogens during fungal pathogen identification. Blast results and *Corylus* sp. leaf pathogens (Table 2) are used for identifying candidate regions for primer design. *Erysiphe corylacearum* specific primers 28S rRNA gene regions of *Erysiphe corylacearum* and *Ramularia* spp., *Alternaria* spp., *Phaeosphaeriopsis* spp. and *Leptospora* spp. ITS sequences were analyzed by multiple sequence alignment. Five regions are identified for candidate sequences that are different with *Erysiphe corylacearum* and other fungi species (Figure 29). Two regions are used for forward primer design and three regions are used for reverse primer design (Table 5).

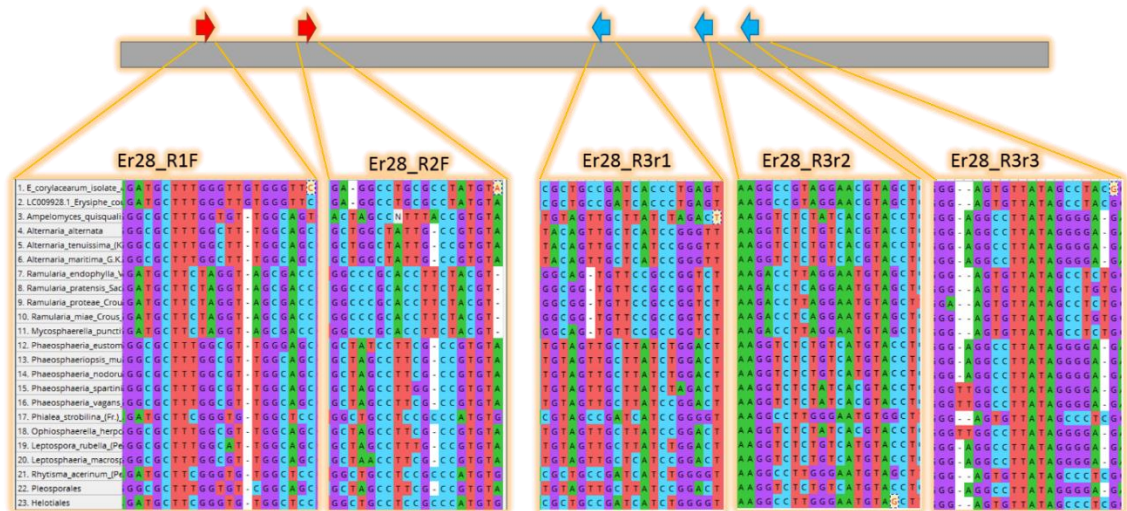


**Figure 32:** Sequence differences of the *Erysiphe corylacearum* and other leaf infecting fungal pathogens. Grey rectangle represents the whole ITS rRNA gene region and the arrows symbolize the primers; red for forward primers and blue for reverse primers.

**Table 5:** Designed primer for *Erysiphe corylacearum* specific fungal identification.

Type	Name	Sequence (5'→3')	Length	Start	Stop	Tm	GC%
F	Ec28_R1F	GATGCTTTGGGTTGTGGGTTTC	21	57	77	60.00	52.38
F	Ec28_R2F	AGGCCTGCGCCTATGTAAA	19	134	152	59.09	52.63
R	Ec28_R3r1	GAAAACTCAGGGTGATCGGC	20	365	346	58.91	55.00
R	Ec28_R3r2	GAGGAGCTACGTTCTACGG	20	440	421	59.34	60.00
R	Ec28_R3r3	TGGCACCGTAGGCTATAACA	20	468	449	58.51	50.00

Newly designed primers are tested with both Sabanci University leaf samples infected with *E. corylacearum* and Pasalar old leaf sample (17) infected with *Alternaria spp.* and Artıklı bud sample (51) infected with *Ramularia spp.*. Newly designed primers are tested with DNA and PCR amplicons with primers PM3-TW14 to see if nested PCR is necessary for designed primers. Expected amplicon sizes for R1-R3r1 is 309bp, R1-R3r2 is 384bp, R1-R3r3 is 412bp, R2-R3r1 is 232, R2-R3r2 is 307bp and R2-R3r3 is 335 bp (Figure 30). All newly designed primers give positive result for *E. corylacearum* infection and previously negative result for powdery mildew infection but positive for opportunistic fungal infection. All designed primers work effectively for *Erysiphe corylacearum* identification. Also designed primer works perfectly with the direct DNA usage rather than nested PCR amplicons. Meaning no nested PCR needed for *E. corylacearum* powdery mildew infection identification.

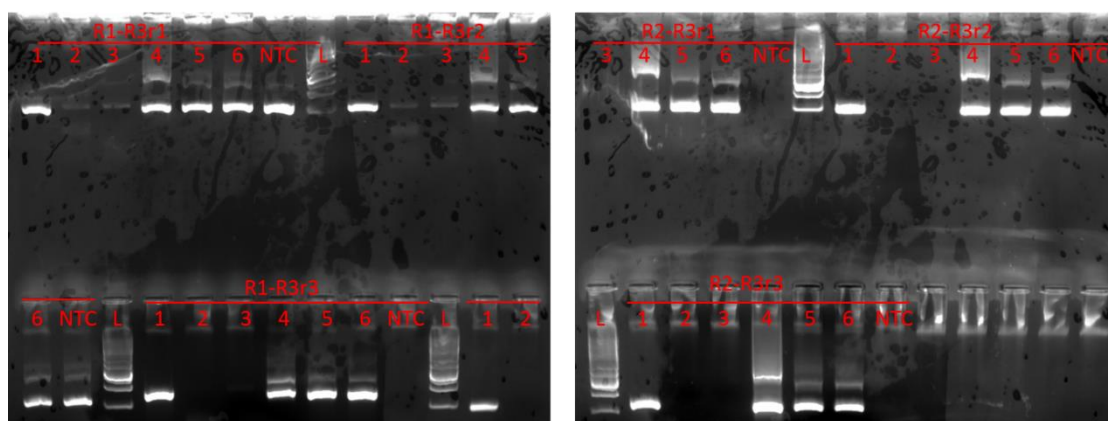


**Figure 33:** Gel results of newly designed primers for *Erysiphe corylacearum* identification. 1 and 4: Powdery mildew infected Tombul hazelnut leaf sample (sample 2), fungal agent: *Erysiphe corylacearum*, 2 and 5. Paşalar old leaf sample (sample 17), fungal agent: *Alternaria sp.*, 3-6. Artıklı bud sample (sample 51), fungal agent: *Ramularia sp.*, L: 1kb Ladder, NTC: No template. R1: Forward primer from region 1, R2: Forward primer from region 2, R3r1: Reverse primer from region 3, R3r2: Reverse primer from region 4, R3r3: Reverse primer from region 5.

Achievement with *E. corylacearum* specific primers are eliminating two steps of fungal pathogen identification. Sequencing of PCR amplicons and blasting the results with hazelnut leaf pathogens and other fungal ITS sequences are not needed anymore. Gel electrophoresis result with amplification means sample is infected with *E. corylacearum*. If there is no amplification observed in the gel electrophoresis, then analyzed samples are not infected with *E. corylacearum*. Designed *E. corylacearum* specific primers not only shorten the time of fungal pathogen identification but also lower the price for validation of pathogen.

### **3.7 Analyzing collected leaf samples with newly designed *E.corylacearum* specific primers**

Newly designed primers are tested on all collected samples to compare with microscope observation and validate the infected agent as *E. corylacearum*. Ec\_R1-R3r3 primers are chosen to be tested for *E. corylacearum* powdery mildew infection analysis (Figure 31-34). Gel electrophoresis with amplification are confirmed positive for powdery mildew infection with pathogen is *E. corylacearum*. PCR analysis with Ec\_R1-R3r3 are summarized in Appendix B.

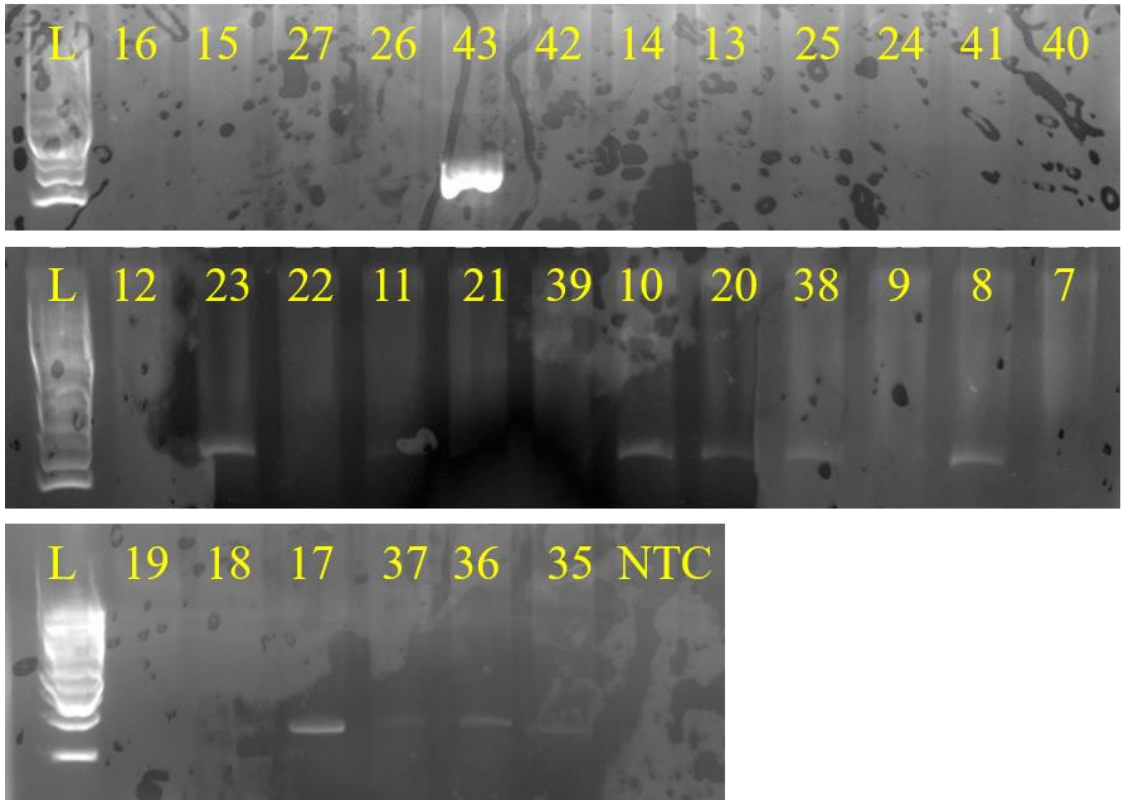


**Figure 34:** All 2018 samples sent from Sakarya and Düzce orchards agarose gel image result of PCR with primers Ec\_F1-R3. Samples 43, 23, 11, 10, 20, 38, 8, 17, 37, 36 are infected with *E. corylacearum*. L: 1kb Ladder, NTC: No template

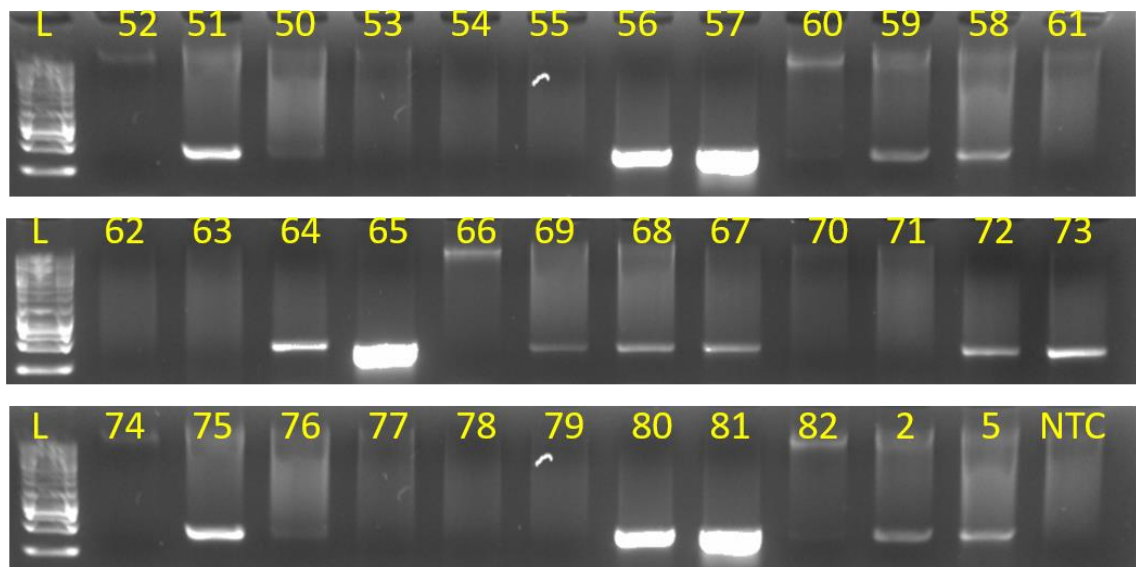


**Figure 7:** Ordu orchard samples agarose gel image result of PCR with primers Ec\_F1-R3. Sample 51, 56, 57, 59, 58, 64, 65, 69, 68, 67, 72, 73, 75, 80, 81 are infected with *E. corylacearum*. L: 1kb Ladder, NTC: No template

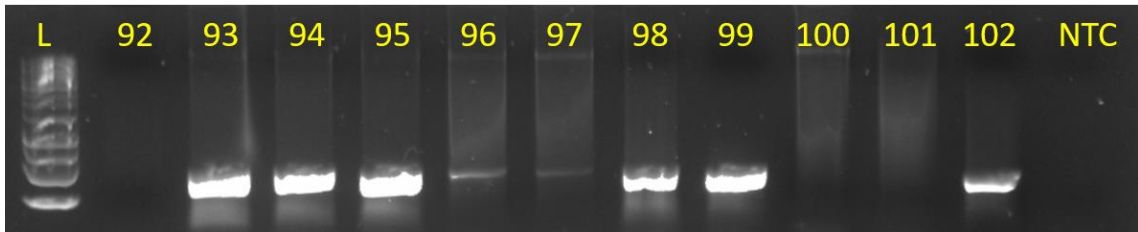


**Figure 35:** Different hazelnut cultivar samples agarose gel image result of PCR with primers Ec\_F1-R3. Sample 93, 94, 95, 96, 97, 98, 99 and 102 are infected with *E. corylacearum*. L: 1kb Ladder, NTC: No template

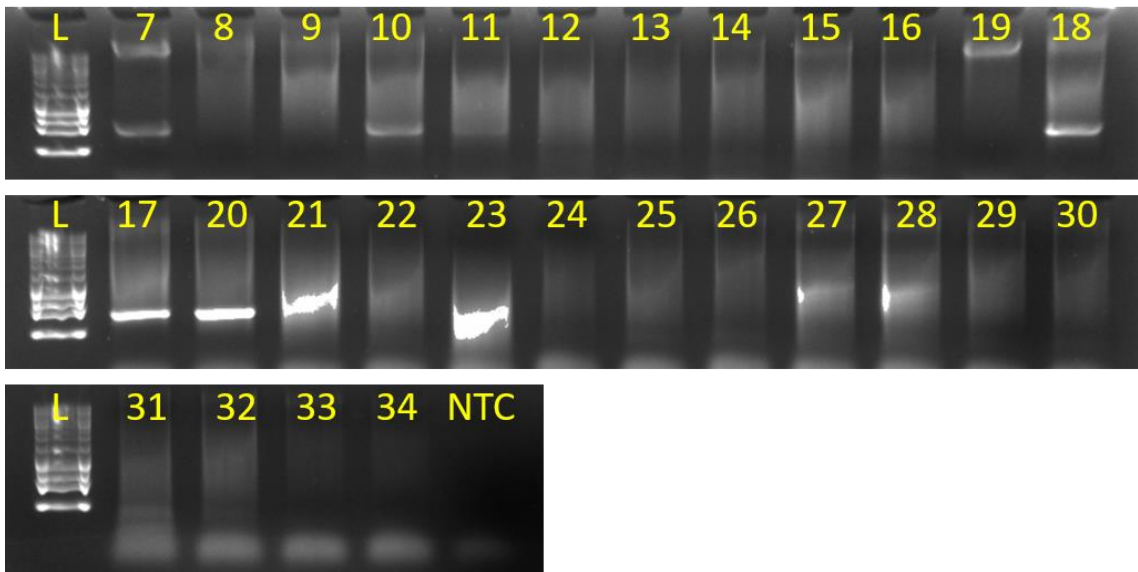


**Figure 36:** Düzce orchard samples agarose gel image result of PCR with primers Ec\_F1-R3. Sample 7, 10, 18, 17, 20 are infected with *E. corylacearum*. L: 1kb Ladder, NTC: No template.

Collected leaf samples from all orchards between 2018 and 2019 are infected with powdery mildew infecting agents *E. corylacearum*. Pathogen identification with *E. corylacearum* specific primers are more effective than pathogen identification with

Universal ITS primers. One of the disadvantages with pathogen identification by Universal ITS primers is instead of the target pathogen; primers can amplify opportunistic fungal pathogens or hyperparasite of targeted pathogen or even an unstudied fungi species. *E. corylacearum* specific primers eliminate the chances of amplification of other fungi species. Another disadvantage of universal ITS primers is each amplicon should be tested by sequencing and blast analysis since these primers are only selective for fungal identification rather than species specific identification. *E. corylacearum* specific primers are designed just to target *Erysiphe corylacearum* infection so positive result means there is 100% infection with *E. corylacearum*. Universal ITS primer pathogen identification consists of several steps most crucial step being sequencing, since not all universities and companies own a sequencing machine this step is the time and money consuming step. *E. corylacearum* specific primers eliminating sequencing step by lowering the cost and time for pathogen identification.

### **3.8 Powdery mildew infection copy number calculation**

Previous analysis with Ec\_F1R3 primers shows that with PCR analysis powdery mildew infection are detected in early stages of infection. Early detection of powdery mildew disease is crucial for treatment and protection of healthy scrubs. A limit of detection is created by calculating copy number. Collected samples are used for DNA extraction with covering same area for each sample. Infected leaf samples from Sabancı University, 2019 leaf samples from Düzce, Sakarya, Ordu and Giresun are used for copy number optimization.

Selected samples are firstly analyzed by PCR with Ec\_F1-R3 primers. Samples numbered 28-32 from Tahirli orchard, 44-47 from Süngüt orchard, 74-79 from Uzunisa orchard, 83-88 from Yağlıdere orchard and finally 2 and 4 from Sabancı university are selected. Amplicon results are positive for samples 2, 78, 79, 85, 88, 46, 47, 31 and 32. These samples are proven to be positive for powdery mildew infection with *E. corylacearum* (Figure 35).



**Figure 37:** Gel result of the 2019 season leaf samples tested with Ec\_F1-R3 primers.

A standard curve was set up by calculating the amounts of the Ec\_F1-R3 amplicons. Assuming each fungus cell contains one copy of the F1-R3 region, the number of copies of PCR product can be used as a measure of the number of fungus cells present in a sample. By diluting sample in constant ratio and measuring each diluted sample with qPCR, these results can be used for drawing a graph. Through graph the copy number estimation can be calculated.

Extracted DNA from leaf samples contain DNA of both *C. avellana* and *E. corylacearum*. Sample 2 (Tombul infected leaf) is selected for qPCR standart curve creation. Sample2 is amplified with Ec\_F1-R3 primers. Aim of the PCR to increase the fungal DNA concentration and eliminate the any plant DNA. PCR amplicon mixture is measured for DNA concentration and identified as 41,9ng for 1µL of sample. Copy number calculation formula is used for identifying the copy numbers of Ec\_F1-R3 amplicons (Equation1). Ec\_F1-R3 amplicon size is 414 bp. Molecular weight of the amplicon is calculated as 254.455,97 Da/bp.

$$\text{Copy number calculation formula: } \frac{\text{amount} \times \text{Avogadro number}}{\text{length of amplicon} \times 1 \times 10^9 \times \text{Molecular Weight}}$$

**Equation 1:** Copy number calculation formula.

Copy number of amplified infected sample is calculated as  $9,94 \times 10^7$  for 1  $\mu\text{L}$  of sample. Set of dilution is prepared by 1:10 ratio and slope-intercept equation ( $y=mx+b$ ) is used to create standard curve. Amplification curves are drawn for plant sample and each diluted sample (Figure 36). Plant sample with lowest Ct value, PCR amplicons highest Ct value and the Ct values decrease with the diluted amplicons.

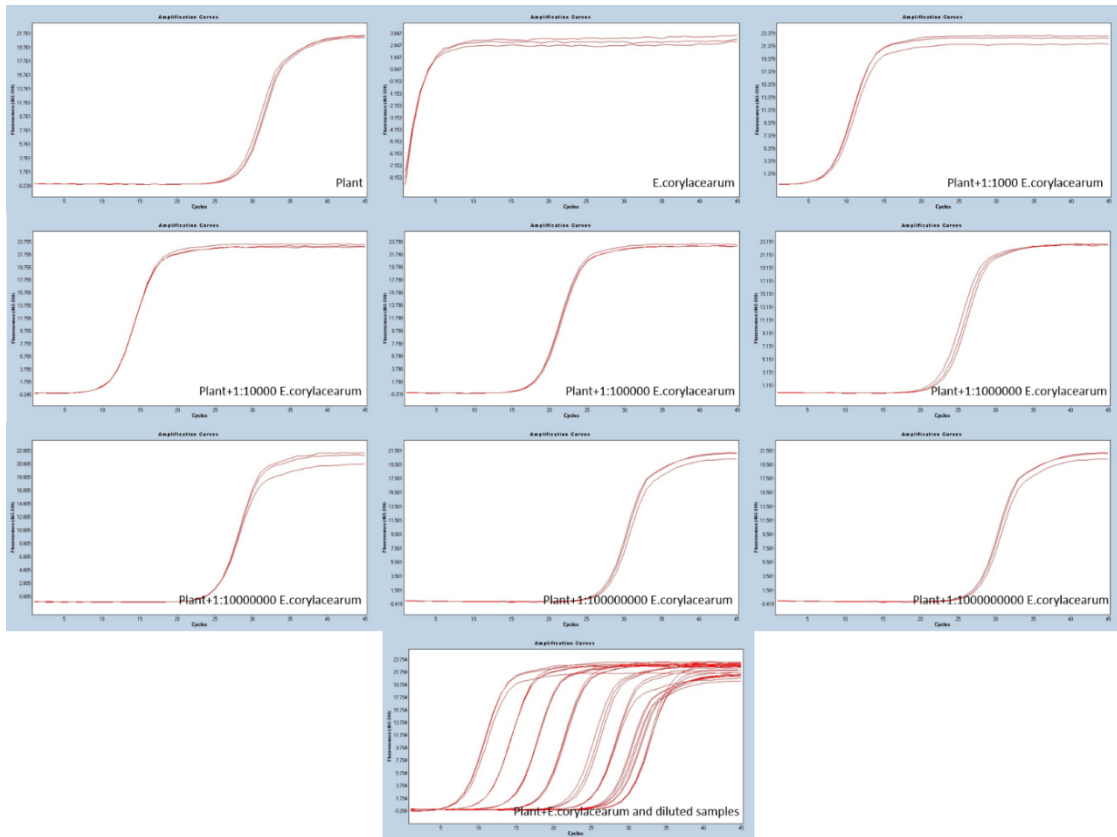


**Figure 38:** Amplification curves of plant, *E.corylacearum* amplicon and diluted samples with 1:10 ratio. Diluted samples and Ct values are proportionally decreasing. Plant sample is healthy sample collected from Sabanci University.

DNA extraction with analyzed samples contain both hazelnut and *E. corylacearum* DNA. Calculated DNA concentrations are formed of two species, to eliminate plant DNA concentration and increase the *E. corylacearum* concentration a standard PCR is done with Ec\_F1-R3 primers. PCR amplicons are measured for DNA concentration and recorded the value is 41,9ng. PCR amplicon is diluted with conserved 1:10 ratio and each dilute sample is measured for DNA concentration to validate the qPCR analysis. Diluted samples and healthy leaf sample are analyzed with qPCR. Each sample is loaded with

three technical replicates. Known concentration and calculated Ct values are used for creating standard curve. NTC and healthy leaf sample showing similar values meaning PCR amplification was necessary for a creating correct standard curved calculation.

Copy number calculation are done with known copy number calculation formula, but also without the formula calculation can be done manually. 1 µl samples are loaded for qPCR and PCR with recorded concentrations. Molecular weight is calculated from amplicon sequence of with each nucleic acid with previously known molecular weight (dATP 491.2 g/mol, dCTP 467.2 g/mol, dGTP 507.2 g/mol, dTTP 482.2 g/mol). Molecular weight of total amplicon is calculated as 254.455,97 Da/bp. Number of moles calculated by concentration divided by molecular weight and calculated as  $2,37 \times 10^{12}$  and multiply by Avogadro number ( $6,022 \times 10^{23} \text{ mol}^{-1}$ ). Diluted sample with 1:10 ratio copy number is calculated by decreasing one decimal of calculated copy number. Diluted sample 1:100 is selected as technical standard to be used in every copy number calculation experiments.

### **3.9 Limit of detection for *E. corylaearum* infection**

Samples collected on 2019 from each orchard are selected for copy number calculation. qPCR analysis is done by collected leaf samples, selected technical standard, healthy and infected sample. Each experiment is done with three technical replicates and average of each measurements are calculated. Result of qPCR is summarized in table 6.

Amplifications curve with no template and 1:100 dilute technical standard are set as the border of the measurements. Gel electrophoresis intensity are correlated with Amplifications curves. Uzunisa-5 sample gel electrophoresis is the dimmest sample and the amplification curve is closest to NTC, Sabancı infected sample with brightest agarose gel amplicon with closest to 1:100 technical standard (Figure 37).

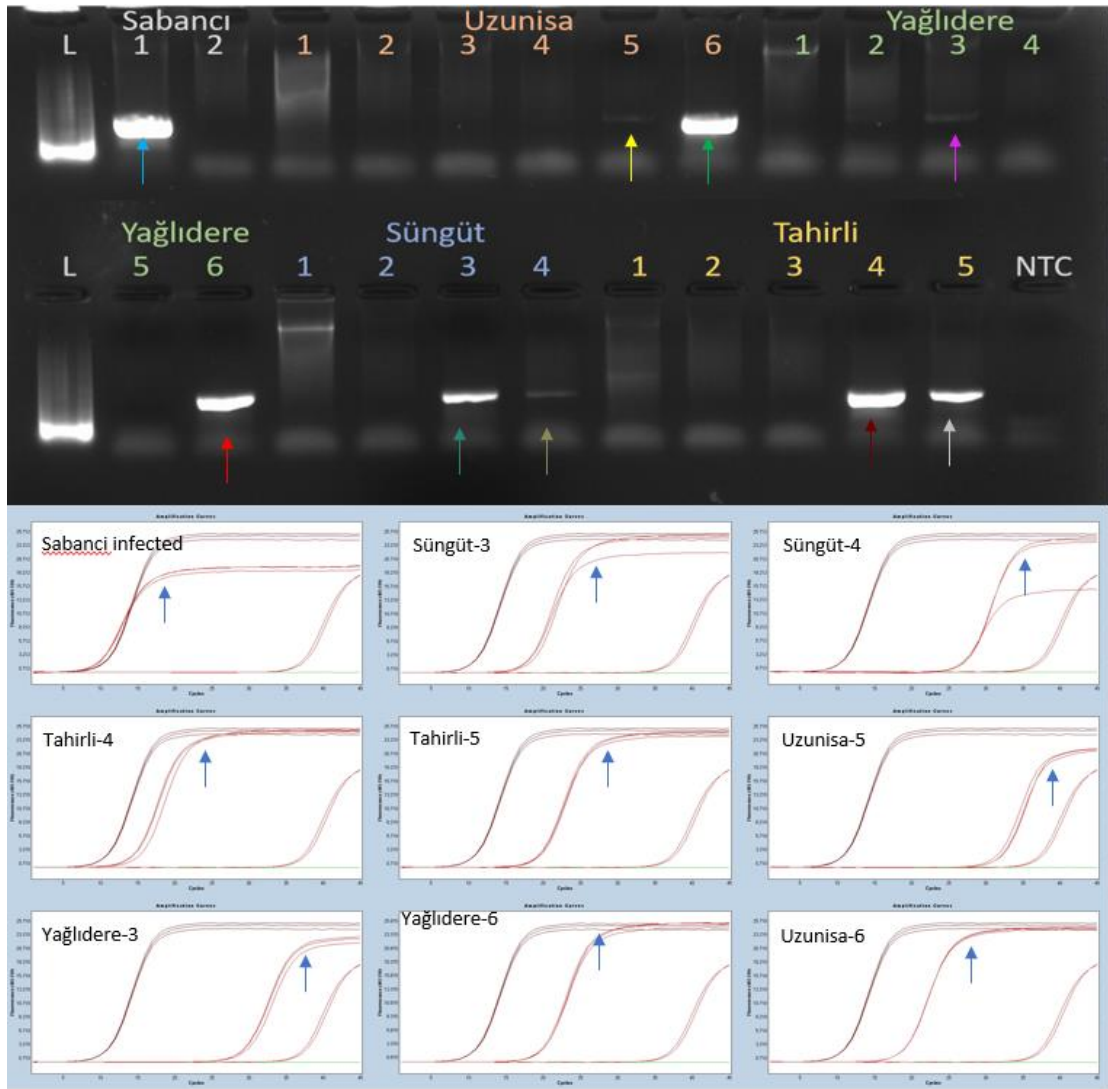


**Figure 39:** Gel electrophoresis result of PCR with Ec\_F1-R3 primers and qPCR analysis. Correlation between the amplicon band intensity and Ct values are identified.

Cq value are describe as number of amplification cycles required to reach a fixed signal threshold or fluorescent signal to cross the threshold. Values above 35 means fluorescent signal detection is less than a single molecule. No template Cq value is measured as 36,93, which prove there is no contamination occurred during experiment preparation. Healty leaf sample with 29,67 Cq value suggesting Cq values around 30 and higher are questionable for *E. corylacearum* infection and values higher are positive for *E. corylacearum* infection.

**Table 6:** Status of *E.corylacearum* infection by limit of detection. The status of the infection; ‘+’ mean sample is infected with *E.corylacearum*, ‘-’ mean there is no infection detected, ‘?’ is used for a weak result that might be positive, but was not significantly higher than the negative control samples.

Name	Cq	Measured Copy number	Status for <i>E.corylacearum</i> infection
NTC	<b>36,93</b>	0,105	Technical control (negative)
PCR Standard (1:100)	10,98	1553333,333	Technical standard (1.55 million copies)
Healthy (4)	<b>29,67</b>	9,713333333	-
Infected (2)	9,697	3540000	+
Uzunisa-5 (78)	<b>31,8</b>	2,486666667	?
Uzunisa-6 (79)	18,95	9383,333333	+
Yaglidere-3 (85)	<b>29,48</b>	5000	?
Yaglidere-6 (8)	19,93	5000	+
Sungut-3 (46)	18,17	15800	+
Sungut-4 (47)	27,13	52,76666667	+
Tahirli-4 (31)	14,83	135833,3333	+
Tahirli-5 (32)	19,61	6143,333333	+

In the “?” samples, the measured presence of *E.corylacearum* DNA is very low (2-12 copies), and could possibly be a result of background contamination, as the negative control gave a similar result. Therefore, the orchards these samples were collected from should be observed and tested again in 1-2 weeks.

‘Measured Copy number’ shows the estimated number of *E. corylacearum* cells found in each leaf sample; positive infection could be detected from c.50 copies (Süngüt-4) up to the most heavily infected samples, with 3-4 million copies of the target DNA region. Samples with infection visible to the naked eye had > 5,000 copies of the target DNA region. All samples are analyzed with qPCR to identify copy number and recorded in Appendix B.

### 3.10 Loop Mediated Isothermal Amplification Assay (LAMP):

28S and ITS regions are selected for primer design (Table 7). LAMP primers are design by PrimerExplorer V5 program and confirmed by Blast with *Corylus avellana* genome and hazelnut leaf fungal pathogen ITS sequences to prevent misamplifications.

**Table 7:** Designed LAMP primers. 28S: primers designed from 28S region, ITS: primers design from ITS region.

Primer ID	Length (nt)	Sequence 5'→3'
Ec28S-F3	18	TGCCGATCACCTGAGTT
Ec28S-B3	19	TGGTCCGTGTTTCAAGACG
Ec28S-FIP	43	ACGGCCTTTATCCAGCCACCTATATCTCAGGTGCACTCGACAG
Ec28S-BIP	43	ATAGCCTACGGTGCCATGCAGATTATACGCCAGCATCCTAGCC
Ec28S-FLP	18	AACCGATGCTGGCCTGTG
Ec28S-BLP	17	GACCGAGGACCGCGCTT
EcITS-F3	20	TGTTTCGAGCGTCATAACACC
EcITS-B3	19	CGAGGTCAACCTGTGATCC
EcITS-FIP	44	ACCGCCACTGTCTTTAAGGGCTTTACTTTGTGTGGTTGCGGTGT
EcITS-BIP	45	GCGTGGGCTCTACGCGTAGTATAAAGTGACTGAGCAAAGGGCTT
EcITS-FLP	18	GCACCGCGACGTGCCCA
EcITS-BLP	19	GCTTCTCGCGACAGAGTGA

LAMP primers 28S and ITS are tested with sample 2 (Sabancı infected Tombul) to define optimum time for primer amplification.. 28S primers started to amplify sample after 10 minutes and ITS primers started to amplify after 20 minutes but the intensity of the band are generally smear (Figure 38).

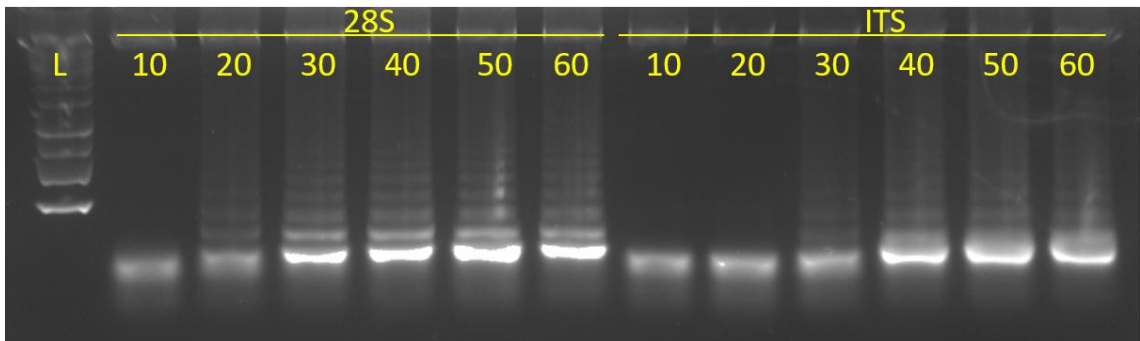


**Figure 40:** Time dependent amplification of LAMP primers ITS and 28S tested on sample2.

Lamp primers are tested for infected (2) and healthy (3) leaf samples. Amplifications with ITS LAMP primers are positive for all samples including NTC. NTC contamination can occur due to a contamination in mixture solution or by primer dimer formation. 28S LAMP primer are clean for healthy leaf sample and NTC (Figure 39). *E. corylacearum* specific 28S LAMP primers can be use for powdery mildew detection.

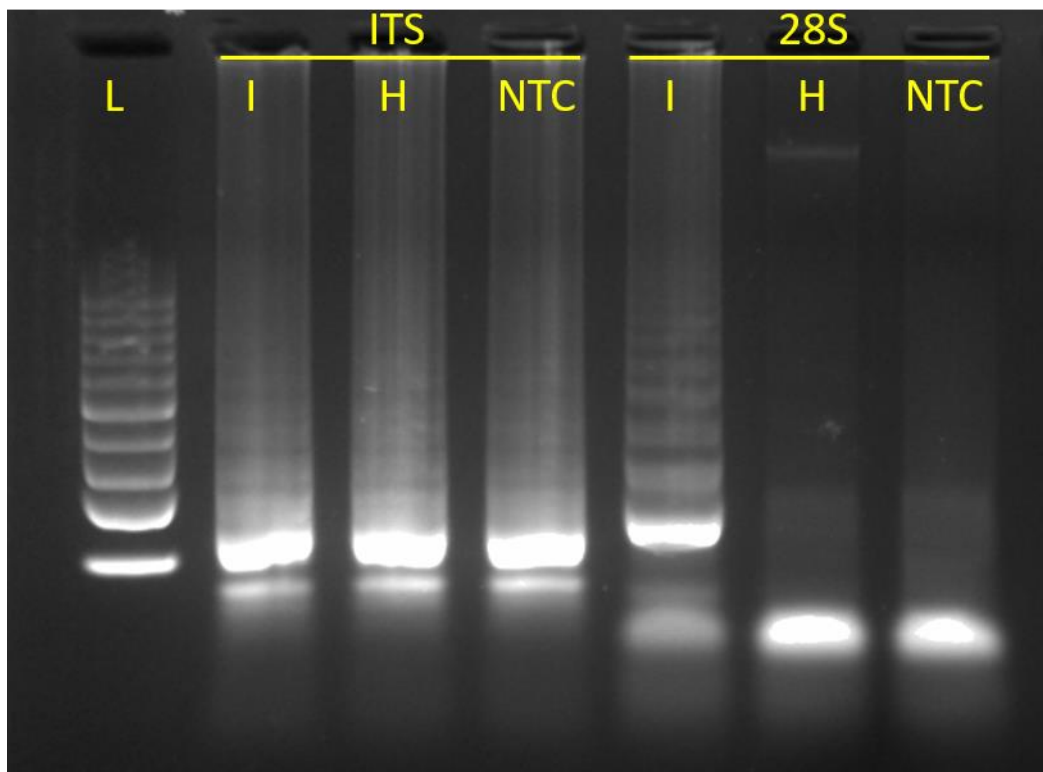


**Figure 41:** *E. corylacearum* specific LAMP primers. I: Infected leaf sample, H: Healthy leaf sample, NTC: No template, L:1kb ladder.

Development of LAMP method was crucial for on field research for pathogen identification since this method eliminate usage of thermocycler. A simple machine-like water bath was enough for species identification. Species specific primers were designed for LAMP based pathogen detection for plant fungal pathogen (Niessen, 2015). Recent studies showed that this method was also used for powdery mildew pathogen detection. LAMP detection was used for identification of *E. necator* a grape powdery mildew pathogen with simple DNA extraction method (Thiessen et al., 2018).

*E.corylacearum* specific primers from ITS and 28S region was designed to be used in LAMP detection. Unfortunately ITS region primers was created non-specific amplifications, but 28S LAMP primers were successful for *E.corylacearum* identification. Previously used simple DNA extraction method and *E.corylacearum* 28S-LAMP primers can be used for powdery mildew pathogen detection on field analysis.

### **3.11 *Phylactinia guttata* identification by Universal primers**

Düzce trip collected leaf samples are analyzed with universal ITS primers NL1-TW14-PM3 and PMITS1-PMITS2-ITS4-ITS5 by nested PCR. Expected amplicon size of *E.corylacearum* from nested PCR with NL1-TW14 is 860bp and for ITS4-ITS5 is 678bp, expected amplicon size of *P. guttata* from nested PCR with NL1-TW14 is 885bp and for ITS4-ITS5 is 683bp. Morphological analysis show sample number 2, 103, 105, 107, 108 and 111 are infected with *E. corylacearum*, sample number 104, 109 and 110 are infected with *P. guttata*, sample number 106 are infected with both pathogen. Gel electrophoresis result with primers NL1-TW14 are samples numbered with 5,6, 8 are higher than other amplicons (Figure 40). Gel electrophoresis result with primers ITS4-ITS5 samples numbered with 2, 4, 6 have lower bands than samples 3, 5, 8, 9 and sample 7 having two bands (Figure 41). Results are questionable with different from observation so samples 4, 5, 6 and 8 are sent for sequencing.

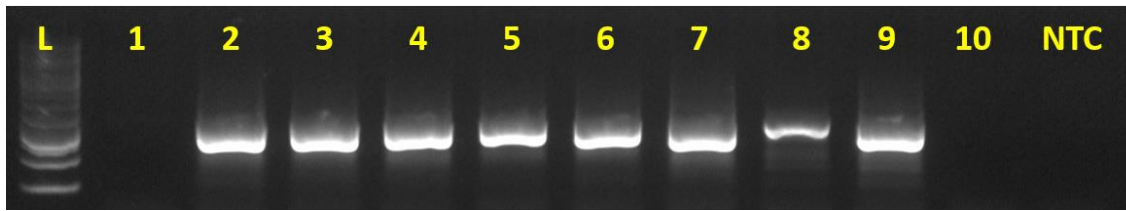


**Figure 42:** Fungal pathogen identification with universal primers NL1-TW14 for Düzce trip samples

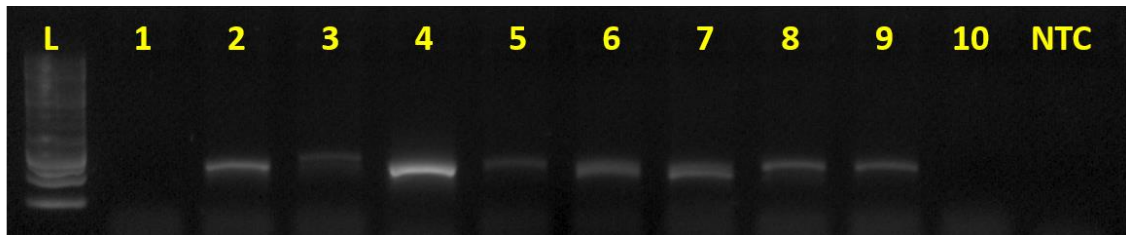


**Figure 43:** Fungal pathogen identification with universal primers ITS4-ITS5 for Düzce trip samples

All amplicons extracted by primers NL1-TW14 and amplicon 6 extracted by primers ITS4-ITS5 were failed in sequencing. Unfortunately, sequenced samples with ITS4-ITS5 primers were not identified by phylogenetic analysis with hazelnut leaf fungal pathogens rather the amplifications occurred due to saprophytic fungi occurrence. Visual observations identify both powdery mildew pathogens were occurred on Düzce field trip collected samples. Different size of amplicons was expected to occur due to the identification of both powdery mildew pathogen on infected leaf samples. However universal ITS primer failed to identify targeted powdery mildew fungal pathogens.

Düzce orchards collected leaf samples were collected in late season where the leaves started to senescence and fall. Occurrence of saprophytic fungi was no surprise. However universal ITS primers failed for detection of minor pathogen infection. Lowering the detection time and eliminating the experiment repeats *P. guttata* specific primer should be designed to identify targeted fungal pathogen.

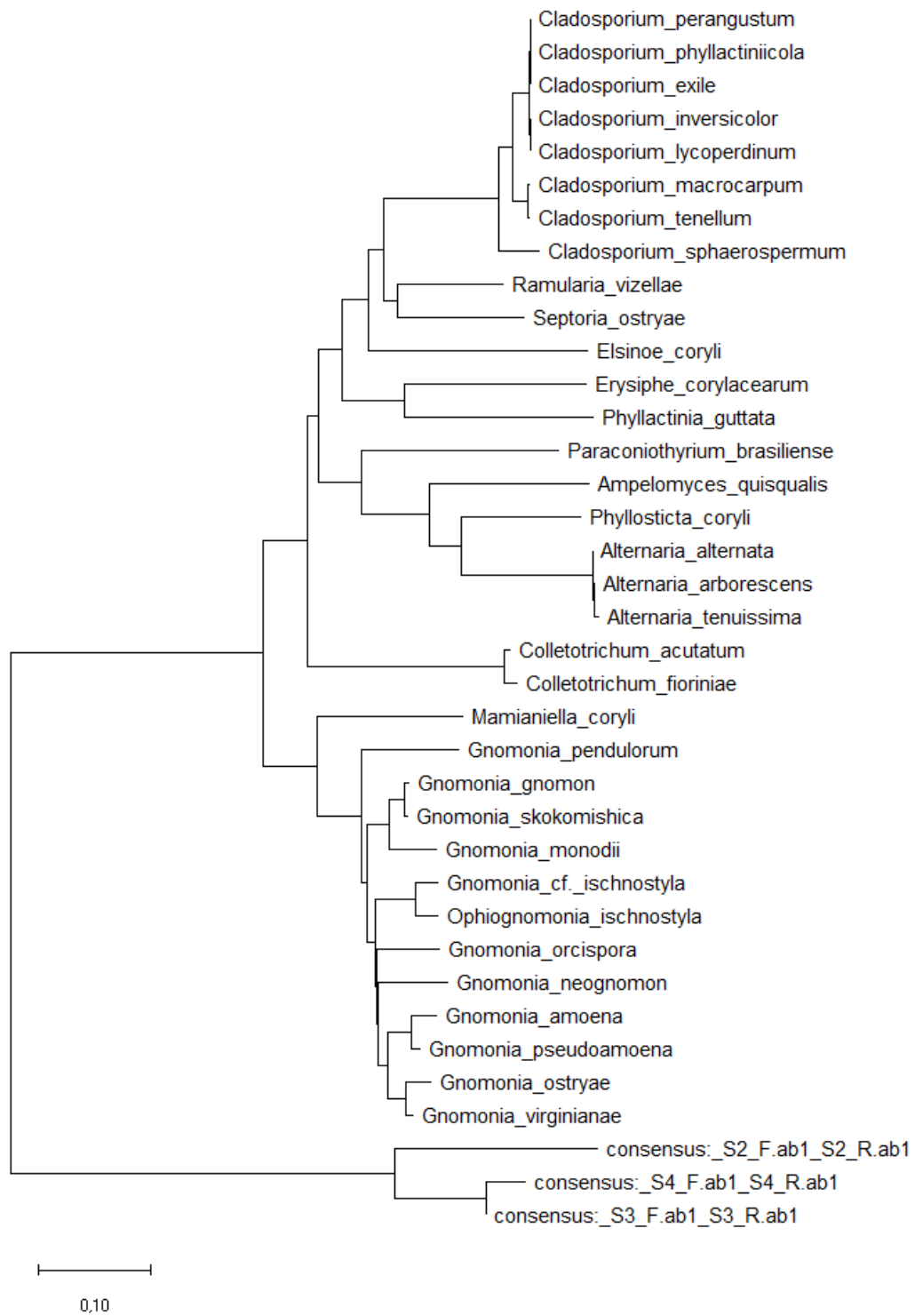


**Figure 44:** *P. guttata* infected leaf sample sequenced analysis result by phylogenetic tree.

### 3.12 *Phylactinia guttata* specific primer design

Three regions are identified that show difference between *Phylactinia guttata* and other fungi species that can be used for primer design. *P. guttata* specific primer sequences are reported in table 8. Expected amplicon size for Pg1 is 179bp and for Pg2 is 375bp.

**Table 8:** *Phylactinia guttata* specific primers.

Type	Name	Sequence (5'→3')	Length	Start	Stop	Tm	GC%
F	Pg1-F	GTGAAGACTCTCGGCCCC	18	37	54	59.42	66.67
R	Pg1-R	TCAAGTTTTCTCTGGCAGGC	20	196	215	58,39	50
F	Pg2-F	CGTGCCTGCCAGAGAAAAC	19	193	211	59,42	57,89
R	Pg2-R	TCGTCTTTTGGCTGGATCCA	20	551	567	59,31	50

Gel electrophoresis result of *P. guttata* specific primer Pg1 show two different sized amplicons.

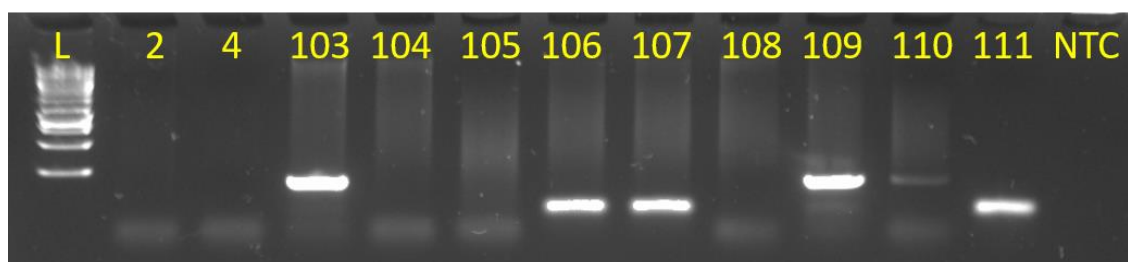


**Figure 45:** Gel electrophoresis result of *P. guttata* specific primer Pg1. L: 1kb Ladder, NTC: No template, expected amplicon size 179bp.

Gel electrophoresis result of *P. guttata* specific primer Pg2 amplicon sizes matches to expected amplicon size. Sample 2 is *E. corylacearum* infected and Sample 4 is healthy leaf sample. Suggesting *P. guttata* specific primers Pg2 intercept with these samples. For further validation these samples should be sequenced and identify by blasting fungal ITS sequences.



**Figure 46:** Gel electrophoresis result of *P. guttata* specific primer Pg2. L: 1kb Ladder, NTC: No template, expected amplicon size 375bp.

Powdery mildew on hazelnut were caused by two pathogens *E. corylacearum* and *P. guttata*. *P. guttata* were reported to infect diverse range of hard-shelled fruiting plants (Saenz and Taylor, 2015). However, this pathogen causes no significant damage to hazelnut scrubs and unlikely to threaten the long-term survival of infected hazelnut scrubs. Our aim was to develop hazelnut powdery mildew specific pathogen detection so both *E. corylacearum* and *P. guttata* hazelnut powdery mildew pathogen specific primer was developed in this process.

#### 4.8 Identification of MLO gene family

The InterPro domain IPR004326, ‘MLO-related protein’ are annotated to the *Corylus avellana* genome and 24 gene models were identified with matching regions. These sequences were re-annotated manually and examined sequence similarity and secondary structure prediction 11 of these gene models were found to encode full-length MLO proteins. In order to identify those most likely to be involved in powdery mildew infection, the predicted protein sequences were aligned with the original MLO protein from barley (HvMLO), *A. thaliana* and apple. Phylogenetic tree was used to cluster the sequences, which formed 8 clades.

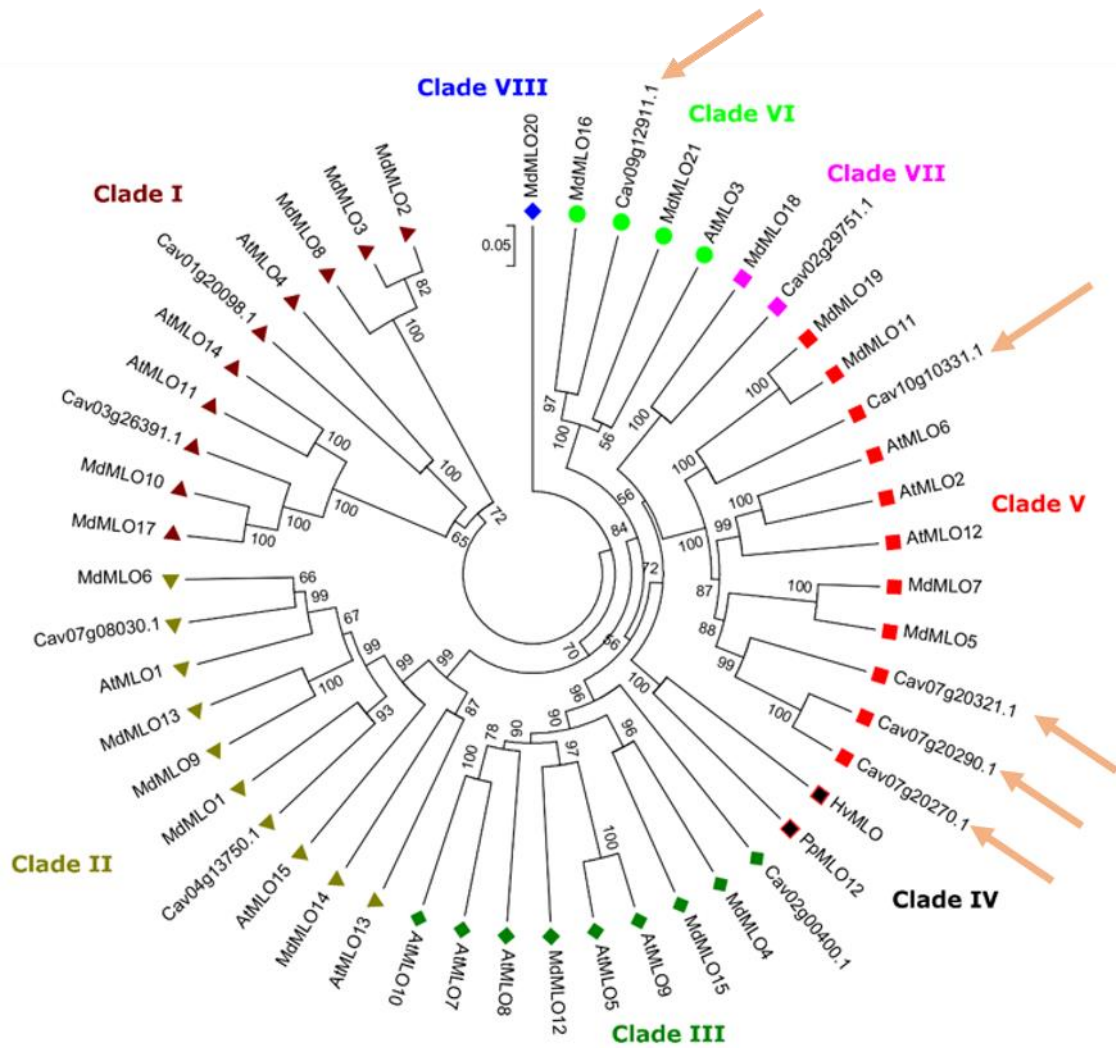


**Figure 47:** A. Phylogenetic clustering of *C.avellana* MLO gene models with those from *A. thaliana* and *Malus domestica*, using the UPGMA approach. Branch lengths are scaled to the number of amino acid differences per site (p-distance method); node confidence values are % of 1000 bootstrap replications. Yellow arrows are showing the selected genes for experimental validation (S. J. Lucas et al., 2019).

Mildew Locus O gene family are membrane proteins that contains calmodulin binding domain located with intracellular carboxy terminus. MLO contains seven membrane-spanning helices and formed by intracellular loop structures (Pessina et al., 2016). MLO proteins have role in several physiological processes such as root morphogenesis and pollen tube. In 1942 a loss of function mutation in MLO gene family caused to develop powdery mildew resistance to *Erysiphe graminis f.sp. hordei* in barley. The mechanism behind the resistance occurred by inhibiting pathogen penetration through cell stoma.

Multiple groups identified the powdery mildew resistance created by MLO resistance. Also, it was showed that MLO gene resistance was not match to the gene-for-gene system process.

Eleven full length MLO proteins were identified from hazelnut genome. Five of these identified protein was matched within the clade V and clade IV. Cav02g2975.1, Cav07g20321.1, Cav07g20270.1, Cav07g20290.1 and Cav19g10331.1 were selected for physical validation.

#### **4.9 Mildew Locus O (MLO) gene family experimentally validation for *Corylus avellana***

MLO specific primers were designed for Cav02g2975.1, Cav07g20321.1, Cav07g20270.1, Cav07g20290.1 and Cav19g10331.1 genes. Expected amplicon size for Cav02g2975.1 is; 494 for cDNA, 1346 for DNA, for Cav07g20321.1 is; 314 for cDNA, 1335 for DNA, for Cav07g20270.1 is; 180 for cDNA, 1384 for DNA, for Cav07g20290.1 is; 808 for cDNA, 1774 for DNA and lastly for Cav19g10331.1 is; 329 for cDNA, 737 for DNA. Collected leaf samples from Sabanci University was classified as healthy, mildly infected with powdery mildew and highly infected with powdery mildew. These samples were used for RNA isolation. Also previously identified powdery mildew infected leaf samples gDNA were used for validation. Gel amplification were occurred for Cav02g2975.1 were higher than expected size, so these amplicons should be sent for sequencing for further validation.

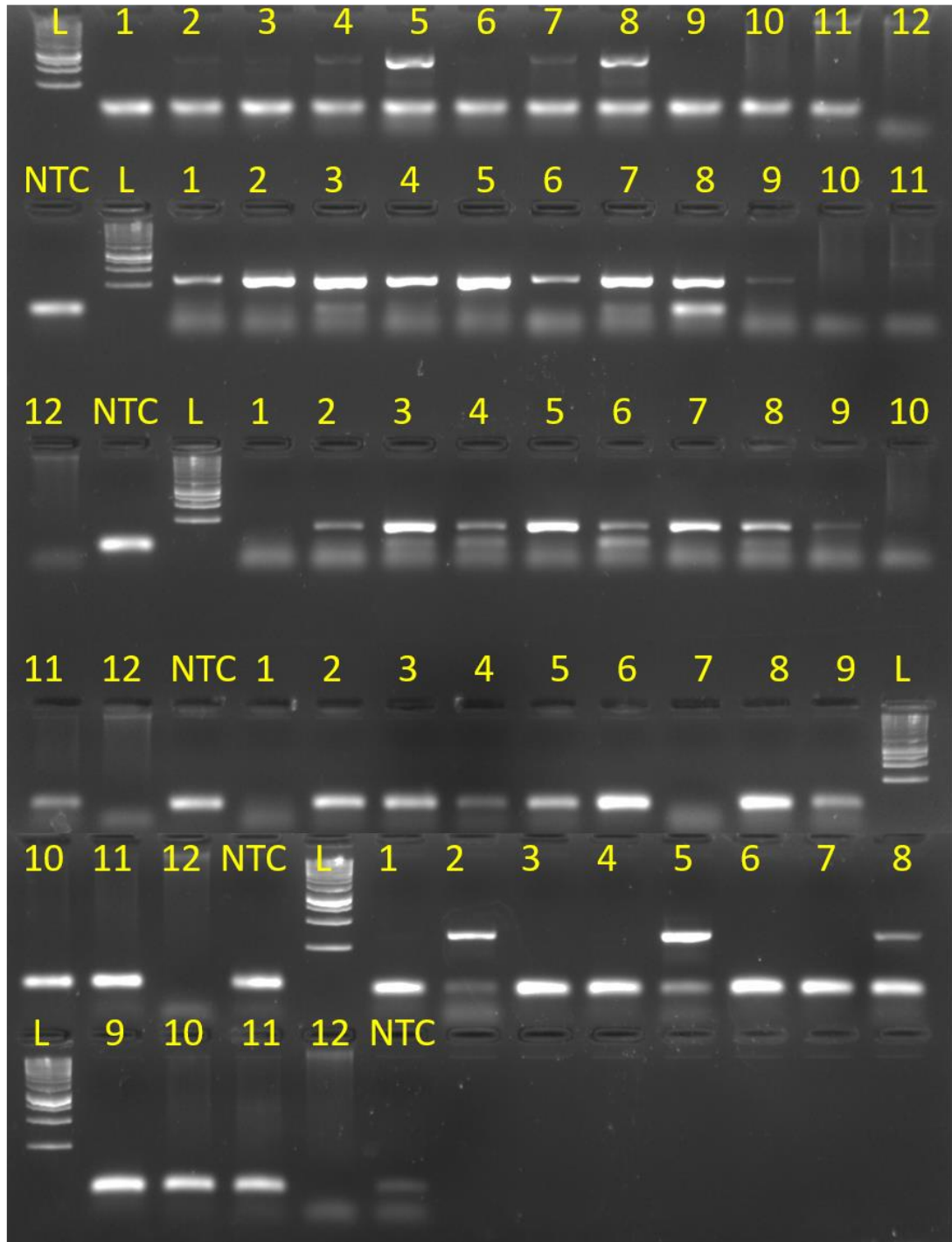


**Figure 48:** Samples with number 1,2,3; Healty leaf cDNA, 4,5,6; Lighty infected leaf cDNA, 7,8,9; Heavly infected cDNA, 10,11; infected leaf DNA, 12; Healty leaf DNA. Order of the amplicons are as flows; Cav02g2975.1, Cav07g20321.1, Cav07g20270.1, Cav07g20290.1 and Cav19g10331.1.

#### 4. CONCLUSION

Powdery mildew infection on *Corylus avellana* are caused by two pathogen *Erysiphe corylacearum* and *Phylactinia guttata*. *P. guttata* have minor effects on hazelnut scrub so usually the disease left untreated. However, *E. corylacearum* have more destructive effects on hazelnut scrub. In 2014 destructive powdery mildew infection started to appear on hazelnut orchards in Karadeniz region of Turkey and by 2015 all orchards are infected by this disease. By 2018 destructive powdery mildew disease caused by *E. corylacearum* have been identified in Europe and Asia. Hazelnut orchards from Düzce, Sakarya, Ordu and Giresun have been selected that show destructive powdery mildew. Sample collection and pathogen identification have been carried out for two years.

Powdery mildew analysis started with the examination of atmospheric conditions. Several studies about the powdery mildew points out the effects of humidity, temperature, wind, rain and solar radiation on the effects of powdery mildew germination and propagation. Weather conditions are collected from selected weather station near the orchards. Propagation about the powdery mildew disease have been explained however amount of collected leaf samples are not enough to correlate any relation between the disease development and atmospheric conditions.

Collected leaf samples from selected orchards are visually examined. Morphological characteristic which are previously described match with our observations. Chasmothecium morphology of *E. corylacearum* appendages are dichotomously branched and curved tips and chasmothecium morphology of *P. guttata* appendages are bulbous swelling at the base and straight to the tip. Morphological analysis is validated with genetic identification.

Universal identification methods of fungal pathogen are done by examination of ITS regions. Identification starts with extracting DNA from fungal pathogen. Followed by PCR amplification with universal ITS primers. Amplified samples are sequenced and blast with the known ITS fungal sequences. We follow the same procedure for fungal pathogen identification however our fungal pathogens are identified as other opportunistic fungal pathogen that are also use hazelnut as hosts.

We decide to develop an enhanced method for pathogen identification that is specific to powdery mildew pathogen *E. corylacearum*. Also hoping to lower the cost and time needed for identification. Started with designing *E. corylacearum* specific primers that

eliminate the risk of encountering by opportunistic pathogens also, by eliminating sequencing and blast analysis these primer save 10 days from our analysis. Newly designed primers are effective for *E. corylacearum* identification however any issues that could be encountered with primers are also presented here especially the risk of contamination while sample preparation to PCR analysis.

*E. corylacearum* specific primer are than use for copy number calculation. Assuming each fungus cell contains one copy of the R1F1-R3R3 region, the number of copies of this PCR product can be used as a measure of the number of fungus cells present in a sample. Copy number of PCR amplicon are calculated by copy number calculation formula and created a set of dilution with known copy number and with slope-intercept equation. All samples are calculated and created a limit of detection.

Lastly for enhancing *E. corylacearum* identification method we designed 28S-LAMP primers that can be adaptable for colorimetric analysis. By further adaptations these methods can be altered to powdery mildew pathogen identification that can be directly use in field or orchards.

We conclude our study by the identification of MLO family sequences from hazelnut genome. There are eleven genes identified for MLO gene family however only five of them were in Clade V and Clade VI that were related for powdery mildew resistant. Selected genes were validated by MLO specific primers.

## **References:**

- Abasova, L. V., Aghayeva, D. N., & Takamatsu, S. (2018). Notes on powdery mildews of the genus *Erysiphe* from Azerbaijan. *Current Research in Environmental and Applied Mycology*, 8(1), 30–53. <https://doi.org/10.5943/cream/8/1/3>
- AGRIOS, G. N. (2005). *chapter eleven - PLANT DISEASES CAUSED BY FUNGI* (G. N. B. T.-P. P. (Fifth E. AGRIOS (ed.); pp. 385–614). Academic Press. <https://doi.org/https://doi.org/10.1016/B978-0-08-047378-9.50017-8>
- Al-Khayri, J. M., Jain, S. M., & Johnson, D. V. (Eds. ). (2019). *Advances in Plant Breeding Strategies : Nut and Beverage Crops* (Vol. 4). [https://doi.org/Al-Khayri, J. M., Jain, S. M., & Johnson, D. V. \(Eds.\). \(2019\). Advances in Plant Breeding Strategies: Nut and Beverage Crops. doi:10.1007/978-3-030-23112-5](https://doi.org/Al-Khayri, J. M., Jain, S. M., & Johnson, D. V. (Eds.). (2019). Advances in Plant Breeding Strategies: Nut and Beverage Crops. doi:10.1007/978-3-030-23112-5)
- Altin, N., & Gülcü, B. (2018). Potential of *Ampelomyces* as a biological control agent against powdery mildew in hazelnut orchards. *International Journal of Agriculture and Biology*, 20(9), 2064–2068. <https://doi.org/10.17957/IJAB/15.0732>
- Amsalem, L., Freeman, S., Rav-David, D., Nitzani, Y., Szejnberg, A., Pertot, I., & Elad, Y. (2006). Effect of Climatic Factors on Powdery Mildew Caused by *Sphaerotheca macularis* f. sp. *Fragariae* on Strawberry. *European Journal of Plant Pathology*, 114(3), 283–292. <https://doi.org/10.1007/s10658-005-5804-6>
- Angeli, D., Pellegrini, E., & Pertot, I. (2009). Occurrence of *Erysiphe necator* chasmothecia and their natural parasitism by *Ampelomyces quisqualis*. *Phytopathology*, 99(6), 704–710. <https://doi.org/10.1094/PHYTO-99-6-0704>
- Arena, M., Auteri, D., Barmaz, S., Bellisai, G., Brancato, A., Brocca, D., Bura, L., Byers, H., Chiusolo, A., Court Marques, D., Crivellente, F., De Lentdecker, C., Egsmose, M., Erdos, Z., Fait, G., Ferreira, L., Goumenou, M., Greco, L., Ippolito, A., ... Villamar-Bouza, L. (2017). Peer review of the pesticide risk assessment of the active substance *Ampelomyces quisqualis* strain AQ10. *EFSA Journal*. *European Food Safety Authority*, 15(12), e05078. <https://doi.org/10.2903/j.efsa.2017.5078>
- Arzanlou, M., Torbati, M., & Golmohammadi, H. (2018). *Powdery mildew on hazelnut*

- (*Corylus avellana*) caused by *Erysiphe corylacearum* in Iran. December 2017, 1–4. <https://doi.org/10.1111/efp.12450>
- Becker, W. F., von Jagow, G., Anke, T., & Steglich, W. (1981). Oudemansin, strobilurin A, strobilurin B and myxothiazol: new inhibitors of the bc1 segment of the respiratory chain with an E-beta-methoxyacrylate system as common structural element. *FEBS Letters*, *132*(2), 329–333. [https://doi.org/10.1016/0014-5793\(81\)81190-8](https://doi.org/10.1016/0014-5793(81)81190-8)
- Beenken, L., Brodtbeck, T., & De Marchi, R. (2020). First record of *Erysiphe corylacearum* on *Corylus avellana* in Switzerland and in central Europe . *New Disease Reports*, *41*, 11. <https://doi.org/10.5197/j.2044-0588.2020.041.011>
- Begerow, D., Nilsson, H., Unterseher, M., & Maier, W. (2010). *Current state and perspectives of fungal DNA barcoding and rapid identification procedures*. 99–108. <https://doi.org/10.1007/s00253-010-2585-4>
- Bensch, K., Groenewald, J. Z., Dijksterhuis, J., Starink-Willemse, M., Andersen, B., Summerell, B. A., Shin, H. D., Dugan, F. M., Schroers, H. J., Braun, U., & Crous, P. W. (2010). Species and ecological diversity within the *Cladosporium cladosporioides* complex (Davidiellaceae, Capnodiales). *Studies in Mycology*, *67*, 1–94. <https://doi.org/10.3114/sim.2010.67.01>
- Carver, T. L. W., Ingerson-Morris, S. M., Thomas, B. J., & Gay, A. P. (1994). Light-mediated delay of primary haustorium formation by *Erysiphe graminis* f.sp *avenae*. *Physiological and Molecular Plant Pathology*, *45*(1), 59–79. [https://doi.org/https://doi.org/10.1016/S0885-5765\(05\)80019-0](https://doi.org/https://doi.org/10.1016/S0885-5765(05)80019-0)
- Celio, G. J., & Hausbeck, M. K. (1998). Conidial Germination, Infection Structure Formation, and Early Colony Development of Powdery Mildew on Poinsettia. *Phytopathology*®, *88*(2), 105–113. <https://doi.org/10.1094/PHYTO.1998.88.2.105>
- Chen, X., Zhang, J., Liu, Q., Guo, W., Zhao, T., Ma, Q., & Wang, G. (2014). Transcriptome sequencing and identification of cold tolerance genes in hardy *Corylus* species (*C. heterophylla* fisch) floral buds. *PLoS ONE*, *9*(9). <https://doi.org/10.1371/journal.pone.0108604>
- Cherrad, S., Charnay, A., Hernandez, C., Steva, H., Belbahri, L., & Vacher, S. (2018). Emergence of boscalid-resistant strains of *Erysiphe necator* in French vineyards.

- Microbiological Research*, 216, 79–84.  
<https://doi.org/10.1016/j.micres.2018.08.007>
- Colburn, B. C., Mehlenbacher, S. A., & Sathuvalli, V. R. (2017). Development and mapping of microsatellite markers from transcriptome sequences of European hazelnut (*Corylus avellana* L.) and use for germplasm characterization. *Molecular Breeding*, 37(2). <https://doi.org/10.1007/s11032-016-0616-2>
- Constantinescu, B., Botany, S., Box, P. O., & Uppsala, S.-. (1983). TAXONOMIC REVISION OF SEPTORIA-LIKE FUNGI PARASITIC ON BETULACEAE. *Transactions of the British Mycological Society*, 83(3), 383–398.  
[https://doi.org/10.1016/S0007-1536\(84\)80035-2](https://doi.org/10.1016/S0007-1536(84)80035-2)
- da Silva Zatti, M., Domingos Arantes, T., & Theodoro, R. C. (2020). Isothermal Nucleic Acid Amplification Techniques for Detection and Identification of Pathogenic Fungi: a review. *Mycoses*. <https://doi.org/10.1111/myc.13140>
- Délye, C., Laigret, F., & Corio-Costet, M. F. (1997). A mutation in the 14 alpha-demethylase gene of *Uncinula necator* that correlates with resistance to a sterol biosynthesis inhibitor. *Applied and Environmental Microbiology*, 63(8), 2966–2970. <https://doi.org/10.1128/AEM.63.8.2966-2970.1997>
- Fan, X. L., Barreto, R. W., Groenewald, J. Z., Bezerra, J. D. P., Pereira, O. L., Cheewangkoon, R., Mostert, L., Tian, C. M., & Crous, P. W. (2017). Phylogeny and taxonomy of the scab and spot anthracnose fungus *Elsinoe* (Myriangiales, Dothideomycetes). *Studies in Mycology*, 87, 1–41.  
<https://doi.org/10.1016/j.simyco.2017.02.001>
- Fernández-Ortuño, D., Pérez-García, A., López-Ruiz, F., Romero, D., de Vicente, A., & Torés, J. A. (2006). Occurrence and distribution of resistance to QoI fungicides in populations of *Podosphaera fusca* in south central Spain. *European Journal of Plant Pathology*, 115(2), 215–222. <https://doi.org/10.1007/s10658-006-9014-7>
- Gisi, U., Sierotzki, H., Cook, A., & McCaffery, A. (2002). Mechanisms influencing the evolution of resistance to Qo inhibitor fungicides. *Pest Management Science*, 58(9), 859–867. <https://doi.org/10.1002/ps.565>
- Goettel, M. S., Koike, M., Kim, J. J., Aiuchi, D., Shinya, R., & Brodeur, J. (2008). Potential of *Lecanicillium* spp. for management of insects, nematodes and plant

- diseases. *Journal of Invertebrate Pathology*, 98(3), 256–261.  
<https://doi.org/10.1016/j.jip.2008.01.009>
- Gürcan, K., & Mehlenbacher, S. A. (2010). Development of microsatellite marker loci for European hazelnut (*Corylus avellana* L.) from ISSR fragments. *Molecular Breeding*, 26(3), 551–559. <https://doi.org/10.1007/s11032-010-9464-7>
- Gürcan, K., Mehlenbacher, S. A., Botta, R., & Boccacci, P. (2010). Development, characterization, segregation, and mapping of microsatellite markers for European hazelnut (*Corylus avellana* L.) from enriched genomic libraries and usefulness in genetic diversity studies. *Tree Genetics and Genomes*, 6(4), 513–531.  
<https://doi.org/10.1007/s11295-010-0269-y>
- Hartney, S., Dean, A., Pathologist, P., Dugan, F., & Ammirati, J. (2005). *First Report of Powdery Mildew on Corylus avellana caused by Phyllactinia guttata in Washington State Plant Health Progress Plant Health Progress*. 42(October), 19–21. <https://doi.org/10.1094/PHP-2005-1121-01-BR.Contorted>
- Helmstetter, A. J., Buggs, R. J. A., & Lucas, S. J. (2019). Repeated long-distance dispersal and convergent evolution in hazel. *Scientific Reports*, 1–12.  
<https://doi.org/10.1038/s41598-019-52403-2>
- Heluta, V. P., Makarenko, N. V., & Al-maali, G. A. (2019). *avellana in Ukraine*. 76(3).
- Hofstein, R., Daoust, R. A., & Aeschlimann, J. P. (1996). Constraints to the development of biofungicides: The example of “AQ10”, a new product for controlling powdery mildews. *Entomophaga*, 41(3), 455–460.  
<https://doi.org/10.1007/BF02765797>
- Hong, S. G., Maccaroni, M., Figuli, P. J., Pryor, B. M., & Belisario, A. (2006). Polyphasic classification of *Alternaria* isolated from hazelnut and walnut fruit in Europe. *Mycological Research*, 110(11), 1290–1300.  
<https://doi.org/10.1016/j.mycres.2006.08.005>
- Husain, S. I., & Akram, M. (1995). Effect of temperature and relative humidity on conidial germination and germ tube elongation of *Sphaerotheca fuliginea* (Schlecht ex Fr.) Poll, on sunflower / Wirkung der Temperatur und relativen Luftfeuchtigkeit auf die Konidienkeimung und auf das Keimsch. *Zeitschrift Für Pflanzenkrankheiten Und Pflanzenschutz / Journal of Plant Diseases and*

- Protection*, 102(5), 509–513. <http://www.jstor.org/stable/43386904>
- Isabel, S., Videira, R., Zacharias, J., Verkley, G. J. M., Braun, U., Willem, P., & Spatafora, J. W. (2015). The rise of *Ramularia* from the *Mycosphaerella* labyrinth. *Fungal Biology*, 119(9), 823–843. <https://doi.org/10.1016/j.funbio.2015.06.003>
- Jin, X., Fitt, B., Hall, A., & Huang, Y. (2013). *The role of chasmothecia in the initiation of epidemics of powdery mildew (Podospheara aphanis) and the role of silicon in controlling the epidemics on strawberry.*
- Johnson, K.B., J.N. Pinkerton, S.A. Mehlenbacher, J. K. S., & Pscheidt., and J. W. (1996). Eastern filbert blight of European hazelnut: It's becoming a manageable disease. *Plant Dis.*, 1308–1316. <https://doi.org/10.1094/PD-80-1308>
- Kafkas, S., Sabir, A., & Turan, A. (2009). Genetic Characterization of Hazelnut (*Corylus avellana* L.) Cultivars from Genetic Characterization of Hazelnut (*Corylus avellana* L.) Cultivars from Turkey Using Molecular Markers. *HortScience: A Publication of the American Society for Horticultural Science*, June. <https://doi.org/10.21273/HORTSCI.44.6.1557>
- Kiss, L, Russell, J. C., Szentiványi, O., Xu, X., & Jeffries, P. (2004). Biology and biocontrol potential of *Ampelomyces* mycoparasites, natural antagonists of powdery mildew fungi *Biology and Biocontrol Potential of Ampelomyces.* *Biocontrol Science and Technology*, 14(7), 635–651. <https://doi.org/10.1080/09583150410001683600>
- Kiss, L, Russell, J. C., Szentiványi, O., Xu, X., & Jeffries, P. (2010). *Biology and biocontrol potential of Ampelomyces mycoparasites, natural antagonists of powdery mildew fungi* *Biology and Biocontrol Potential of Ampelomyces.* 3157. <https://doi.org/10.1080/09583150410001683600>
- Kiss, Levente. (1998). Natural occurrence of *ampelomyces* intracellular mycoparasites in mycelia of powdery mildew fungi. *New Phytol.*, 140, 709–714.
- Kiss, Levente. (2003). A review of fungal antagonists of powdery mildews and their potential as biocontrol agents. *Pest Management Science*, 59(4), 475–483. <https://doi.org/10.1002/ps.689>
- Kumar, S., Stecher, G., Li, M., Knyaz, C., & Tamura, K. (2018). MEGA X: Molecular

- evolutionary genetics analysis across computing platforms. *Molecular Biology and Evolution*, 35(6), 1547–1549. <https://doi.org/10.1093/molbev/msy096>
- Li, J., Xiong, C., Liu, Y., Liang, J., & Zhou, X. (2016). Loop-Mediated Isothermal Amplification (LAMP): Emergence As an Alternative Technology for Herbal Medicine Identification . In *Frontiers in Plant Science* (Vol. 7, p. 1956). <https://www.frontiersin.org/article/10.3389/fpls.2016.01956>
- Lucas, J. A., Hawkins, N. J., & Fraaije, B. A. (2015). The evolution of fungicide resistance. *Advances in Applied Microbiology*, 90, 29–92. <https://doi.org/10.1016/bs.aambs.2014.09.001>
- Lucas, S. J., Kahraman, K., Buggs, R. J. A., & Bilge, I. (2019). A chromosome-scale genome assembly of European Hazel ( *Corylus avellana* L .) reveals targets for crop improvement Running title : European hazel reference genome. *BioRxiv*, 44. <https://doi.org/10.1101/817577>
- Ma, H., Lu, Z., Liu, B., Qiu, Q., & Liu, J. (2013). Transcriptome analyses of a Chinese hazelnut species *Corylus mandshurica*. *BMC Plant Biology*, 13(1). <https://doi.org/10.1186/1471-2229-13-152>
- Marinoni DT, Beltramo C, Akkak A, Destefanis ML, Boccacci P, B. R. (2009). Gene Expression and Sporophytic Self-Incompatibility in Hazelnut. *Acta Horti*, 227–232.
- Mehlenbacher, S. A., Brown, R. N., Nouhra, E. R., Gökirmak, T., Bassil, N. V., & Kubisiak, T. L. (2006). A genetic linkage map for hazelnut (*Corylus avellana* L.) based on RAPD and SSR markers. *Genome*, 49(2), 122–133. <https://doi.org/10.1139/G05-091>
- Miles, L. A., Miles, T. D., Kirk, W. W., & Schilder, A. M. C. (2012). Strobilurin (QoI) Resistance in Populations of *Erysiphe necator* on Grapes in Michigan. *Plant Disease*, 96(11), 1621–1628. <https://doi.org/10.1094/PDIS-01-12-0041-RE>
- Miller, T. C., Gubler, W. D., Geng, S., & Rizzo, D. M. (2003). Effects of Temperature and Water Vapor Pressure on Conidial Germination and Lesion Expansion of *Sphaerotheca macularis* f. sp. *fragariae*. *Plant Disease*, 87(5), 484–492. <https://doi.org/10.1094/PDIS.2003.87.5.484>

- Molnar, Thomas and Capik, J. (2012). Advances in hazelnut research in North America  
Advances in Hazelnut Research in North America. *Acta Horticulturae, December 2012*. <https://doi.org/10.17660/ActaHortic.2012.940.6>
- Morgan-Jones, J. F. (1981). Ascocarp Development in *Mamianiella Coryli* Var. *Spiralis*. *Mycologia*, 73(3), 429–439.  
<https://doi.org/10.1080/00275514.1981.12021365>
- Mosquera, S., Chen, L.-H., Aegerter, B., Miyao, E., Salvucci, A., Chang, T.-C., Epstein, L., & Stergiopoulos, I. (2019). Cloning of the Cytochrome b Gene From the Tomato Powdery Mildew Fungus *Leveillula taurica* Reveals High Levels of Allelic Variation and Heteroplasmy for the G143A Mutation. *Frontiers in Microbiology*, 10, 663. <https://doi.org/10.3389/fmicb.2019.00663>
- Niessen, L. (2015). Current state and future perspectives of loop-mediated isothermal amplification (LAMP)-based diagnosis of filamentous fungi and yeasts. *Applied Microbiology and Biotechnology*, 99(2), 553–574. <https://doi.org/10.1007/s00253-014-6196-3>
- Notomi, T., Okayama, H., Masubuchi, H., Yonekawa, T., Watanabe, K., Amino, N., & Hase, T. (2000). Notomi et al LAMP.pdf. *Nucleic Acids Research*, 28(12), e63.  
<https://doi.org/10.1093/nar/28.12.e63>
- Oh, S. J., Park, B. H., Jung, J. H., Choi, G., Lee, D. C., Kim, D. H., & Seo, T. S. (2016). Centrifugal loop-mediated isothermal amplification microdevice for rapid, multiplex and colorimetric foodborne pathogen detection. *Biosensors & Bioelectronics*, 75, 293–300. <https://doi.org/10.1016/j.bios.2015.08.052>
- Öztürk, S. C., Göktay, M., Allmer, J., Doğanlar, S., & Frary, A. (2018). Development of Simple Sequence Repeat Markers in Hazelnut (*Corylus avellana* L.) by Next-Generation Sequencing and Discrimination of Turkish Hazelnut Cultivars. *Plant Molecular Biology Reporter*, 36(5–6), 800–811. <https://doi.org/10.1007/s11105-018-1120-0>
- PERIES, O. S. (1962). Studies on strawberry mildew, caused by *Sphaerotheca macularis* (Wallr. ex Fries) Jaczewski\*. *Annals of Applied Biology*, 50(2), 211–224. <https://doi.org/doi:10.1111/j.1744-7348.1962.tb06004.x>
- Pessina, S., Lenzi, L., Perazzolli, M., Campa, M., Dalla Costa, L., Urso, S., Valè, G.,

- Salamini, F., Velasco, R., & Malnoy, M. (2016). Knockdown of MLO genes reduces susceptibility to powdery mildew in grapevine. *Horticulture Research*, 3(1), 16016. <https://doi.org/10.1038/hortres.2016.16>
- Pirondi, A., Nanni, I. M., Brunelli, A., & Collina, M. (2014). First Report of Resistance to Cyflufenamid in *Podosphaera xanthii*, Causal Agent of Powdery Mildew, from Melon and Zucchini Fields in Italy. *Plant Disease*, 98(11), 1581. <https://doi.org/10.1094/PDIS-02-14-0210-PDN>
- Qin, L., Zhou, Z., Li, Q., Zhai, C., Liu, L., Quilichini, T. D., Gao, P., Kessler, S. A., Jaillais, Y., Datla, R., Peng, G., Xiang, D., & Wei, Y. (2020). Specific Recruitment of Phosphoinositide Species to the Plant-Pathogen Interfacial Membrane Underlies Arabidopsis Susceptibility to Fungal Infection. *The Plant Cell*. <https://doi.org/10.1105/tpc.19.00970>
- Rankovic, B. (1997). Hyperparasites of the genus *Ampelomyces* on powdery mildew fungi in Serbia. *Mycopathologia*, 139, 157–164.
- Romero, D., Rivera, M. E., Cazorla, F. M., de Vicente, A., & Pérez-García, A. (2003). Effect of mycoparasitic fungi on the development of *Sphaerotheca fusca* in melon leaves. *Mycological Research*, 107(Pt 1), 64–71. <https://doi.org/10.1017/s0953756202006974>
- Rowley, E. R., Fox, S. E., Bryant, D. W., Sullivan, C. M., Priest, H. D., Givan, S. A., Mehlenbacher, S. A., & Mockler, T. C. (2012). Assembly and characterization of the European hazelnut “Jefferson” transcriptome. *Crop Science*, 52(6), 2679–2686. <https://doi.org/10.2135/cropsci2012.02.0065>
- Rowley, E. R., VanBuren, R., Bryant, D. W., Priest, H. D., Mehlenbacher, S. A., & Mockler, T. C. (2018). A draft genome and high-density genetic map of European hazelnut (*Corylus avellana* L.). *BioRxiv*, 469015(1), doi: <https://doi.org/10.1101/469015>. <https://doi.org/10.1101/469015>
- Saenz, G. S., & Taylor, J. W. (2015). *Phylogeny of the Erysiphales ( powdery mildews ) inferred from internal transcribed spacer ribosomal DNA sequences*. December. <https://doi.org/10.1139/b98-235>
- Saghai-Marooif, M. A., Soliman, K. M., Jorgensen, R. A., & Allard, R. W. (1984). Ribosomal DNA spacer-length polymorphisms in barley: mendelian inheritance,

- chromosomal location, and population dynamics. *Proceedings of the National Academy of Sciences*, 81(24), 8014 LP – 8018.  
<https://doi.org/10.1073/pnas.81.24.8014>
- Salehi, M. (2019). Elicitors derived from endophytic fungi *Chaetomium globosum* and *Paraconiothyrium brasiliense* enhance paclitaxel production in *Corylus avellana* cell suspension culture Elicitors derived from endophytic fungi *Chaetomium globosum* and *Paraconiothyrium brasiliense*. *Plant Cell, Tissue and Organ Culture (PCTOC)*, 136(1), 161–171. <https://doi.org/10.1007/s11240-018-1503-9>
- Sathuvalli, V., Mehlenbacher, S. A., & Smith, D. C. (2017). *High-Resolution Genetic and Physical Mapping of the Eastern Filbert Blight Resistance Region in ‘ Jefferson ’ Hazelnut ( Corylus avellana L . )*. July.  
<https://doi.org/10.3835/plantgenome2016.12.0123>
- Sathuvalli, V. R., & Mehlenbacher, S. A. (2011). *A bacterial artificial chromosome library for ‘ Jefferson ’ hazelnut and identification of clones associated with eastern filbert blight resistance and pollen – stigma incompatibility*. 867, 862–867.  
<https://doi.org/10.1139/G11-048>
- Schoch, C. L., Seifert, K. A., Huhndorf, S., Robert, V., Spouge, J. L., & Levesque, C. A. (2012). *Nuclear ribosomal internal transcribed spacer ( ITS ) region as a universal DNA barcode marker for Fungi*. 109(16), 6241–6246.  
<https://doi.org/10.1073/pnas.1117018109>
- Sezer, A., & Dolar, F. S. (2012). *Colletotrichum acutatum*, a new pathogen of hazelnut. *Journal of Phytopathology*, 160(7–8), 428–430. <https://doi.org/10.1111/j.1439-0434.2012.01910.x>
- Sezer, A., Dolar, F. S., Lucas, S. J., Köse, Ç., & Gümüş, E. (2017a). First report of the recently introduced, destructive powdery mildew *Erysiphe corylacearum* on hazelnut in Turkey. *Phytoparasitica*, 45(4), 577–581.  
<https://doi.org/10.1007/s12600-017-0610-1>
- Sezer, A., Dolar, F. S., Lucas, S. J., Köse, Ç., & Gümüş, E. (2017b). First report of the recently introduced, destructive powdery mildew *Erysiphe corylacearum* on hazelnut in Turkey. *Phytoparasitica*, 45(4), 577–581.  
<https://doi.org/10.1007/s12600-017-0610-1>

- Sivapalan, A. (1993). Effects of water on germination of powdery mildew conidia. *Mycological Research*, 97(1), 71–76. [https://doi.org/https://doi.org/10.1016/S0953-7562\(09\)81115-5](https://doi.org/https://doi.org/10.1016/S0953-7562(09)81115-5)
- Sogonov, M. V., Castlebury, L. A., Rossman, A. Y., Mejía, L. C., & White, J. F. (2008). Leaf-inhabiting genera of the Gnomoniaceae, Diaporthales. *Studies in Mycology*, 62(1), 1–77. <https://doi.org/10.3114/sim.2008.62.01>
- Sreerama Kumar, P., & Singh, L. (2009). Lasiodiplodia theobromae is a Mycoparasite of a Powdery Mildew Pathogen. *Mycobiology*, 37(4), 308–309. <https://doi.org/10.4489/MYCO.2009.37.4.308>
- Sugai, K., Inoue, H., Inoue, C., Sato, M., Wakazaki, M., Kobayashi, K., Nishiguchi, M., Toyooka, K., Yamaoka, N., & Yaeno, T. (2020). High Humidity Causes Abnormalities in the Process of Appressorial Formation of Blumeria graminis f. sp. hordei. *Pathogens (Basel, Switzerland)*, 9(1). <https://doi.org/10.3390/pathogens9010045>
- Takamatsu, S., & Kano, Y. (2001). PCR primers useful for nucleotide sequencing of rDNA of the powdery mildew fungi. *Mycoscience*, 42(1), 135–139. <https://doi.org/10.1007/BF02463987>
- Takamatsu, Susumu, Inagaki, M., Niinomi, S., & Voglmayr, H. (2008). *Comprehensive molecular phylogenetic analysis and evolution of the genus Phyllactinia ( Ascomycota : Erysiphales ) and its allied genera. 112, 299–315.* <https://doi.org/10.1016/j.mycres.2007.11.014>
- Thiessen, L. D., Neill, T. M., & Mahaffee, W. F. (2018). Development of a quantitative loop-mediated isothermal amplification assay for the field detection of Erysiphe necator. *PeerJ*, 6, e4639. <https://doi.org/10.7717/peerj.4639>
- Tucker, M. A., Lopez-Ruiz, F., Cools, H. J., Mullins, J. G., Jayasena, K., & Oliver, R. P. (2020). Analysis of mutations in West Australian populations of Blumeria graminis f. sp. hordei CYP51 conferring resistance to DMI fungicides. *Pest Management Science*, 76(4), 1265–1272. <https://doi.org/10.1002/ps.5636>
- Vela-Corcía, D., Romero, D., de Vicente, A., & Pérez-García, A. (2018). Analysis of  $\beta$ -tubulin-carbendazim interaction reveals that binding site for MBC fungicides does not include residues involved in fungicide resistance. *Scientific Reports*, 8(1),

7161. <https://doi.org/10.1038/s41598-018-25336-5>

Vielba-Fernández, A., de Vicente, A., Pérez-García, A., & Fernández-Ortuño, D. (2019). Monitoring Methyl Benzimidazole Carbamate-Resistant Isolates of the Cucurbit Powdery Mildew Pathogen, *Podosphaera xanthii*, Using Loop-Mediated Isothermal Amplification. *Plant Disease*, *103*(7), 1515–1524.  
<https://doi.org/10.1094/PDIS-12-18-2256-RE>

Yan, W., Wang, X., Li, K., Li, T.-X., Wang, J.-J., Yao, K.-C., Cao, L.-L., Zhao, S.-S., & Ye, Y.-H. (2019). Design, synthesis, and antifungal activity of carboxamide derivatives possessing 1,2,3-triazole as potential succinate dehydrogenase inhibitors. *Pesticide Biochemistry and Physiology*, *156*, 160–169.  
<https://doi.org/10.1016/j.pestbp.2019.02.017>

White TJ, Bruns TD, Lee S, Taylor JW (1990) Amplification and direct sequencing of fungal ribosomal RNA genes for phylogenetics. In 'PCR protocols: a guide to methods and applications'. (Eds MA Innis, DH Gelfand, JJ Sninsky, TJ White) pp. 315–322. (Academic Press Inc: San Diego, California, US

APPENDICES

APPENDIX A. Location data for sample collected orchards in Turkey

**Table 9:** Hazelnut orchard location and selected weather stations in Sakarya and Düzce. Orchard ID (chosen according to village name), city, district names are recorded. Latitude (Lat.) and longitude (Long.) are recorded in decimal degrees (DD) and degrees minutes seconds (DMS). Altitudes recorded in meters (m).

Orchard ID (Village)	City	District	Lat. (DD)	Lat. (DMS)	Long. (DD)	Long. (DMS)	Altitude (m)	Weather Station ID
Yeşiltepe	Düzce	Cumayarı	40,937	40°56'11.78"	30,902	30°54'7.31"	658	Çikolata-Dededüzü
Paşalar	Düzce	Akçakoca	41,062	41°3'44.33"	31,029	31°1'45.74"	148	Cikolata-Pasalar
Süngüt	Sakarya	Kocaali	40,958	40°57'28.54"	30,875	30°52'28.89"	514	Cikolata-Ballıkaya
Tahirli	Düzce	Akçakoca	41,055	41°3'19.56"	31,074	31°4'26.28"	133	Cikolata-Pasalar
Artıklı	Ordu	Merkez	40,921	40°55'14"	37,865	37°51'53"	165	Cikolata-Kovanci
Dedeli	Ordu	Merkez	40,907	40°54'26"	37,829	37°49'46"	172	Cikolata-Kovanci
Uzunisa	Ordu	Merkez	40,923	40°55'21"	37,863	37°51'47"	140	Cikolata-Kovanci

Kekiktep	Giresu	Eynesil	41,04	41°2'	39,09	39° 5'		Cikolata-
e	n		3	36.38"	4	37.14"	50	Eynesil



Figure 11: Map of hazelnut orchards and nearest weather stations on Ordu. a. Map of weather station; Kovancı is labelled in yellow, b. map of hazelnut orchards Artıklı, Dedeli and Uzunisa are labelled in yellow.



Figure 12: Map of hazelnut orchard and nearest weather station on Giresun. a. Map of weather station; Eynesil is labelled in yellow, b. map of hazelnut orchards Pasalar, Süngüt, Tahirli and Yeşiltepe are labelled in yellow.

APPENDIX B. List of collected leaf samples

**Table 10:** Collected leaf sample

Location	Date	Sample type	Sample number	Microscope observation	PCR with Ec_F1-R3	qPCR with Ec_F1-R3
Sabancı University	26.09.2018	Tombul leaf healthy	1	hy	i	i
	26.09.2018	Tombul leaf infected-L	2	i	i	i
	26.09.2018	Tombul leaf infected-U	3	i	i	i
	26.09.2018	Çakıldak leaf healthy	4	n		n
	26.09.2018	Çakıldak leaf infected-L	5	i	i	i
	26.09.2018	Çakıldak leaf infected-U	6	i	i	i
Yeşiltepe/ Cumayarı/ Düzce	21.03.2018	Old leaf	7	i	i	+
	21.03.2018	Bud	8	hy	i	?
	21.03.2018	Fresh leaf	9	n		?
	3.04.2018	Leaf	10	hy	i	+
	12.04.2018	Leaf	11	hy	i	?
	9.05.2018	Infected leaf	12	i		+
	24.05.2018	Leaf	13	n		-
	24.05.2018	Infected leaf	14	i		?
	6.06.2018	Leaf	15	hy		?
	6.06.2018	Infected leaf	16	i		
Paşalar/ Akcakoca/ Düzce	21.03.2018	Old leaf	17	i	i	+
	21.03.2018	Bud	18	hy	i	?
	21.03.2018	Fresh leaf	19	n		-
	3.04.2018	Leaf	20	n	i	+
	12.04.2018	Leaf	21	hy		+
	9.05.2018	Leaf	22			
	9.05.2018	Infected leaf	23	i	i	+
	24.05.2018	Leaf	24	hy		?
	24.05.2018	Infected leaf	25	i	i	
	6.06.2018	Leaf	26	i	i	-
	6.06.2018	Infected leaf	27	i	i	
Tahirli/ Akcakoca/ Düzce	7.05.2019	old leaf	28	i	i	+
	7.05.2019	fresh leaf	29	n	n	?
	7.05.2019	fungus infected leaf	30	hy	i	+
	31.05.2019	fungus infected leaf	31	hy	i	+
	31.05.2019	leaf	32	hy	i	+
	26.06.2019	fungus infected leaf	33	i		+
	26.06.2019	leaf	34	n		+
	21.03.2018	Old leaf	35	hy	i	?
	21.03.2018	Bud	36	hy	i	?

Süngüt/ Kocaali/ Sakarya	21.03.2018	Fresh leaf	37	n	i	-
	3.04.2018	Leaf	38	n	i	+
	12.04.2018	Leaf	39	n	n	?
	24.05.2018	Leaf	40	hy	i	+
	24.05.2018	Infected leaf	41	hy	i	
	11.06.2018	Leaf	42	hy		?
	11.06.2018	Infected leaf	43	i	i	+
Süngüt/ Kocaali/ Sakarya	7.05.2019	old leaf	44	i	i	+
	7.05.2019	fresh leaf	45	n	n	-
	31.05.2019	fungus infected leaf	46	i	i	+
	31.05.2019	leaf	47	n	i	+
	26.06.2019	fungus infected leaf	48		i	+
	26.06.2019	leaf	49	n	i	?
Artıklı/ Merkez/ Ordu	20.03.2018	Old leaf	50	i		
	20.03.2018	Bud	51	hy	i	+
	20.03.2018	Fresh leaf	52	i		
	30.03.2018	Leaf	53	n		
	2.04.2018	Leaf	54	hy		
	11.04.2018	Leaf	55	hy		
	7.05.2018	Leaf	56	i	i	+
	28.05.2018	Leaf	57	i	i	+
Dedeli/ Merkez/ Ordu	20.03.2018	Old leaf	58	i	i	+
	20.03.2018	Bud	59	i	i	?
	20.03.2018	Fresh leaf	60	n		?
	30.03.2018	Leaf	61	n		
	2.04.2018	Leaf	62	hy		?
	11.04.2018	Leaf	63	hy		
	7.05.2018	Leaf	64	hy	i	?
	28.05.2018	Leaf	65	i	i	+
Uzunisa/ Merkez/ Ordu	20.03.2018	Old leaf	66	i		
	20.03.2018	Bud	67	i	i	?
	20.03.2018	Fresh leaf	68	n	i	?
	30.03.2018	Leaf	69	n	i	-
	2.04.2018	Leaf	70	n		-
	11.04.2018	Leaf	71	hy		+
	7.05.2018	Leaf	72	hy	i	+
	28.05.2018	Leaf	73	i	i	+
Uzunisa/ Altınordu/ Ordu	19.04.2019	old leaf	74	i		+
	19.04.2019	fresh leaf	75	n	i	?
	7.05.2019	leaf	76	hy		
	20.05.2019	leaf (returned)	77	n		
	27.05.2019	leaf	78	hy	i	+
	14.06.2019	leaf	79	i	i	+

	1.07.2019	leaf	80	hy	i	+
	12.06.2019	involucre	81	hy	i	+
	12.06.2019	involucre	82	n		
Yağlıdere/ Ömerli/ Giresun	19.04.2019	old leaf	83	i		+
	19.04.2019	fresh leaf	84	n		-
	7.05.2019	leaf	85	hy	i	?
	20.05.2019	leaf (returned)	86	n		-
	27.05.2019	leaf	87	hy		-
	14.06.2019	leaf	88	i	i	+
	1.07.2019	leaf	89	i		+
	1.07.2019	involucre	90	hy	i	+
	1.07.2019	involucre	91	n		?
Dedeli- Şimşek	28.05.2018	Treated	92			+
Dedeli- Şimşek	28.05.2018	Tombul	93		i	+
Dedeli- Şimşek	28.05.2018	Çakıldak	94		i	+
Kadioğlu- 2	28.05.2018	Tombul, no treatment	95		i	+
Kadioğlu- 2	28.05.2018	Tombul	96		i	+
Kadioğlu- 1	28.05.2018	Palaz yağlı	97		i	
Kadioğlu- 1	28.05.2018	Yağlı fındık Tombul	98		i	+
Kadioğlu- 1	28.05.2018	Yabani fındık	99		i	+
Örnek bahçe	28.05.2018	Tombul-palaz	100			
Sulama bahçesi	28.05.2018	Tombul	101			
Ordu Sulama bahçesi	28.05.2018	Palaz yağlı	102		i	+
Hendek / Yeşilyurt- 2	21.11.2018	leaf	103	i		
Hendek / Şeyhler	21.11.2018	leaf	104	i (P.guttata)		
Hendek / Şeyhler	21.11.2018	leaf	105	i		
Süngüt	21.11.2018	leaf	106	i (both)		
Süngüt	21.11.2018	leaf	107	i		
Cumayeri	21.11.2018	leaf	108	i		
Cumayeri	21.11.2018	leaf	109	i (P.guttata)		
Hendek merkez	21.11.2018	leaf	110	i (P.guttata)		
Hendek merkez	21.11.2018	leaf	111	i		

